NSTX Upgrade

FDR Calculation Executive Summaries

May   2011

Prepared By:
the NSTX Upgrade Team

Introduction:

This is a compilation of the executive summaries of the NSTX Upgrade calculations currently prepared and under review. This is expected to be somewhat disjointed and will have minimal commonality in format, but it should give an indication of the scope of the analysis work performed to support the NSTX Upgrade design effort.   Some, but not most, have been reviewed and signed by a checker. The status of the calculations and the full version undergoing checking may be found at the project web site

NSTXU   Calculation   Web   page   (http://nstx-upgrade.pppl.gov/Engineering/Calculations/index_Calcs.htm >)

An important input to the calculations is the design point spreadsheet that is maintained on the web by Charlie Neumeyer. This includes all the coil specs, design scenarios, load summations, coil temperatures, inductance matrices and many other specifics of the coil systems.

http://www.pppl.gov/~neumeyer/NSTX_CSU/Design_Point.html

 It is the projects intent to have all the calculations in the review process at the time of the Peer Review and to have then checked and signed at the time of the FDR. realistically, both the Peer Review and the FDR will find some areas where corrections and clarifications will be required. All these calculations are being prepared and reviewed in accordance with the Engineering Department Requirements Document ENG-033.
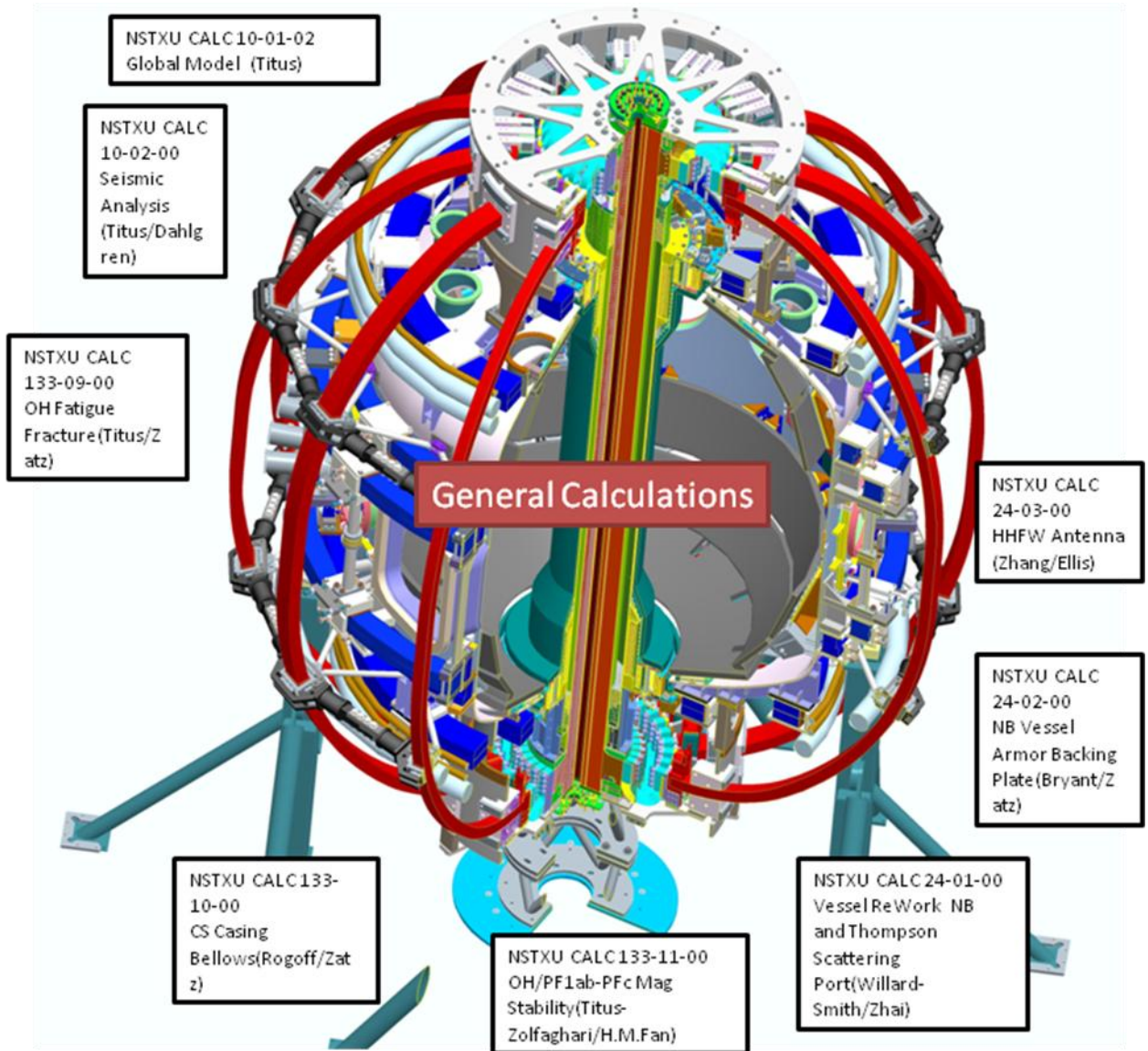
A list of the calculations follow. A few figures follow the list which show the correlation between the calculation with the system or component. The presentation at the Peer Review will discuss the major performance challenges and how the calculations have qualified the Upgrade for the increased Lorentz and thermal loads.
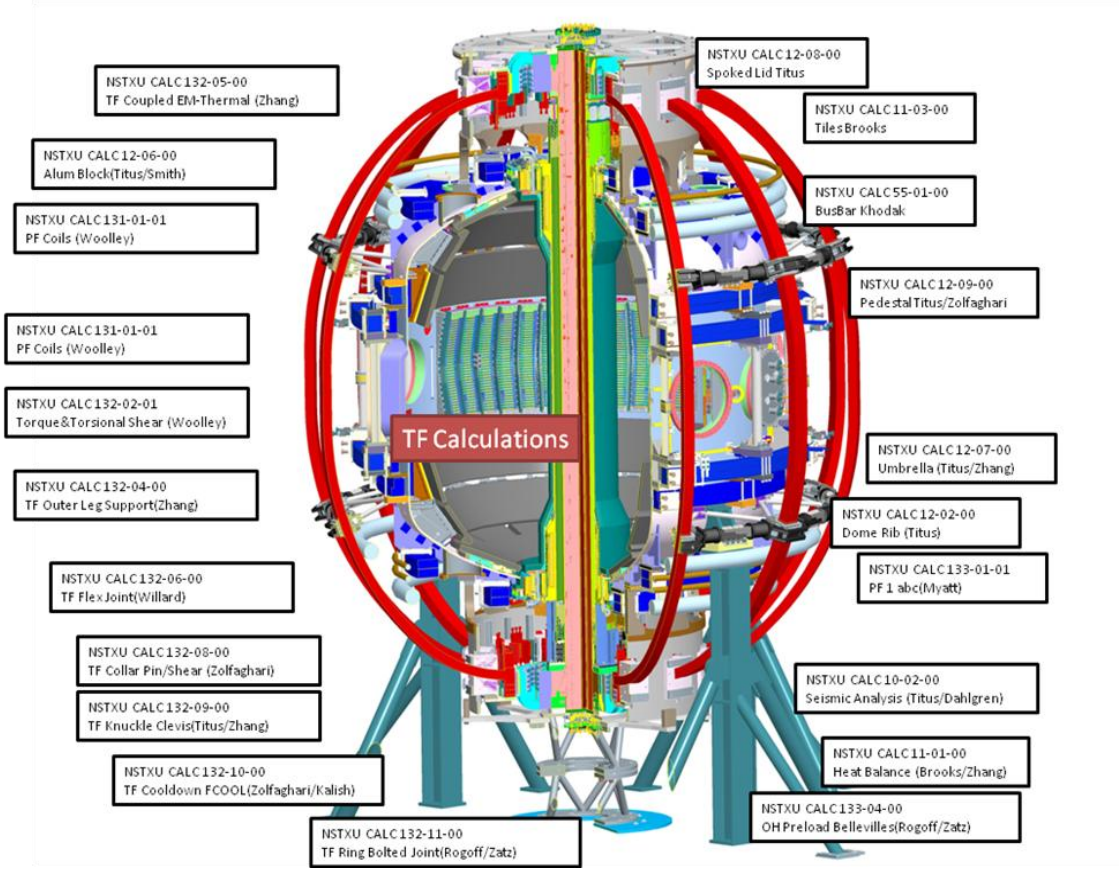
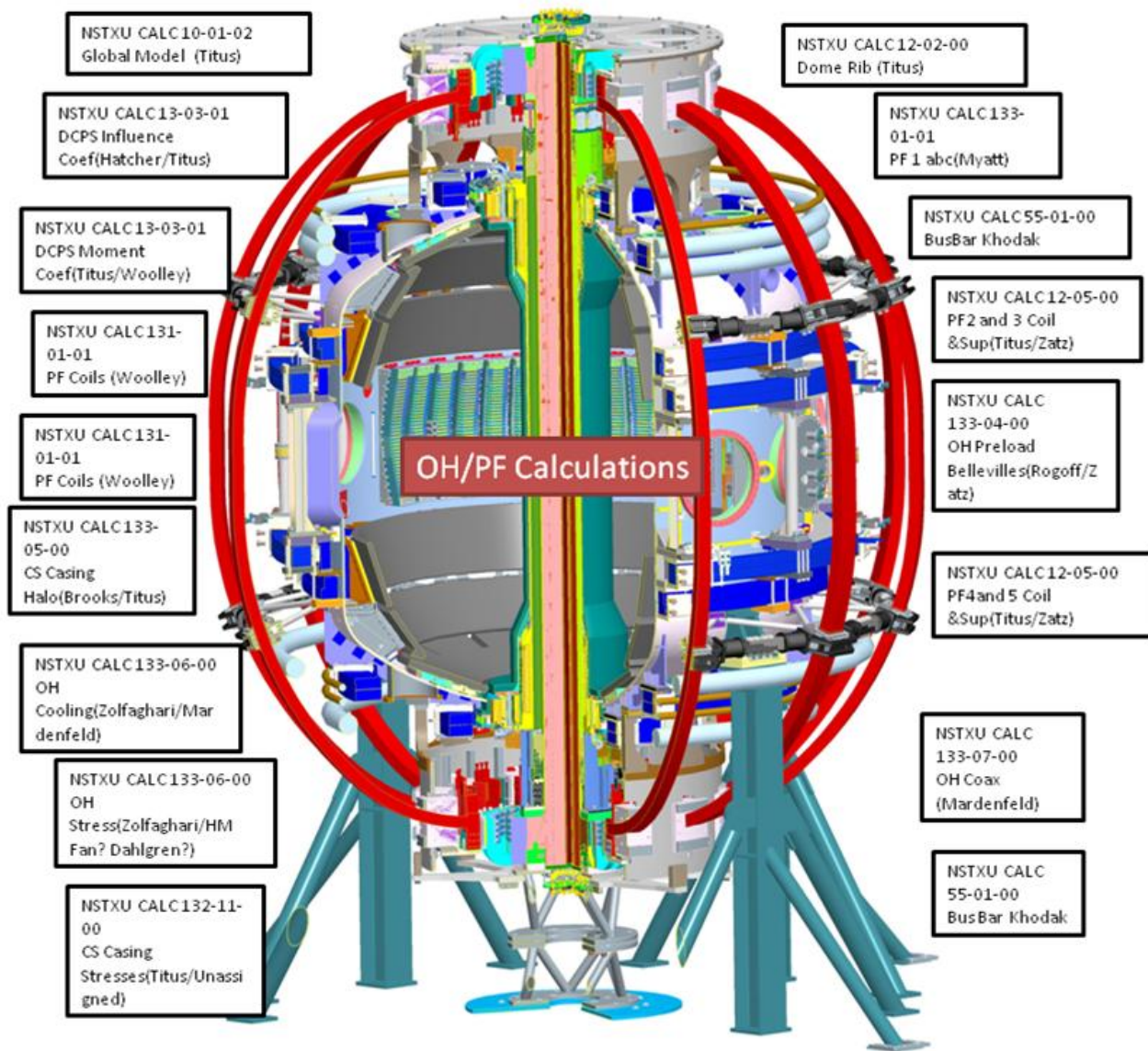| WBS	Calc #	Calc Title	Preparer
1.1.0	NSTXU-CALC-132-03-00	Torque Egns for Design Point	Woolley
1.1.1	NSTXU-CALC-10-01-02	Global Model	P.Titus
1.1.1	NSTXU-CALC-10-02-00	Seismic Analysis	P. Titus
1.1.1	*NSTXU-CALC-11-01-00*	Heat Balance	A. Brooks
1.1.1	*NSTXU-CALC-11-02-00*	General Tile Program	J. Boales
1.1.1	*NSTXU-CALC-11-03-00*	Final Tile Stress Analysis (ATJ Tiles)	A. Brooks
1.1.1	*NSTXU-CALC-11-04-00*	Fastener Analysis	A. Brooks
1.1.1	NSTXU-CALC-12-01-01	Update of Analysis of Vacuum Vessel & Passive Plates	P. Titus
1.1.1	*NSTXU-CALC-12-03-00*	OPERA 2D Disruption Analyses	Hatcher
1.1.2	*NSTXU-CALC-12-02-00*	Dome/PF Rib Stresses	P. Titus
1.1.2	*NSTXU-CALC-12-04-00*	PF2 / PF3 Bolting, Bracket, and weld Stress	P. Titus
1.1.2	*NSTXU-CALC-12-05-00*	PF4 and PF5 Support Analysis	P. Titus
1.1.2	*NSTXU-CALC-12-06-00*	Aluminum Block (To Be Revised by Pete T.)	P. Titus
1.1.2	*NSTXU-CALC-12-07-00*	Umbrella Reinforcement Details	P. Titus
1.1.2	*NSTXU-CALC-12-08-00*	Lid/Spoke Assembly, Upper and Lower	P. Titus/Smith
1.1.2	*NSTXU-CALC-12-09-00*	Pedestal Analysis	P. Titus/Smith
1.1.2	NSTXU-CALC-132-04-00	Analysis of TF Outer Leg	Han Zhang
1.1.2	*NSTXU-CALC-132-09-00*	Analysis of Knuckle Clevis	P. Titus
1.1.2	*NSTXU-CALC-132-11-00*	Ring Bolted Joint	Peter Rogoff
1.1.3	NSTXU-CALC-131-01-00	Analysis of CSU Poloidal Field Coils	Woolley
1.1.3	NSTXU-CALC-131-02-00	Poloidal Magnetic Quantities for the Feb 2010 Provisional Design	Woolley
1.1.3	NSTXU-CALC-131-03-00	Poloidal Magnetic Quantities for the May 2010 Design Point	Woolley
1.1.3	NSTXU-CALC-132-05-00	Coupled EM-Thermal Analysis	Han Zhang
1.1.3	NSTXU-CALC-132-06-00	TF Flex Joint and Bundle Stub	T. Willard
1.1.3	NSTXU-CALC-132-07-00	Maximum Torsional Shear Stress	P. Titus
1.1.3	NSTXU-CALC-132-08-00	Determination of shear Forces Between the TF conductors and Insulation and the G-10 Insulating Crown.	A. Zolfaghari
1.1.3	*NSTXU-CALC-132-10-00*	TF Cool-down using FCOOL	A. Zolfaghari
1.1.3	NSTXU-CALC-133-01-01	Structural Analysis of the PF1 Coils, leads and Supports, Rev 1	L. Myatt
1.1.3	NSTXU-CALC-133-02-00	Thermal Stresses on OH-TF Coils	S. Avasarala

1.1.3	NSTXU-CALC-133-03-00	Center Stack Casing Disruption Inductive and Halo Current Loads	P. Titus
1.1.3	NSTXU-CALC-133-04-00	OH Preload System and Belleville Spring Design	Peter Rogoff
1.1.3	*NSTXU-CALC-133-05-00*	CS Casing Halo Ind and Res Cur	A. Brooks
1.1.3	*NSTXU-CALC-133-06-00*	OH Coolant Hole Optimization	A. Zolfaghari
1.1.3	*NSTXU-CALC-133-07-00*	OH Coax Lead Analysis	M. Mardenfeld
1.1.3	*NSTXU-CALC-133-08-00*	OH Stress Analyses	A. Zolfaghari
1.1.3	*NSTXU-CALC-133-09-00*	OH Fatigue and Fracture Mechanics	P. Titus
1.1.3	*NSTXU-CALC-133-10-00*	Center Stack Casing Bellows	Peter Rogoff
1.1.3	*NSTXU-CALC-133-11-00*	OH & PF1 Electromagnectic Stability Analysis	P. Titus/Zolfaghari
1.1.4	*NSTXU-CALC-133-12-00*	Centerstack Manufacturing Fixtures	
1.2.3	*NSTXU-CALC-40-01-00*	Diagnostics Review and Database	J. Boales
1.2.4	*NSTXU-CALC-24-01-00*	Vessel Port Re-Work for NB and Thompson Scattering Port	T. Willard
1.2.4	*NSTXU-CALC-24-02-00*	Armor Plate Backing Plate	L. Bryant
1.2.4	*NSTXU-CALC-24-03-00*	HHFW Antenna (needs to be modified for upgrade loads)	Han Zhang/Ellis
1.2.4	*NSTXU-CALC-24-04-00*	Magnetic Shielding Calculation	L. Bryant
1.5.2	NSTXU-CALC-13-03-01	DCPS Force Influence Coefficients	Hatcher
1.5.2	*NSTXU-CALC-13-05-00*	DCPS Moment Influence Coefficients	Woolley/Titus
1.5.5	*NSTXU-CALC-55-01-00*	Bus Bar Analysis	A. Khodak

NSTXU Calculation Web page (http://nstx-upgrade.pppl.gov/Engineering/Calculations/index_Calcs.htm >)

NSTXU CALC 10-01-02 Global Model (Titus)

NSTXU CALC 10-02-00 Seismic Analysis (Titus/Dahlgren)

NSTXU CALC 133-09-00 OH Fatigue Fracture(Titus/Zatz)

General Calculations

NSTXU CALC 24-03-00 HHFW Antenna (Zhang/Ellis)

NSTXU CALC 24-02-00 NB Vessel Armor Backing Plate(Bryant/Zatz)

NSTXU CALC 133-10-00 CS Casing Bellows(Rogoff/Zatz)

NSTXU CALC 133-11-00 OH/PF1ab-PFc Mag Stability(Titus-Zolfaghari/H.M.Fan)

NSTXU CALC 24-01-00 Vessel ReWork NB and Thompson Scattering Port(Willard-Smith/Zhai)

NSTXU CALC 132-05-00
TF Coupled EM-Thermal (Zhang)

NSTXU CALC 12-06-00
Alum Block(Titus/Smith)

NSTXU CALC 131-01-01
PF Coils (Woolley)

NSTXU CALC 131-01-01
PF Coils (Woolley)

NSTXU CALC 132-02-01
Torque&Torsional Shear (Woolley)

NSTXU CALC 132-04-00
TF Outer Leg Support(Zhang)

NSTXU CALC 132-06-00
TF Flex Joint(Willard)

NSTXU CALC 132-08-00
TF Collar Pin/Shear (Zolfaghari)

NSTXU CALC 132-09-00
TF Knuckle Clevis(Titus/Zhang)

NSTXU CALC 132-10-00
TF Cooldown FCOOL(Zolfaghari/Kalish)

NSTXU CALC 132-11-00
TF Ring Bolted Joint(Rogoff/Zatz)

NSTXU CALC 12-08-00
Spoked Lid Titus

NSTXU CALC 11-03-00
Tiles Brooks

NSTXU CALC 55-01-00
BusBar Khodak

NSTXU CALC 12-09-00
Pedestal Titus/Zolfaghari

NSTXU CALC 12-07-00
Umbrella (Titus/Zhang)

NSTXU CALC 12-02-00
Dome Rib (Titus)

NSTXU CALC 133-01-01
PF 1 abc(Myatt)

NSTXU CALC 10-02-00
Seismic Analysis (Titus/Dahlgren)

NSTXU CALC 11-01-00
Heat Balance (Brooks/Zhang)

NSTXU CALC 133-04-00
OH Preload Bellevilles(Rogoff/Zatz)

TF Calculations

NSTXU CALC 10-01-02 Global Model (Titus)

NSTXU CALC 13-03-01 DCPS Influence Coef(Hatcher/Titus)

NSTXU CALC 13-03-01 DCPS Moment Coef(Titus/Woolley)

NSTXU CALC 131-01-01 PF Coils (Woolley)

NSTXU CALC 131-01-01 PF Coils (Woolley)

NSTXU CALC 133-05-00 CS Casing Halo(Brooks/Titus)

NSTXU CALC 133-06-00 OH Cooling(Zolfaghari/Mardenfeld)

NSTXU CALC 133-06-00 OH Stress(Zolfaghari/HM Fan? Dahlgren?)

NSTXU CALC 132-11-00 CS Casing Stresses(Titus/Unassigned)

NSTXU CALC 12-02-00 Dome Rib (Titus)

NSTXU CALC 133-01-01 PF 1 abc(Myatt)

NSTXU CALC 55-01-00 BusBar Khodak

NSTXU CALC 12-05-00 PF2 and 3 Coil &Sup(Titus/Zatz)

NSTXU CALC 133-04-00 OH Preload Bellevilles(Rogoff/Zatz)

NSTXU CALC 12-05-00 PF4and 5 Coil &Sup(Titus/Zatz)

NSTXU CALC 133-07-00 OH Coax (Mardenfeld)

NSTXU CALC 55-01-00 BusBar Khodak

OH/PF Calculations

NSTXU CALC 132-02-01
Torque&Torsional Shear (Woolley)

NSTXU CALC 133-01-01
PF 1 abc(Myatt)

NSTXU CALC 12-05-00
PF2 and 3 Coil
&Sup(Titus/Zatz)

NSTXU CALC 13-03-01
DCPS Influence
Coef(Hatcher/Titus)

NSTXU CALC 13-03-01
DCPS Moment
Coef(Titus/Woolley)

NSTXU CALC 55-01-00
BusBar Khodak

NSTXU CALC 12-09-00
Pedestal Titus/Zolfaghari

NSTXU CALC 12-08-00
Spoked Lid (Titus)

NSTXU CALC 12-06-00
Alum Block(Titus/Smith)

NSTXU CALC 12-02-00
Dome Rib (Titus)

NSTXU CALC 12-07-00
Umbrella
(Titus/Zhang)

NSTXU CALC 12-05-00
PF4and 5 Coil
&Sup(Titus/Zatz)

NSTXU CALC 132-04-00
TF Outer Leg
Support(Zhang)

NSTXU CALC 12-06-00
Alum Block(Titus/Smith)

NSTXU CALC 12-08-00
Spoked Lid (Titus)

External Structures

NSTXU CALC132-05-00
TF Coupled EM-Thermal (Zhang)

NSTXU CALC12-06-00
Alum Block(Titus/Smith)

NSTXU CALC131-01-01
PF Coils (Woolley)

NSTXU CALC131-01-01
PF Coils (Woolley)

NSTXU CALC132-02-01
Torque&Torsional Shear (Woolley)

NSTXU CALC132-04-00
TF Outer Leg Support(Zhang)

NSTXU CALC132-06-00
TF Flex Joint(Willard)

NSTXU CALC132-08-00
TF Collar Pin/Shear (Zolfaghari)

NSTXU CALC132-09-00
TF Knuckle Clevis(Titus/Zhang)

NSTXU CALC132-10-00
TF Cooldown FCOOL(Zolfaghari/Kalish)

NSTXU CALC132-11-00
TF Ring Bolted Joint(Rogoff/Zatz)

NSTXU CALC12-08-00
Spoked Lid Titus

NSTXU CALC11-03-00
Tiles Brooks

NSTXU CALC55-01-00
BusBar Khodak

NSTXU CALC12-09-00
Pedestal Titus/Zolfaghari

NSTXU CALC12-07-00
Umbrella (Titus/Zhang)

NSTXU CALC12-02-00
Dome Rib (Titus)

NSTXU CALC133-01-01
PF 1 abc(Myatt)

NSTXU CALC10-02-00
Seismic Analysis (Titus/Dahlgren)

NSTXU CALC11-01-00
Heat Balance (Brooks/Zhang)

NSTXU CALC133-04-00
OH Preload Bellevilles(Rogoff/Zatz)

TF Calculations

WBS 1.1.0 NSTXU 132-03-00, Torques On TF Conductors & Resulting Torsion & Shear Stress in NSTX CSU, 04 May2010 Design Point,
Prepared by R. Woolley **Reviewed by** Peter Titus**, Cognizant Engineer:** Peter Titus

<u>References:</u>
1. **R. Woolley memo 13-260709, "Out-Of-Plane (OOP) PF/TF Torques On TF Conductors in NSTX CSU", 26 July 2009,**
2. **P. Titus memo, "Maximum TF Torsional Shear", 29 July 2009**
3. **P. Titus paper, "Provisions for Out-of-Plane Support of the TF Coils in Recent Tokamaks",28September1999**

<u>Summary</u>
This updates Ref.1 bringing its calculation of out-o-plane (OOP) torques on TF coil conductors up to date for the design point adopted on 04May2010. It also includes a linear elastic model for the TF conductors and their supporting structures to estimate TF conductor torsion for any specified set of currents in the PF coils, OH coil, and plasma. For the 96 previously defined plasma equilibria and for the +24 kA maximum OH precharge case, the **peak torsional shear stress in the TF centerstack calculated by these methods is <u>25.18 MPa</u>.**

As in Ref.1, this memo advances a simple but accurate algorithm for evaluating out-of-plane torques due to magnetic interactions of poloidal magnetic fields with TF conductor current. This is the subject of pages 1-14 and Appendix 1 (pages 43-50). The torsional response model is the subject of pages 15- -42 and Appendix 2 (pages 51-69). Instead of the conventional complicated approach involving numerical integration of vector cross products of position vectors, current density vectors and poloidal magnetic field vectors at many evaluation points chosen along a segment of the TF conductor, this torque algorithm multiplies the [(130kA)(36turn)=4,680,000 A] TF current magnitude by the difference of the per radian poloidal magnetic fluxes evaluated at the two ends of the segment. (Note that the product of amperes and webers has the torque units, newton-meters.) The results are mathematically equivalent to numerically integrating the vector cross product of position and force over the TF conductor, but the torque algorithm advanced herein requires far less computation and is subject to far less numerical error. A full exposition of the torque algorithm is given in Appendix 1.

This torque algorithm is applied to the NSTX CS upgrade, using the latest layout for the TF conductor outline and using the PF/OH coil set of the 04May2010 design point. To increase numerical accuracy the TF conductor is partitioned into sub-regions separated by internal current streamlines estimated by equally subdividing the conductor cross section area. Torque loading densities for current ranges in each of the 12 PF and 1 OH coil circuits and for the plasma current are plotted. MATLAB version R2010b was used for all numerical calculations and plots.

A formula for net torque on the top half of the TF system is as follows:

$$\left[\frac{\text{Net Upper Half TF System Torque}}{1\,\text{N-m}}\right] = 13563.1\left[\frac{I_{OH}}{1\,\text{kA}}\right] + 2260.9\left[\frac{I_{PF1AU} + I_{PF1AL}}{1\,\text{kA}}\right]$$

$$+ 1580.6\left[\frac{I_{PF1BU} + I_{PF1BL}}{1\,\text{kA}}\right] + 1851.5\left[\frac{I_{PF1CU} + I_{PF1CL}}{1\,\text{kA}}\right]$$

$$+ 5197.5\left[\frac{I_{PF2U} + I_{PF2L}}{1\,\text{kA}}\right] + 21915.7\left[\frac{I_{PF3U} + I_{PF3L}}{1\,\text{kA}}\right]$$

$$+ 56813.9\left[\frac{I_{PF4}}{1\,\text{kA}}\right] + 118636.5\left[\frac{I_{PF5U}}{1\,\text{kA}}\right] + 713308.9\left[\frac{I_{plasma}}{1\,\text{MA}}\right]$$

M = 4.13E6 lbf-in

R = 41.3 inch

$\Theta = s/r$ => .085343 inch/41.3 inch = 0.002066 radians

K2a = T/Θ = 4.13E6 lbf-in/0.002066 radians
K2a = 1.99E9 lbf-in/radians

K2a = 3.48827E7 lbf-in/°

Mark Smith's Global Model Provided Torsional Stiffness's

M = 4.13E6 lbf-in

R = 14 inch

$\Theta = s/r$ => 0.14196 inch/14 inch = 0.01014 radians

$K_{p\,new}$ = T/Θ = 4.13E6 lbf-in/0.01014 radians
$K_{p\,new}$ = 4.073e8 lbf-in/radians

$K_{p\,new}$ = 7.109e6 lbf-in/°

Mark Smith's Global Model Data 6

ANALYSIS RESULTS

For the stiffness parameter values chosen herein and for each of 97 coil current combination cases including the 96 plasma equilibria (specified previously by J. Menard) and a single OH-only +24 kA precharge case, the model's solution was obtained via MATLAB. Once the fixed currents i1 and i2 for a parameter case were numerically found that were used to determine the corresponding internal torque and shear stress profile in the TF centerstack. The resulting shear stress profiles are plotted in Appendix 2.

The maximum peak absolute shear stress over all 97 cases examined was 25.18 MPa, but many cases had almost this large a value of peak absolute shear stress. Inspection of the profiles shows that the OH coil's effect on peak shear stress is far stronger than the combined effects of the other PF coils or the plasma. All cases with peak shear stresses near 25 MPa had the absolute value of OH current at 24 kA, and all cases with smaller absolute values of OH current had correspondingly smaller values of peak shear stress.

WP 1.1.0 NSTX Upgrade Global Model – Model Description, Mesh Generation, and Results NSTXU-CALC-10-01-02 Prepared by Peter Titus, Reviewed by Unassigned, Cognizant Engineer: Peter Titus

4.0 Executive Summary

   The Global model of NSTX Center Stack Upgrade (NSTX-CSU) provides a simulation of the overall behavior of the machine. It provides boundary conditions for local models and sub Models , or allows inclusion of the detailed models of components in the global model. The global model is used to compare with other models. The global model is also used as the model for computing influence coefficients for various parts of the machine.

   In many cases it has been built from from other available model segments – The upper and lower head sections of the vessel model come from H.M. Fan's early vessel models. The cylindrical shell that contains the mid plane ports comes from a vessel model built by Srinivasa Avasarala from the Pro–E model of the vessel. It has been updated with the latest neutral beam port frame. In some instances parts of the global model were exported to be evaluateds in more detail. Multiple scenarios from the NSTX design point are run using the global model. The design points are publised on the web and are maintained by C. Neumeyer. Loads from normal operating current sets are in general much less severe than loads that are based on worst case power supply currents. In order to compare the global model results with some of the local models that have been run, some of the "worst case" currents have been run in the global model. The outer TF reinforcements are an example of this. Results reported in sub paragraphs of section 8 have been used to qualify components, check results and guide the need for further analyses. The outer TF leg reinforcements discussed in section 8.3 and in NSTX calculation number 132-04-00 [4] include some load sets which are based on two severe current sets. These are intended to maximize the out-of-plane loading on the TF outer legs for an up-down symmetric loading and an up-down asymmetric loading that causes large net torques on the outer legs. These two current sets were included in the loading analyzed in the global model. Behavior of the global model and reference [4] is consistent. Section 8.3 discusses these results and adds a qualifiucationn of the bending related bond shear in the TF outer leg. Section 8.1 documents the acceptable stresses in the diaphram plate that replaces the gear tooth torsional connection between the centerstack and the outer umbrella structure. This analysis has been essentially superseded by reference [23].
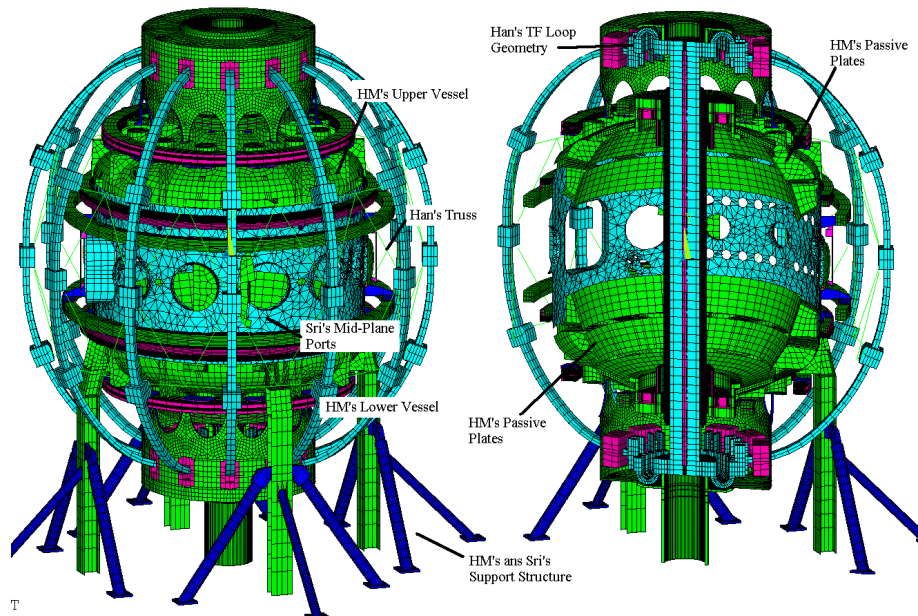
Figure 4.0-1 Global Model Status as of June 22 2009

Section 8.5 provided global displacements to the detailed analysis of the flex joint [7] Section 8.6 has been expanded and split off into another calculation, ref [15]. Section 8.9 similarly profided guidance on global twist in the evaluation of the centerstack OH support details. Section 8.8 shows the stresses and loading

around the I beam column attachments to the vessel and points to the need to evaluate the weld details of this connection.

The global model has been extensively used to investigate various alternative designs to support the out-of-plane TF loads. In October of 2010, the enlargement of the vacuum pumping duct to add the Thompson scattering diagnostic increased the vessel stresses because there was insufficient metal left between the neutral beam ports and the larger Thompson scattering port. Vessel reinforcements were investigated [25] . Also studied was an option which connected a vertically extended umbrella structure to the cell walls via long struts. The global model was used to study this and it confirmed the virtues claimed by M. Smith and T. Willard - but the hardware additions proved much more expensive that the vessel reinforcements.
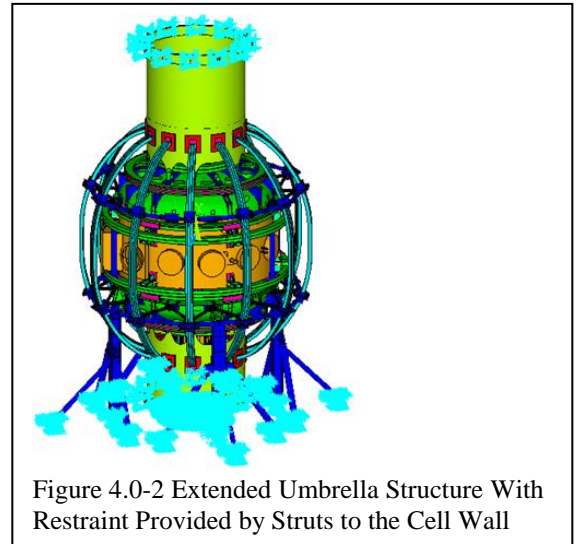
Figure 4.0-2 Extended Umbrella Structure With Restraint Provided by Struts to the Cell Wall

Run # 29 with Bent Lower Spoked Lid and "Vee" Pipe Truss Pedestal - Colored by Real Constants
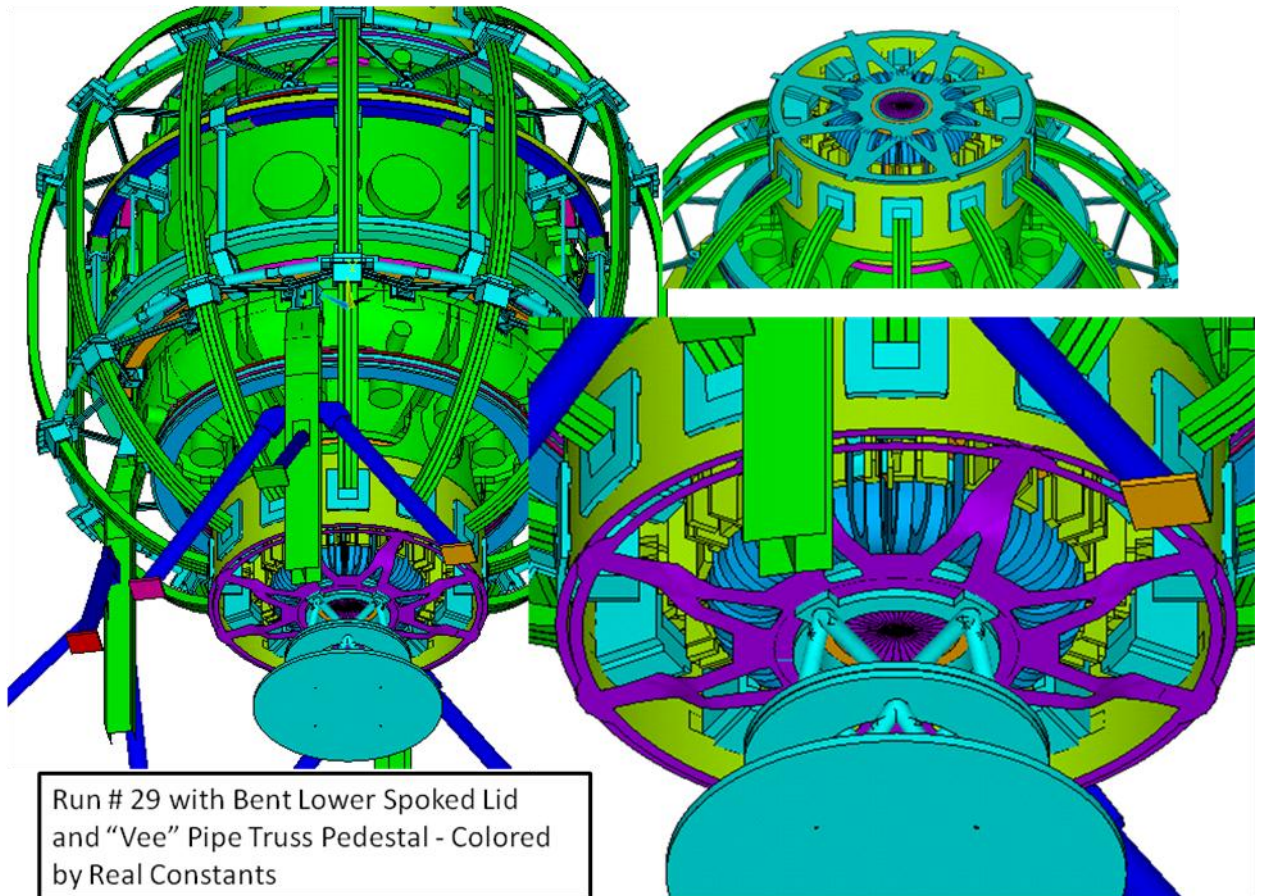
Figure 4.0-3 Global Model Status as of May 2011

The global model described in this calculation has been used to analyze a number of components and loads that are considered in separate calculations. In some instances the global model provides some of the boundary conditions. In others, like the seismic analysis, the global model is the same as the seismic analysis model. A list of calculations in which the global model is directly used follows:

NSTX Upgrade Seismic Analysis NSTXU-CALC-10-02-00 Rev 0 February 9 2011 Prepared By: Peter Titus, Reference [18]

TF Inner Leg Torsional Shear, Including Input to the DCPS, P. H. Titus NSTXU-CALC-132-07-00 Reference [15]

Umbrella Reinforcement Details, by P. Titus and H. Zhang NSTXU CALC 12-07-00, ref [19]

Analysis of Existing & Upgrade PF4/5 Coils & Supports – With Alternating Columns, NSTXU-CALC-12-05-00, Prepared By: Peter Titus, Reviewed by Irv Zatz, Cognizant Engineer: Mark Smith WBS 1.1.2. PF5 stress influence coefficients are computed by applying load files derived from using unit currents.

Lid/Spoke Assembly, Upper & Lower NSTX-CALC-12-08-00 Rev 0 May 2011 Prepared by: Peter Titus, Reference [23] In this calculation the global model is used to compare torsional load distributions for different spoked lid designs.

Analysis of the NSTX Upgrade Centerstack Support Pedestal NSTXU-CALC-12-09-00 May 2011 Prepared By: Peter Titus Reference [24] In this calculation the global model is used to compare torsional load distributions for different pedestal designs.

Calculations which utilize output from the global model as boundary conditons are:

Bellows Qualification Calc # NSTXU CALC 133-10-00, by Peter Rogoff', Reference [13] in which the global model is used to quantify the torsional moment applied on the bellows from the TF out-of plane loading

TF Flex Joint and TF Bundle Stub, T. Willard, NSTX-CALC-132-06-00, reference [7]. The differential toroidal displacements imposed on the inner and outer radius of the TF flex model come from the global model.

Structural Calculation of the TF Flag Key, NSTXU-CALC-132-08-00 , A. Zolfaghari, Reference [21] . The load at the connection of the TF flags to the upper crown and lid are derived from the global model simulations, and similar loads at the connections at the bottom flags of the TF central column are also sized using loads from the global model.

The global model uses separate model "pieces" which are brought into ANSYS as text listings similar to a CDWRITE or *.anf ANSYS file, using the /INPUT command. These segments are created in a separate program. The magnet components are meshed and the loading is computed from a model with only the magnets. Each piece is brought into ANSYS with a NUMOFF command. The last group of elements entered into the ANSYS program is the magnet model. Lorentz forces are computed in the same program used to mesh the structural components. This program is described in section 6.2. Load files are also read into ANSYS in the solution phase. This approach allows computation of loading and re-use of the load files - as long as the magnet model does not change. Structural model "pieces" may be modified and the problem re-run without alteration of the load files. This is a practical way to limit run times for the multiple current sets required by the NSTX GRD.

2.0 Executive Summary:

NSTX is structurally adequate to survive a prescribed seismic event, with minor modifications to improve the shear load capability of the angled brace concrete anchors. Most components of NSTX are lightly loaded during an earthquake.

For the PDR, a response spectra modal analysis has been performed. At the PDR, only a static analysis of the NSTX global model had been done. This is conservative with respect to the original NSTX seismic analysis which was a static overturning analysis. In the PDR analysis of the global model, .5 g's lateral were applied vs. the original .135g requirement. The high acceleration was partially intended to address unknown masses (essentially diagnostics) not included in the global model. The appropriateness of this assumption is born out by the global reactions, tabulated below which show a more rigorous response spectra analysis is more severe than a .5g static evaluation. Coil Stresses are small due to a seismic event. These can be ignored in the evaluation of coil stresses.

Global Model Used for Seismic Analysis
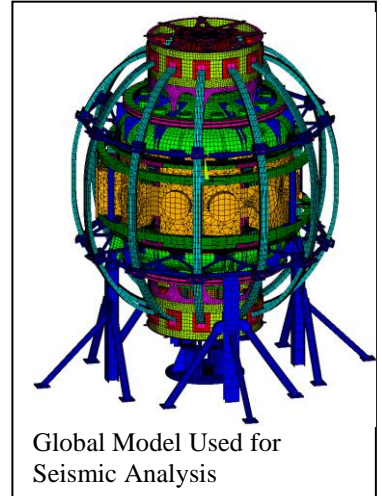
Analysis results show the outboard braces as limiting. A shear design capacity of 13000 lbs and a tensile capacity of 9000lbs are recommended

Global Reaction Summations

	FX Sum (N)	FY Sum (vert)(N)	Fz
Static Analysis	.3581e6 (.5g)	.715e6	0
Modal Analysis	.916e6	2.42e6	.913e6

Hilti Drop-In
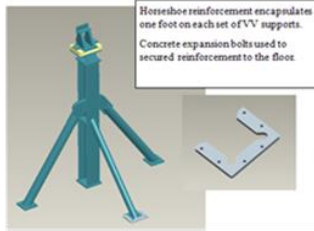
Hilti HDI Concrete Flush Anchor Tests

Horseshoe reinforcement encapsulates one foot on each set of VV supports.
Concrete expansion bolts used to secured reinforcement to the floor.

	2000 psi	Concrete	4000 psi	Concrete	6000 psi	Concrete
Anchor Size	Tension	Shear	Tension	Shear	Tension	Shear
HDI – ¼	1904	1738	2251	1781	3075	3050
HDI – 3/8	3174	3970	4942	4225	5650	5900
HDI – 1/2	3997	5873	6751	6224	10200	9350
HDI – 5/8	5549	8883	9696	12205	10400	13600
HDI – 3/4	8857	15195	16034	17609	16400	21200

Allowable Design Loads are ¼ these Values, i.e. a F.S. of 4 is recommended

A shear design capacity of 13000 lbs and a tensile capacity of 9000lbs is recommended.
For shear, use 13000/6224*4 = 8 ½ " Hiltis, For Tension use 9000/6751*4=5 ½ "Hilties
13 ½ " Hiltis Total per Leg
-or For shear use 13000/9696*4 = 4 5/8 Hiltis, for Tension use 4 5/8 Hiltis
Or 8 5/8 Hilti's Total per Leg
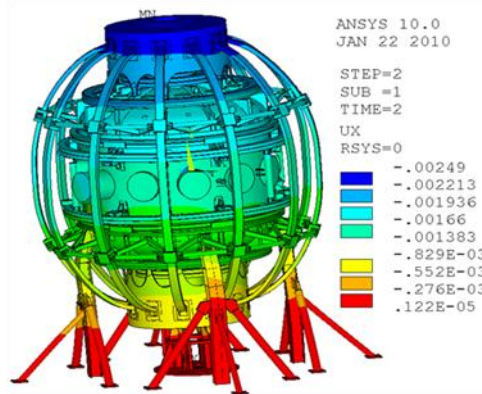
.5g + deadweight Static Analysis
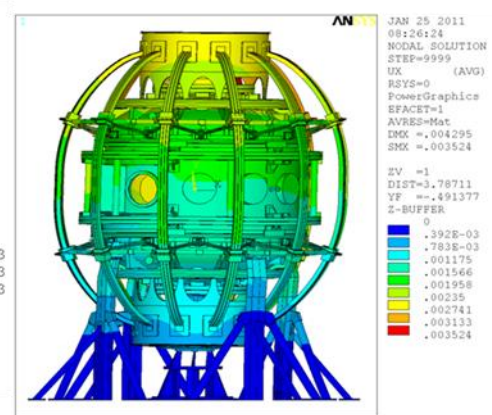
Response Spectra Modal Analysis

Two types of analysis were performed; both based on the global analysis model - Ref [8]

MODE	FREQUENCY	DAMPING	SV	MODE COEF.
1	7.552	0.0000	7.0560	-0.2180
2	7.737	0.0000	7.0560	-0.5650
3	7.892	0.0000	7.0560	0.4051
4	19.11	0.0000	7.0560	0.4360E-01
5	19.46	0.0000	7.0560	-0.1304E-01
6	23.89	0.0000	6.3763	-0.5626E-02
7	23.94	0.0000	6.3687	-0.3525E-02
8	26.01	0.0000	6.0761	0.1780E-02
11	31.03	0.0000	5.4951	0.5901E-03
13	32.82	0.0000	5.3223	0.1096E-02

Horseshoe reinforcement encapsulates one foot on each set of VV supports.
Concrete expansion bolts used to secured reinforcement to the floor.
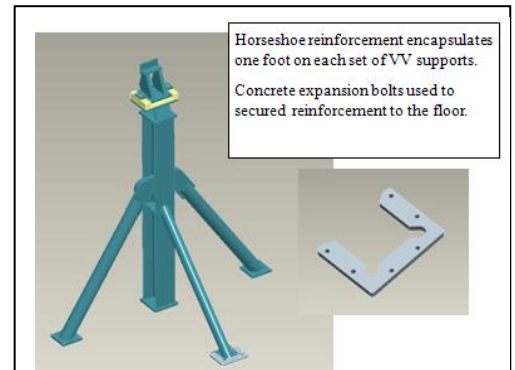
Horseshoe bracing needed at four of the Brace Feet.

WBS 1.1.1 Plasma Facing Components,
Global Thermal Analysis of Center Stack – Heat Balance NSTX-CALC-11-01-00
Prepared By: Art Brooks**, Reviewed by:** TBD**, Cognizant Engineer:** Jim Chrzanowski

Executive Summary:

An analysis was done to assess the thermal response of the Center Stack (CS) during normal operation. The resulting temperature distributions and heat flows to active and passive cooling systems are presented. These results will feed further qualification analysis of associated components and systems.

The cooled sections at the inboard diverter are needed to protect the neighboring coils as well as limiting temperatures in the CS casing. Earlier analysis recommended removing the Grafoil under the tiles because the enhanced heat flow would exceed the capacity of the coolant tubes leading to excessive heating of the water. Since then the cooling capacity has been increased by doubling the number of cooling circuits and the analysis refined to show boiling of the water can be avoided with modest back pressure in the water system.

For the un-cooled portion of the CS casing Grafoil has less of an impact. With or without Grafoil, the CS casing ratchets up to roughly the same temperature. The time to reach the max temperature however is shorter with the Grafoil. Its use should be based on other considerations.

The results assumed the PP, VV and OD were actively cooled with surface temperatures staying below 100C. If the temperatures of those components are allowed to increase to 200C, there is only a modest increase in IBD temperature (~1 C) and the power to the cooling system. The CS casing is more sensitive since it is only cooled by radiation. Its temperature increases ~50 C from 250 C to 300 C.

The figures below show the fully ratcheted temperature distribution in the VV, PP and CS, including the max temperature which occurs in the IBDhs. As seen in the figure to the right, the IBDhs, labeled Tmax, shows very little thermal ratcheting with the Grafoil and enhanced cooling while still providing adequate protection to the coils adjacent to the IBD and bellows.
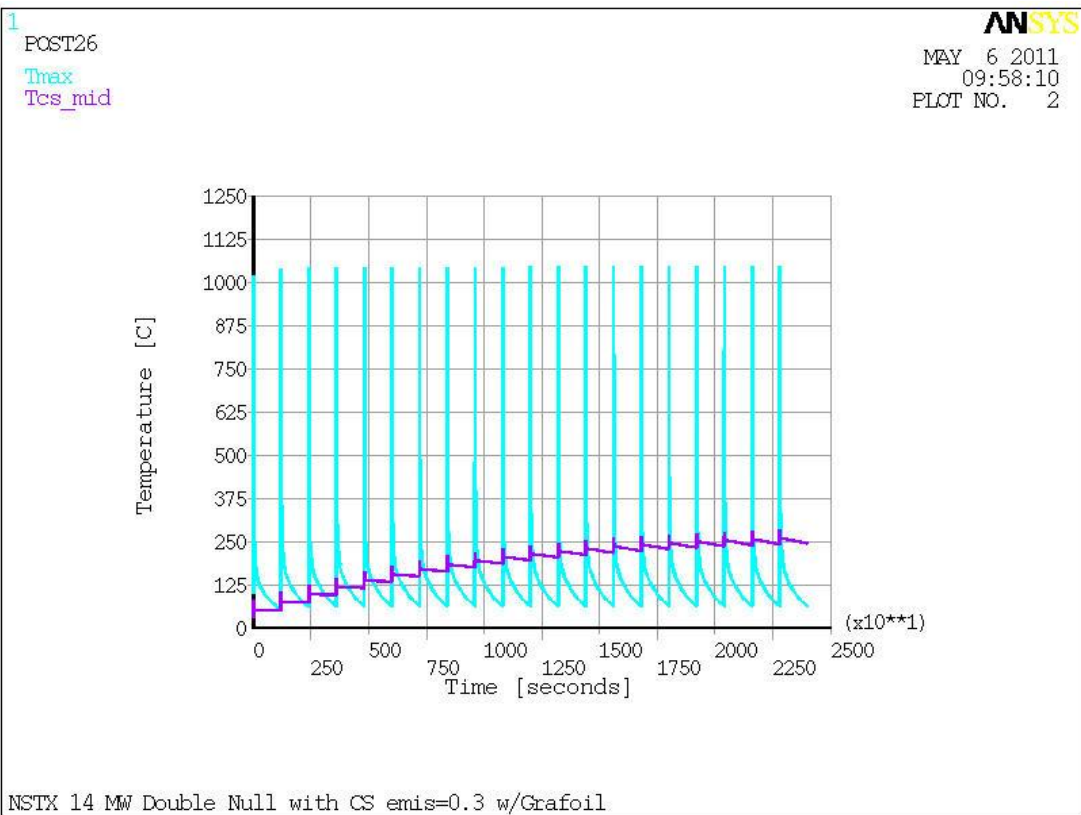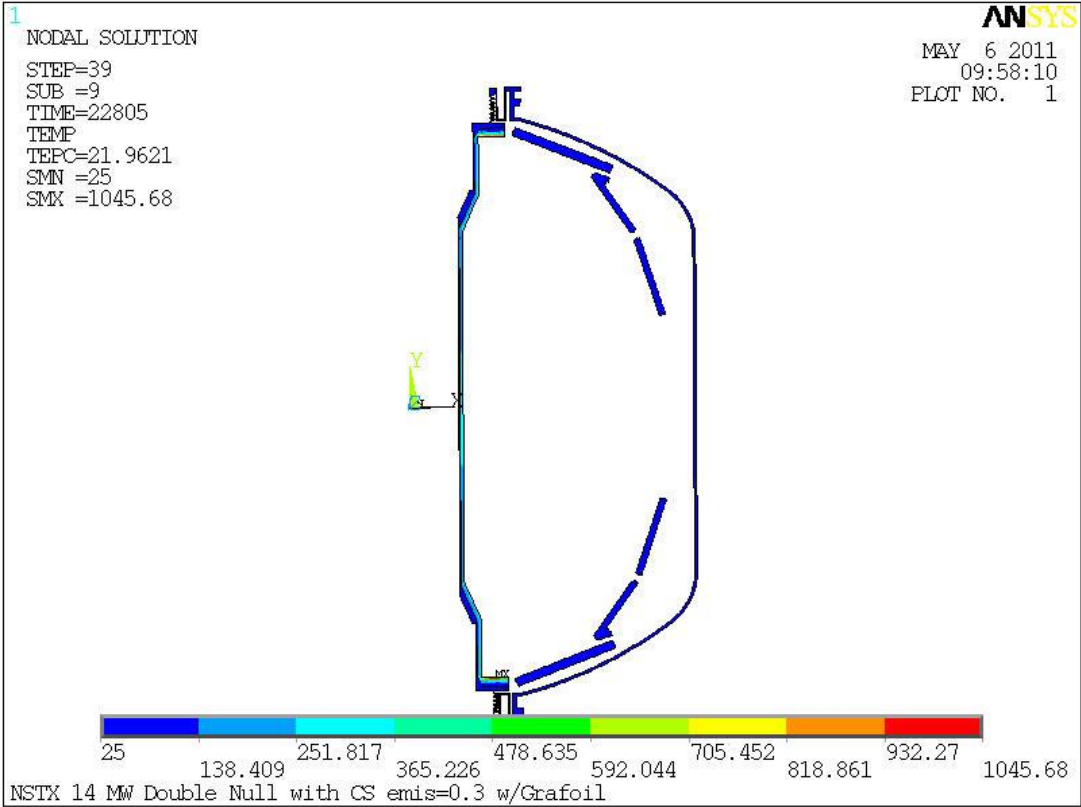
NSTX 14 MW Double Null with CS emis=0.3 w/Grafoil

NSTX 14 MW Double Null with CS emis=0.3 w/Grafoil

Overview

The purpose of this script is to serve as a basic analysis for the general geometry of the tiles to be used for the NSTX-CSU. It is by no means a thorough analysis of the tile geometry or mounting system and is therefore subject to error. It is used primarily to find the worst case given a general scenario (i.e., over-constraining a tile and finding the worst case stresses that may develop due to thermal expansion, eddy currents, and halo currents). It may also be used to find the locations on a tile that may present a problem in a given situation. The script will perform eddy current, halo current and thermal analyses on the tile and plot the von Mises stress for the combined loads upon completion.
The tile geometry that is used in this script is a basic block with a T-slot running the length of the tile, centered horizontally. Several sample images (with dimension labels) are below.
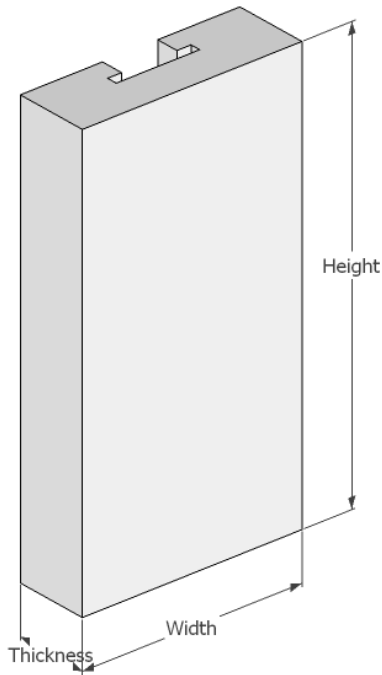
Figure 1. *General overview of the tile geometry including thickness, width, and height dimensions.*
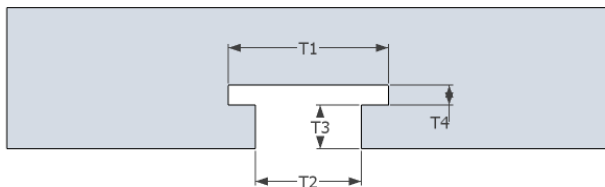
Figure 2. *Top view of the tile geometry including t1, t2, t3, and t4 dimensions, which are used to size the T-slot.*

The geometry used in the ANSYS model is susceptible to high corner stresses, which can generally be ignored as the true tile geometry will include chamfers and fillets to avoid these stresses. This is assumed based on the way in which the stresses appear to develop and has been demonstrated in other models where similar stresses have emerged. The stresses are calculated by reading in forces from each of the individual analysis types and specifying constraints.

How to Use This Script

There are several files that are required to be in the working directory in order to successfully run this script: 'BasicTile.txt', 'input.txt', 'constraints.txt', and 'b_mac.mac'. 'BasicTile.txt' is the actual script. It reads table data from 'input.txt' and the constraint information from 'constraints.txt'. If these files are missing or improperly formatted, the script may generate unexpected results. To change the input parameters used for the tile analysis, the user simply needs to change the numbers that are stored in the second column of 'input.txt'. The first column is the indexing column and never needs to be modified unless the structure of 'BasicTile.txt' is changed. There are eighteen rows and two columns. The variable that is stored in each row is below. There is also a comment at the bottom of the file describing each of the variables.

Index	Variable	Index	Variable
1	Material type	10	Horizontal Bdot (in T/s)
2	Tile width (in inches)	11	Vertical Bdot (in T/s)
3	Tile height (in inches)	12	Normal Bdot (in T/s)
4	Tile Thickness (in inches)	13	Horizontal B (in Tesla)
5	T1 (in inches)	14	Vertical B (in Tesla)
6	T2 (in inches)	15	Normal B(in Tesla)
7	T3 (in inches)	16	Horizontal halo current density (in A/m^2)
8	T4 (in inches)	17	Vertical halo current density (in A/m^2)
9	Heat flux (in W/m^2)	18	Normal halo current density (in A/m^2)

There are eight material types to choose from. They are specified by their index numbers which are listed below.

Index number	Material
1	ATJ Graphite
2	Poco AXF-5Q Graphite
3	Sigrabond CFC 1501G (2D weave)
4	Isostatic Graphite R*510 (unknown source)
5	Annealed Molybdenum
6	Annealed Tungsten
7	Thermagard (2D weave CFC)
8	Meggagard (3D weave CFC)

The 'constraints.txt' file is constructed in an entirely different manner. The user must input the commands to be used for the physical constraints on the tile. The reason that a more user-friendly approach wasn't developed is that the results are very sensitive to the constraints, so the constraints may need to be finely modified to achieve a reasonable result. For most analyses, the tile is over-constrained in order to find the worst case stresses. High stresses at locations of nodal constraints are generally ignored. The high stresses develop because a small number of nodes are constrained to represent the way in which a piece of hardware (such as a T-bar or pin) will hold the tile. The small numbers of nodes that are chosen develop unrealistically high stresses. Calculating the bearing stress for the true geometry based on the reaction forces from the analysis can tell you whether or not the assumption is correct in a particular case. The reaction force on a group of constrained nodes is independent (at least for small scale changes) of the number of nodes chosen.

After the entire script has run once, the stress solution may be repeatedly run until you are confident with the results. To do this, modify the 'constraints.txt' file, clear all of the current constraints, use the command '/input,constraints,txt', and then use the command 'solve'. This will simply re-run the solution using different physical constraints.

The force types used may also be selected by deleting all forces and body forces then loading in the desired forces using the 'ldread' command.

'b_mac.mac' is simply used to impose a uniform vector potential on all of the selected

WBS 1.1.1 Plasma Facing Components, Stress Analysis of Tiles
NSTXU-CALC-11-03-00
Prepared By: Art Brooks**, Reviewed by:** TBD**, Cognizant Engineer:** Kelsey Tresemer

Executive Summary:

The Center Stack Tiles for the NSTX-CSU program are shown to be capable of withstanding the original GRD heat flux requirements using the prescribed ATJ graphite. The tile mounting scheme, consisting of T-bar supports for the CS Angle Section (CSAS) Tiles and the Inboard Divertor Horizontal (IBDhs) and Vertical (IBDvs) Tiles, and the tray support for the Center Stack First Wall (CSFW) Tiles is adequate to support the tiles against the anticipated thermal, eddy current and halo current loads with acceptable bolt loads.

This is premised on the poloidal flowing halo current's interaction with the TF field always results in tile forces which are away from the plasma, regardless of the plasma current and TF field directions as observed in NSTX operation. While the interaction of toroidal flowing halo currents, which will be in both directions due to the Toroidal Peaking, with the PF field produce forces both toward and away from the plasma, they are shown to be small relative to the poloidal current forces and result in net forces away from the plasma. If net forces were reversed, halo currents from a 2 MA plasma may not be tolerable due to high tensile stresses in the ATJ.

The analysis shows that the inclusion of Grafoil under the CSAS, IBDvs and IBDhs combined with the active cooling will significantly limit the thermal ratcheting of the tiles whether Li coated (with assumed emissivity of 0.3) or uncoated (with assumed emissivity of 0.7). The active cooling also offers adequate protection of the neighboring PF and OH coils and reduces the heating of the CS Casing. The flow rate and back pressure are high enough to avoid boiling of the water.

The Grafoil is shown to be structural compliant to allow relatively free thermal expansion of the tiles provided the bolts are only lightly preloaded and do not over compress the Grafoil.

IBhs and IBDvs (top) and CSAS and CSFW (bot) Thermal and EM Stresses are within acceptable limits for ATJ graphite.
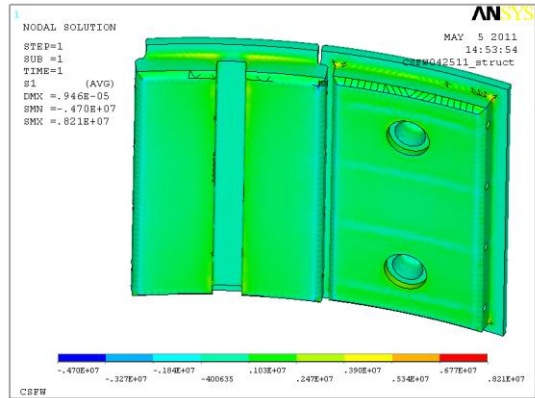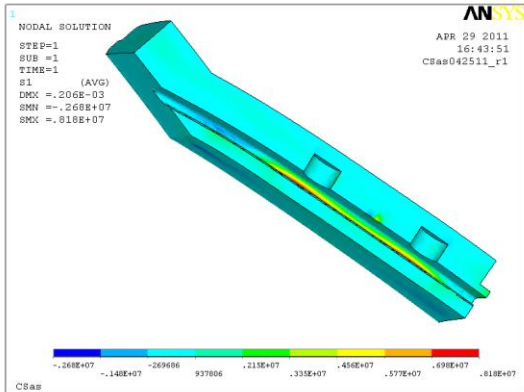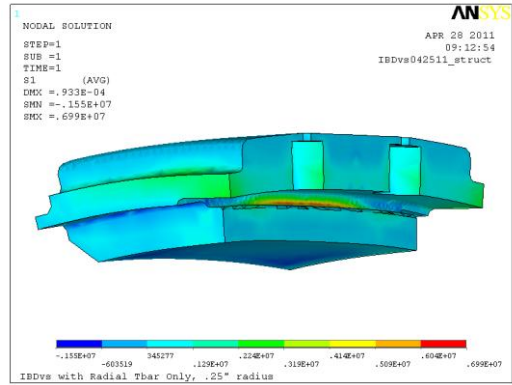
WBS 1.1.1 Disruption Analysis of Passive Plates, Vacuum Vessel & Components
NSTXU-CALC-12-01-01 Rev 1 April, 2011
Prepared By: Peter Titus, **Contributing Authors**: A. Brooks, Srinivas Avasarala,
J. Boales **Reviewed By:** Yu Hu Zhai, **Cognizant Engineer:** Peter Titus

4.0 Executive Summary

The objective of this analysis is to estimate and
assess the stresses in the vacuum vessel, selected
internal components, and passive plates caused by
the plasma disruption. Bake-out stresses on the
passive plates have been considered in the original
design and are addressed in calculation #NSTX-
CALC-11-6. [1]

Mid-plane disruptions and quenches are
manageable. For these events, the loads required
some modest upgrades of the mounting hardware.
The slow VDE's may be more severe for the
secondary passive plate. These appear to be
generating large counter currents in the plate as the
plasma approaches it. - as would be expected from
passive plates.

Development of this procedure began in the
Summer of 2009 and was worked on by Srinivas
Avasarala, Ron Hatcher, Art Brooks, Larry Bryant,
and Joseph Boales. Early test runs are included in
Section 7 as illustrations of the procedure.

The Vector Potential solution for a 2D
axisymmetric simulation of a disruption in OPERA
is imposed on the 3-D model in ANSYS to obtain
the eddy currents and Lorentz forces. A static and
dynamic stress pass is then run and the stresses are
computed. A number of other calculations address

Figure 4.0-1 View of Passive Plates and
Lower Divertor During an Outage. Divertor
Tiles have been removed an a protective
cover is on the secondary passive plate

components not covered in this calculation. Some components like the vessel port region,
and the bellows, are considered in this calculation, and in greater depth in other
calculations. The divertor tiles, diagnostic shutters are some of the components
addressed in other calculations. The primary purpose of these calculations is to address
the passive plates. Other components have been added because the procedures developed
for the passive plates are useful for many components.

Vector potentials obtained from OPERA are arranged in 80x80 tabular forms so that they
can be fed into ANSYS. In the early analyses, 11 tables were considered for the study
and these tables were spaced 0.5 ms apart. Macros are developed that read these values

into ANSYS. The meshes in OPERA and ANSYS are dissimilar, but since ANSYS interpolates the tables between two adjacent indices, proper indexing of the coordinates yields a reasonable approximation of the Vector Potentials. The element type used was SOLID 97 and the material properties used are that of Stainless Steel except for the passive plates which are made up of Copper Chrome Zircaloy allow. This model is then solved for eddy currents and Lorentz forces.

The model is then converted into a structural model by switching the SOLID 97s into SOLID 45s. For the test cases, eleven load steps, 5ms apart are written for the stress pass. Later analyses use up to 45 steps. Forces are read from the earlier E-mag results by using LDREAD command and both the static and dynamic analyses are performed. A 0.5% damping factor is used in the dynamic run.
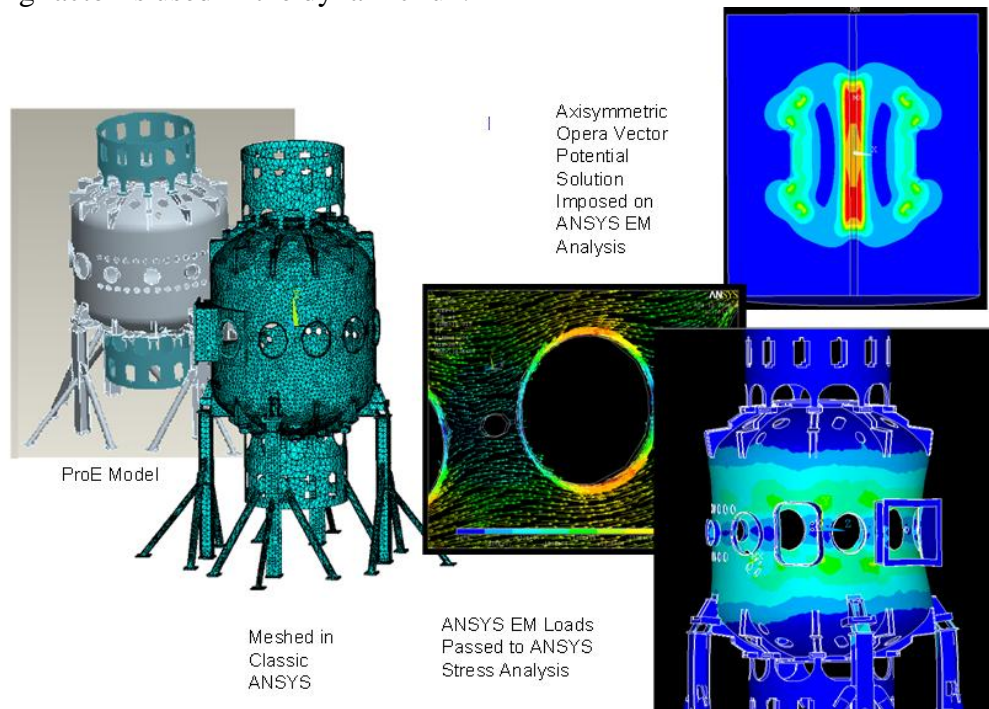
The procedure has been multiply checked. In section 7 of this calculation the consistency with the OPERA analysis was checked. Poloidal and toroidal field plots were checked. In section 7.6.1, results were compared with disruption simulations done only in ANSYS for the HHFW antenna. Results for the mid plane disruption were similar. In section 9.2.2 the total currents in the major components of the toroidal elements that would inductively pick up the plasma current, were summed. These included the vessel, the passive plates and the Centerstack casing. They approximately add to the plasma current. This should be the case for inductively coupled closely nested current loops.

Stress Summary (Dynamic Unless Otherwise Noted)

Component	Section	Damp	Disruption	Stress	Allowable
Vessel At Port Ligaments Near Bay L NB and Thom		.5%	Mid Plane Disruption	40 MPa	40 MPa*

Scattering Ports					
Vessel Support Column Intersection with Vessel		.5%	Mid Plane Disruption	40 MPa	40 MPa*
Secondary Passive Plate		.5%	Mid Plane Disruption	90 MPa	171 MPa
Secondary Passive Plate			Fast Quench Plasma 4	180 MPa	171 MPa
Secondary Passive Plate		.5%	P1-P5 Slow	360 MPa	***
Tresca from Shear Stress in Passive Plate Counter-bore	9.5	.5%	Fast Quench Plasma 4	232 MPa	171 MPa
Centerstack Casing (No Halo)	11.2	.5%	Mid Plane Disruption	1 MPa	1 MPa*
TAE Antenna Moly Shield	14.0	.5%	Mid-Plane Disruption	200	600 Yield

* These are values passed on to other calculations to be added to normal operational loads. Comparison with the allowable needs to be performed in these calculations.

*** Analysis of the response to the slow VDE is on-going. The passive plates may require more elaborate reinforcement .
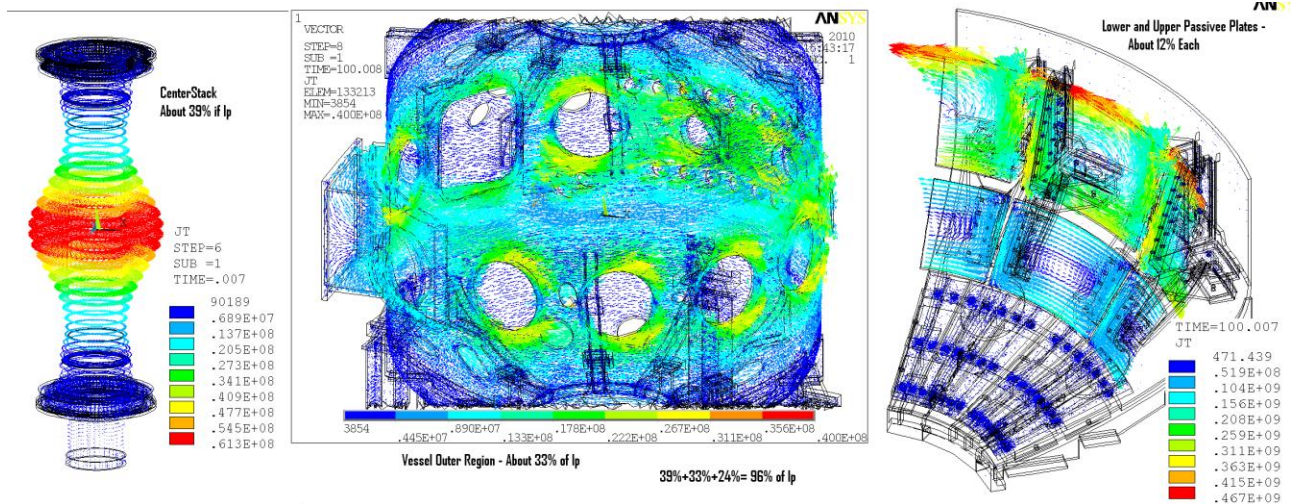
As of May 2011, the current distributions in the major components of the tokamak have been checked for the mid-plane disruption and compared with the OPERA 2D results. Yuhu Zhai has also checked the currents using an OPERA 3D model. Tom Willard ran a mid plane disruption in MAXWELL.   All the analyses have similar currents.

Opera 2D Electromagnetic Analysis NSTXU-CALC-12-03-00
Prepared by: Ron Hatcher, **Reviewed by:** Art Brooks**, Cognizant Engineer:** Peter Titus

The NSTX CSU device is modeled as a set of axisymmetric (2D) conducting elements in the Opera electromagnetic design and analysis package. The goal of the analysis is to determine magnetic fields and conducting structure currents and forces resulting from simulated axisymmetric plasma current quenches and displacement events. The project identified a set of twenty two (22) scenarios using five plasmas to cover the expected experimental behavior that are enumerated in the memo.

In the simulations, the plasma is modeled as a driven conductor with zero conductivity. The coils, depending on the analysis, are modeled with or without current (background fields) and with and without conductivity (induced voltage effects). The remaining conducting structures are modeled with conductivities modified to approximate non-axisymmetric behavior. Two types of simulations are described: 1) simulations that directly determine Lorentz forces on conducting elements; and 2) simulation that save the vector potential solution for export and use as background fields for smaller more focused 3D simulations.
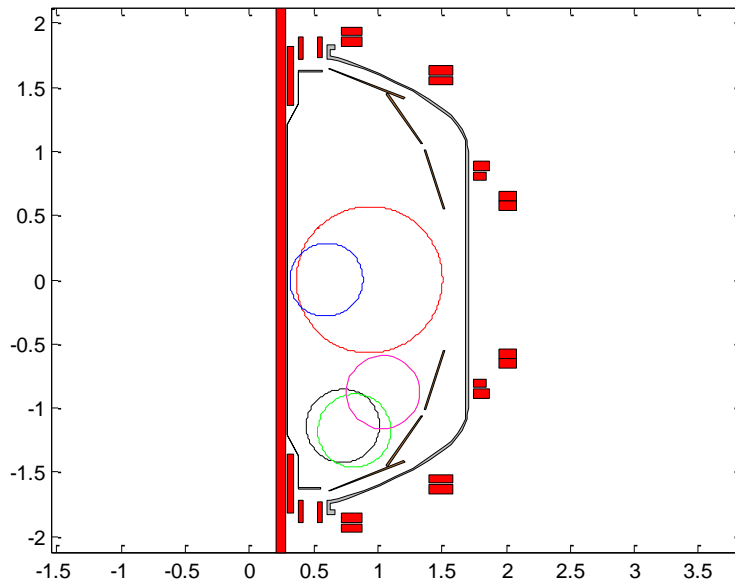
Figure 3 NSTX CSU axisymmetric model including plasma model outlines
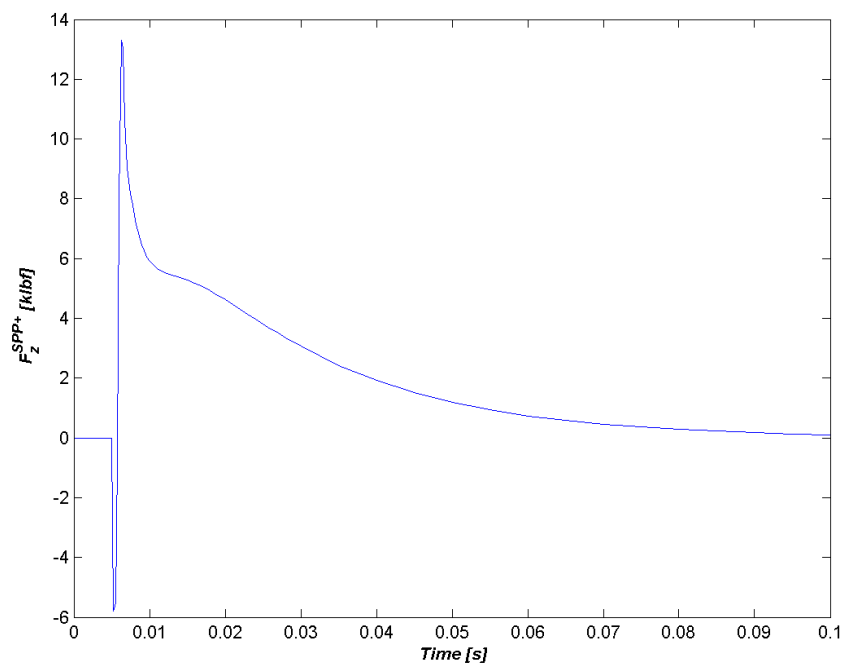
**Figure 4 Vertical force on the upper secondary plasma plate
during a mid-plane plasma quench (disruption) simulation**

WBS 1.1.2 PF2 and PF3 Coils and Support Analysis
NSTXU-CALC-12-04-00
Rev0, March 2011 Prepared By: Peter Titus Reviewed By: Irv Zatz, Cognizant Engineer: Mark Smith

3.0 Executive Summary:

Stresses in the coils are relatively low. Hoop stress due to the radial loading is small. Stresses are predominantly driven by coil bending due to the vertical load and the spans created by the discrete supports. Coil stiffness is sufficient to transmit only a small portion of the bending moments to the supports and clamps. Coils and support hardware meet the requirements of the NSTX structural criteria with the exception that the 1/8 inch fillet welds used on the PF3 support are still judged unacceptable with respect to the AWS, AISC and ASME criteria for min weld size for given plate thicknesses. The Stainless section of the AWS code is under review to determine if the small welds are acceptable for stainless steel.

PF2 and 3 are supported on sliding plate supports that are lubricated with Magnaplate. The sliding surfaces are primarily intended for the bake-out differential thermal growth of the vessel. Hoop strains produce minimal radial expansion. For PF2 and 3, bolt stresses for the net vertical loading in the coils are being checked to qualify the coil supports and coil stresses (vertical meaning upward for the upper PF2/3 and downward for the lower PF2/3). This is based on the expectation that there is a large margin in the hoop stresses in the coils, and centering loads are taken by compressive loads into the support plates and ribs,- and that the centering loads produce low stresses. Traditionally NSTX has not checked coil hoop stresses in the existing coil protection system. Only vertical loading has been addressed. Part of the purpose of this calculation is to re-visit this assumption.
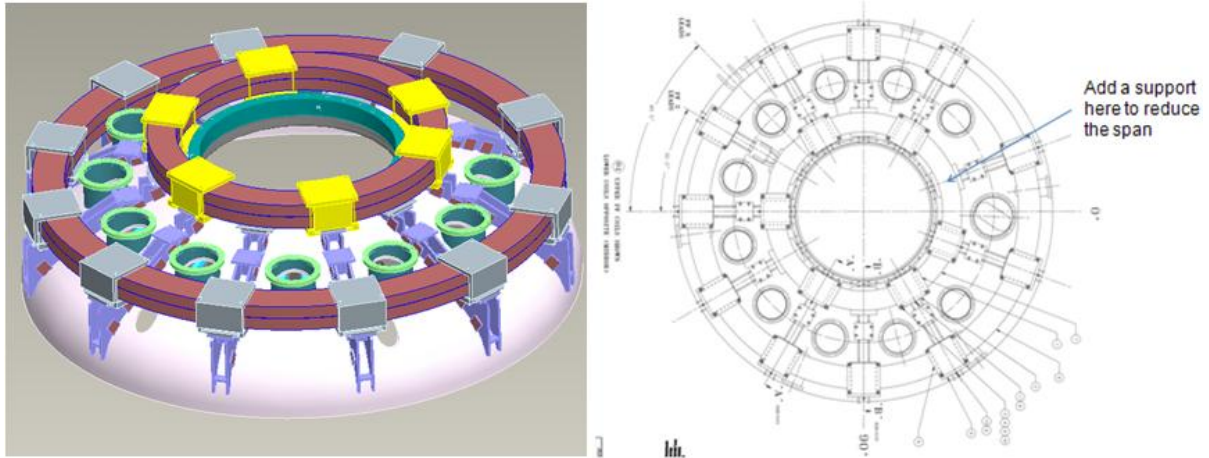
Current (2010) locations of the PF2 supports, and the proposed location of the seventh support

Existing PF 2 Supports - PF2 Supports are in Yellow

Low hoop and support stresses have been shown with a three dimensional model of the coils, vessel domes and ribs. The coil pancakes and individual conductors and insulation are modeled. Other structures besides the PF2/3 supports are not included in order to isolate the effects of the PF2 and 3 loads. Representative scenarios are selected for the Lorentz load calculation. Coil and vessel stresses are very low, justifying the limited stress and bolt load checks recommended for the DCPS.

PF2 is currently supported at 6 places with brackets that use four 1/2 inch bolts or studs to clamp the coil. For the worst case upward vertical load, the bolt P/A stress is 47150/6/4/.1416=13,830 psi for the 96 scenario max tensile load (see Section 5 for a Design Point Load Summary). This is true if evenly distributed at 6 locations, but it is not evenly distributed. An additional support has been recommended to help with the uniformity of loading, but even with the extra support, loads vary around the perimeter of the coil

Currently there is one span that is about 90 degrees. This would distribute the bolt loads more like Fvert/4/4 rather than Fvert/6/4. There would be some rotation as well that might change the loads in the bolt pattern at the clamp. This has been considered in a 360 degree model of the coil and support system. The non-uniform support distribution could probably be qualified to the 96 scenario loading, but would have no margin for faulted loads or any headroom for the DCPS. Dividing the vertical load from the design point spreadsheet by the total stress area of the bolts = 47456/4/4/.1416 = 20ksi, which is OK for standard bolts. An analysis of the toroidal distribution of loading on one side of the clamp vs. the other (i.e. the rotation effect) was carried out in section 7.5. The toroidal variation in loading was found to be 105 lbs.

If the 7th support is added then one side looks like Fvert/6/4 and the other side looks like Fvert/8/4. The actual non-uniformity in support distribution was analyzed for one of the scenarios and the effective number of supports is 5.32 supports:

For all of PF2, (Old Scenario 12)
the net vertical loading is:
FX= 11350 N
Fy=-13 N
Fz=376330 N

The peak Vertical Load in the PF
supports is 70719 N
The effective number of supports is
376330/70719 = 5.32
while there are actually 7 supports

FX 3423
Fy 2003
Fz 36515

FX 2638
Fy -2244
Fz 33282

FX 805
Fy -6869
Fz 61861

FX 1737
Fy 5271
Fz 48656

Scenario 12
Reactions are in the
Cylindrical System 5
(Z up)

MN
MX

FX 50
Fy 3593
Fz 70719

FX 688
Fy -759
Fz 65329

FX 2009
Fy -1008
Fz 59970
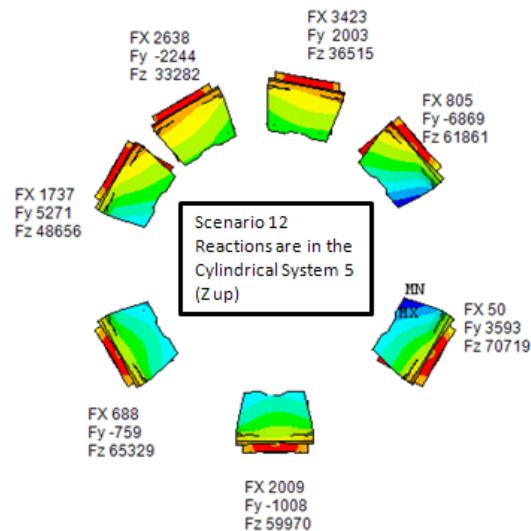
The model with the actual support arrangement is discussed in section 6.2. Bolt stress is then 47456/5.32/4/.1416 = 16ksi. This is within the capacity of many studs, but the studs are a generic 316. Replacing the studs with a known material with a sufficient yield to allow 16 ksi or above is recommended. The bolts should be preloaded above this level to avoid any significant cycling.

The PF2 weld drawing shows 3/16 inch fillets as under the PF2 support plate. With a weld efficiency of .7 the allowable for a fillet is 14ksi, or 96 MPa. The plate is 9 inches long. There are four 3/16 inch fillets for a total weld area of 4*9*3/16*.707 = 4.77 square inches per pad. There are effectively 5.23 pads; this would produce a capacity of 5.23 * 4.77* 14,000 = 450,000 lbs. This would even satisfy the worst case power supply loading.

PF3 support pads are also distributed non-uniformly. For the same scenario 12 used for PF2, the net vertical load is 16103N. The maximum individual support load is 1782 N and the effective number of supports is 9, while there are actually 11 supports PF3 is supported with brackets that use 4 1/2 inch bolts or studs to clamp the coil. The bolt P/A stress is 98989/9/4/.1416=19418psi

	Old Scenario 12	**Charlie's Latest Max Load**
PF2 Net Vertical Load lbs Old Scenario 12	84600;	-51374 Lbs (Section 5.5)
PF2 Coil Stress	31.8MPa	19.3 MPa
PF2Insulation Shear	5 MPa	3 MPa
PF3 Net Vertical Load Old Scenario 13	-133009 (Section 6.5)	-138527(Section 5.5)
PF3 Coil Stress	9 MPa	9.5 MPa
PF2 Insulation Shear	4.5 (conservatively assumed 1/2 of Tresca)	5 MPa

Model with 6 Fold Cyclic Symmetry

NODAL SOLUTION

STEP=2
SUB =6
TIME=2
/EXPANDED
U2
R.SY
DMX
SMN
SMX

Vertical Displacement
Dscale,1,500

ANSYS

| -.779E-04 | -.604E-04 | -.429E-04 | -.254E-04 | -.786E-05 |
| -.692E-04 | -.516E-04 | -.341E-04 | -.166E-04 | .895E-06 |

Scenario 12 Mu=0.2

NODAL SOLUTION

STEP=2
SUB =6
TIME=2
/EXPANDED
SINT   (AVG)
DMX =.987E-04
SMN =199948
SMX =.128E+08

Coil Copper Tresca
With Narrower /Contour

ANSYS

MAR 9 2011
11:46:15

| 0 | .200E+07 | .400E+07 | .600E+07 | .800E+07 |
| .100E+07 | .300E+07 | .500E+07 | .700E+07 | .900E+07 |

Scenario 12 Mu=0.2

WBS 1.1.2 Analysis of Existing & Upgrade PF4/5 Coils & Supports – With Alternating Columns, NSTXU-CALC-12-05-00,
Prepared By: Peter Titus, **Reviewed by** Irv Zatz, **Cognizant Engineer:** Mark Smith

Executive Summary:

The design of the outer PF 4/5 supports has gone through a number of iterations. Initially only 6 support points were proposed (twelve including uppers and lowers). The existing support brackets (Figure 3.0-2) were to be bypassed and an additional set of six stronger columns were to be added. This left six strong support points that could react the large attractive loads between PF4/5 upper and PF4/5 lower. If the coils could handle the spans created by the six support points, this option was thought to be attractive because the vessel shell would be off-loaded.

Figure 3.0-1 FDR PF4/5 Supports

The PF5 insulation system is a mylar wrapped fusifab epoxy system. Because of the poor bonding of the mylar to epoxy and to the copper conductors, twelve supports were necessary to reduce the spans and resulting bending stress. Stresses in PF4 and 5 have been calculated in a detailed model of the vessel shell, support hardware, and winding pack. In order to assess the stress in the coils, stress analysis of the winding pack is used in concert with influence coefficients to add localized stress behavior with thermal stress and for all scenarios currently postulated for NSTX - with 10% headroom in currents, with and without plasma. PF5U conductor stress is calculated to be 122 MPa with all effects included. This is below the fatigue allowable developed for the OH coil [7]

The coil support concept is as presented in the PDR, with six existing supports augmented by six new support columns. Elimination of the existing strut or column between the upper and lower existing PF4/5 supports was considered but this overstressed the cantilevered portion of the PF5 support, added loads to the pad welded to the vessel, and added stress in the port ligaments, and so, the strut/column has been retained.

Figure 3.0- 2 Existing PF4/5 Supports

PF4 and 5 have to be aligned with respect to the centerline of the plasma. The current (meaning prior to the upgrade) approach is to connect" pushers and clamps around the coils to push the coils into roundness and concentricity. Currently coil heat up is trivial. For the upgrade the coils will be on for the 5 sec. pulse and will heat to 100C -expanding and fighting the alignment clamps. Table 6.3-2 shows the maximum temperatures expected during upgrade operation. John Menard and Masa Ono were consulted during a Wednesday project meeting. An n=2 error i.e. an elliptical coil is acceptable as long as it is aligned with the plasma centerline - i.e. it precludes a n=1 error, or a net lateral shift. So the coils are radially held with respect to the vessel and have them grow into an oval as they thermally expand. The degree of ovality was accepted by Jon Menard and Masa Ono.

The intention is to fix the sliding blocks on two opposite, existing PF4 and 5 supports. This makes the coils and their supports symmetric about a vertical plane that cuts through both fixed supports. A 180 degree half symmetry modeling is sufficient to capture the full 360 degree behavior of the coils In addition to the alignment issues; there are leads that require support. They currently break out of the coils and are connected to a unistrut frame that fixes them in space, providing support for Lorentz loads but allowing no thermal growth of the coil. If the fixed radial supports are chosen near the leads then the lead supports will work - at least conceptually.

The staggered column design produces 12 support s for the attractive loads on the PF4/5 upper and lower coils. The support points alternate between support by the vessel, and support by the six columns. This analysis assumes that the small columns (that buckled during initial NSTX runs) are retained. They are much less stiff than the new columns, and some loading is transferred to the vessel. The new columns are modeled as 3 inch in diameter and .3 inch with wall thickness. The welds connecting the bracket to the vessel shell concentrate at the corner of the perimeter weld. The weld is nominally 5/16, but the QA report recommends an effective ¼ inch weld .Local corner stresses were high even for the existing NSTX loading, and an inspection of these corner welds was performed to determine if any fatigue failures were initiating.- No indications of cracking or fatigue were found. The six (twelve included uppers and lowers) existing PF4 and 5 brackets are the only support for the assembly of PF 4,5 upper and lower coils. Most loading on the coils is attractive loading between the series connected PF4U&L coils and PF5U&L coils. The net loading is smaller. The attractive loads are intended to be taken by 12 columns, six original and six new columns. Without consideration of elastic effectiveness of the old columns, and considering the columns to resist all the attractive loads, then the weldments to the vessel would only take the net load with acceptable stress levels. Hand calculations of these loads show that these welds satisfy static and fatigue limits. In order for the bracket to vessel welds to be loaded primarily by the net assembly loads rather than the attractive loads between PF4 and 5, the existing columns must be stiffened. Clamp plate studs are currently listed as 316, but no grade or condition is specified. It is recommended that they be replaced with ASTM A193 B8M Class 2 bolting material. These provide assurance that if the launching loads are not equal and opposite on top vs. bottom, then 6 support points can support the net tensile loads on the studs.
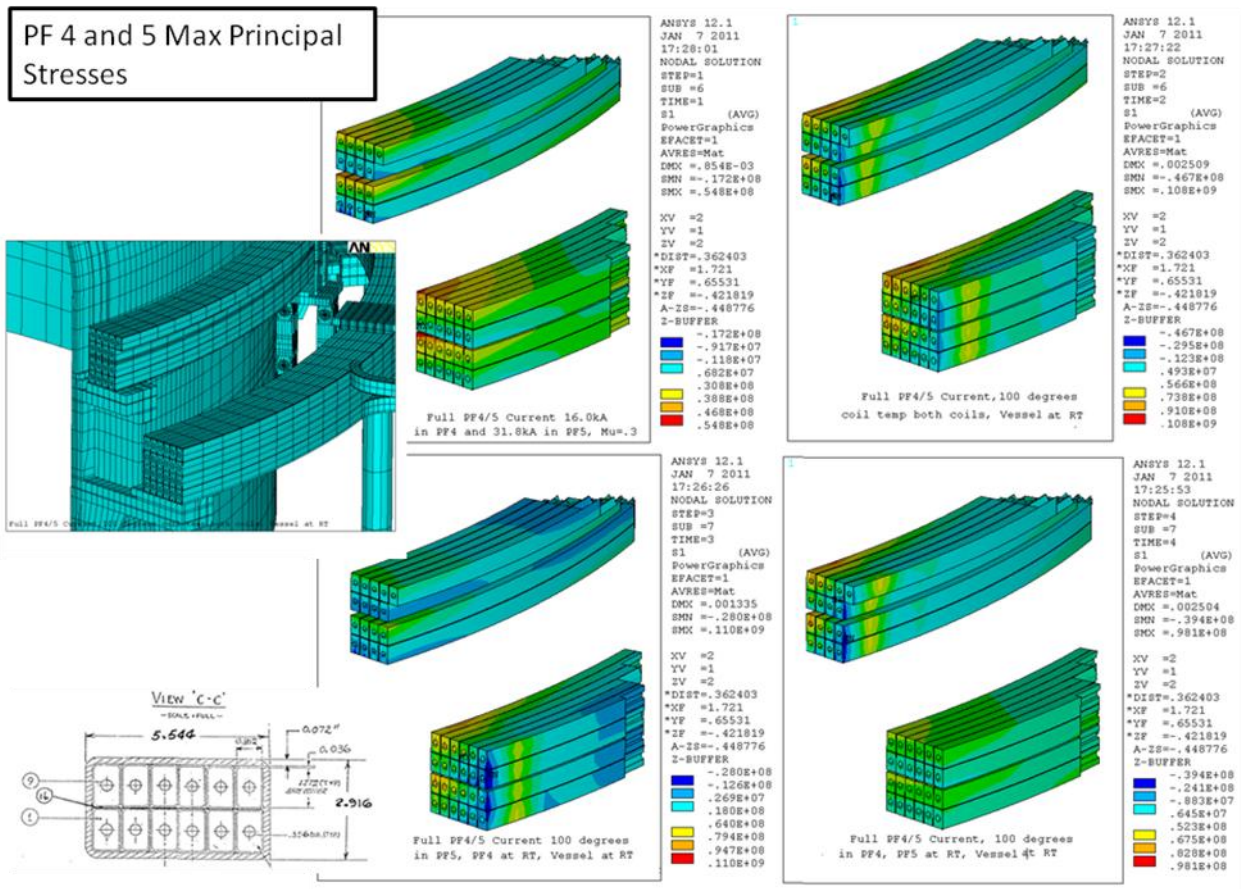
WBS 1.1.2 Upgrade TF to Umbrella Structure Aluminum Block Connection
NSTXU-CALC-12-06-00, Prepared By: Peter Titus,
Reviewed By: Mark Smith, NSTX Cognizant Engineer Mark Smith

Executive Summary:

The aluminum blocks at the top and bottom ends of the TF outer legs react part of the loads from the outer legs of the TF coils. The aluminum blocks are split and clamp the TF coil end with epoxy glass filler. This calculation is intended to investigate the aluminum block stress and the stresses in the 3/4 inch bolts that connect the block to the umbrella shell. This analysis uses conservatively derived OOP loads and moments from the TF outboard leg.

Analysis has progressed through four iterations of recommended reinforcements. The last or "fourth" round of modifications is intended to address the uncertainty in the material properties of the aluminum blocks. If tests or documentation shows adequate properties the last set of additions may not be needed.

With recommended reinforcements, stress levels in the 3/4 inch bolting are less than 36 ksi including bending and are around 20 ksi average axial tension. These satisfy the stress limits for the 316 bolts specified. The bolts are expected to be preloaded, and while only investigated in one of the runs, with the recommended reinforcements, the bolts are expected to be preloaded beyond the design stress and should be isolated from the cyclic loading. The pre-tension needed is 7375 lbs. The torque needed for this is .2*F*D = .2*7375*.75/12= 92 ft-lbs.

Bolt stresses are strongly affected by the flexibility of the umbrella structure shell. Reinforcing the shell has improved stresses in the shell as well as the bolt stress. Also lateral loads are assumed taken by a good fit between the aluminum blocks and umbrella structure cut-out. This may require shimming. If shimming is to be avoided, the preload would have to be tripled and significantly higher strength bolts would be required,
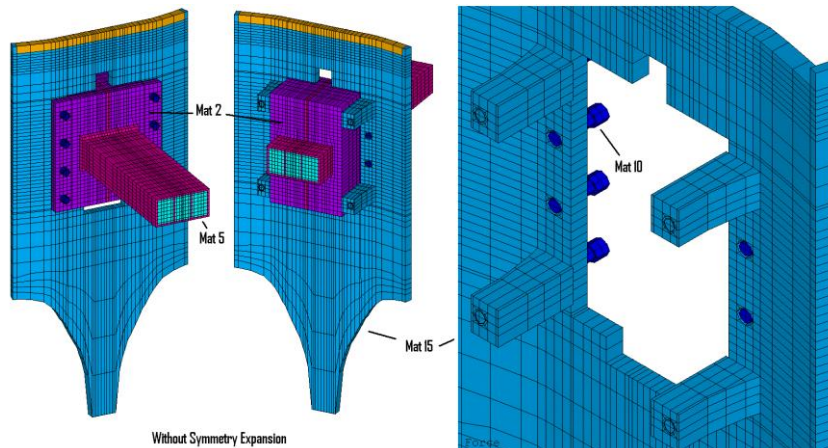
Initial Model Representing the Current (2010) configuration

While this calculation is not intended to address umbrella structure arch stresses, or TF outer leg bending and insulation bond shear, these areas are included in the models and stress values for these areas are consistent with those reported in other analyses.
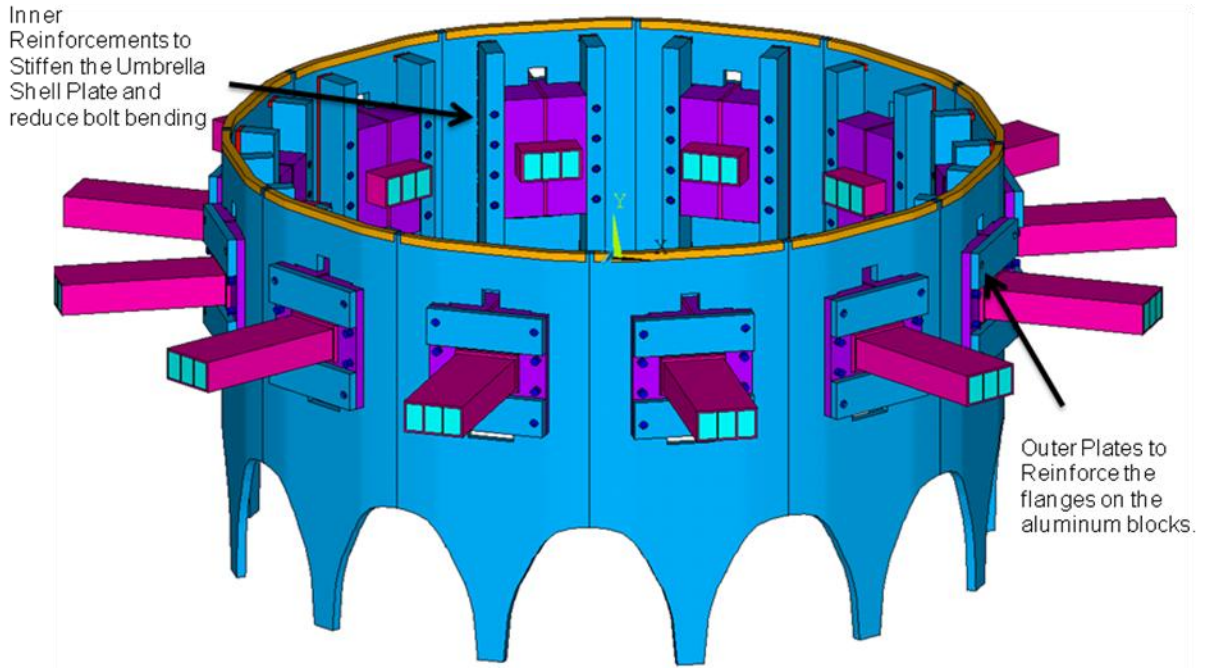
Symmetry expansion of the model with recommended reinforcements added

The external bars or outer plates are 1 inch thick, 4.25 high and 13.5 inches wide. There are two, one above the TF conductor and one below held by 3/4 inch bolts that thread into the reinforcing bars on the inside of the umbrella structure.
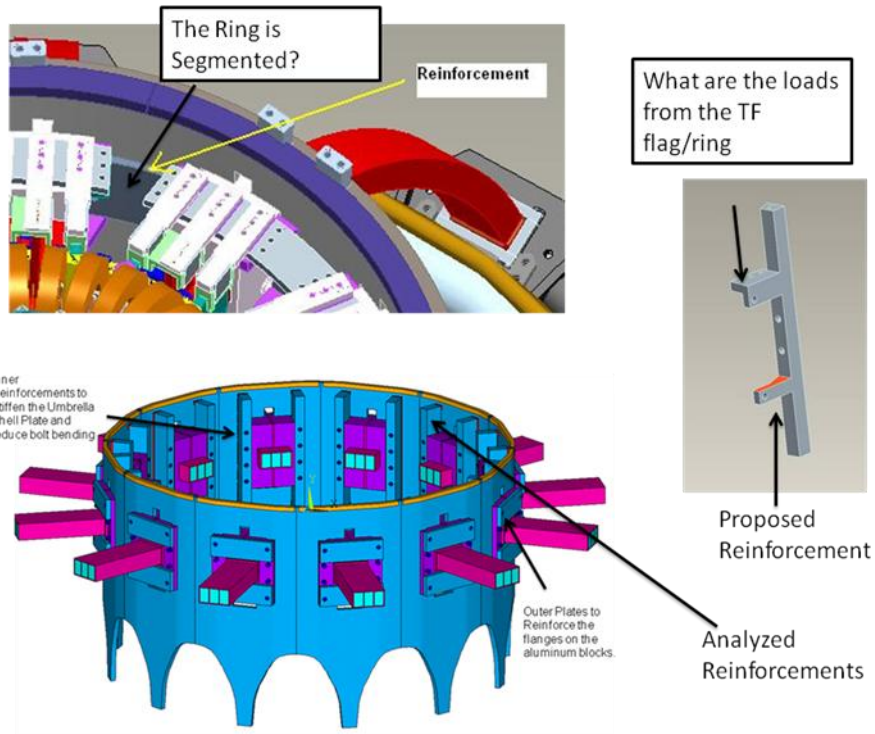
WBS 1.1.2 Lid/Spoke Assembly, Upper & Lower
NSTX-CALC-12-08-00 Rev 0 May 2011
Prepared by: Peter Titus, Reviewed By: Unassigned,
Cognizant Engineer: Mark Smith,

1.2 Executive Summary:

The purpose of this calculation is to qualify the upper and lower lid assemblies. These assemblies bridge between the upper or lower rims of the umbrella structures to the inner TF flags. The upper lid must allow thermal growth of the TF inner leg as it heats up during a pulse. The flexing of the upper lid produces bending stresses in the spokes as they flex.
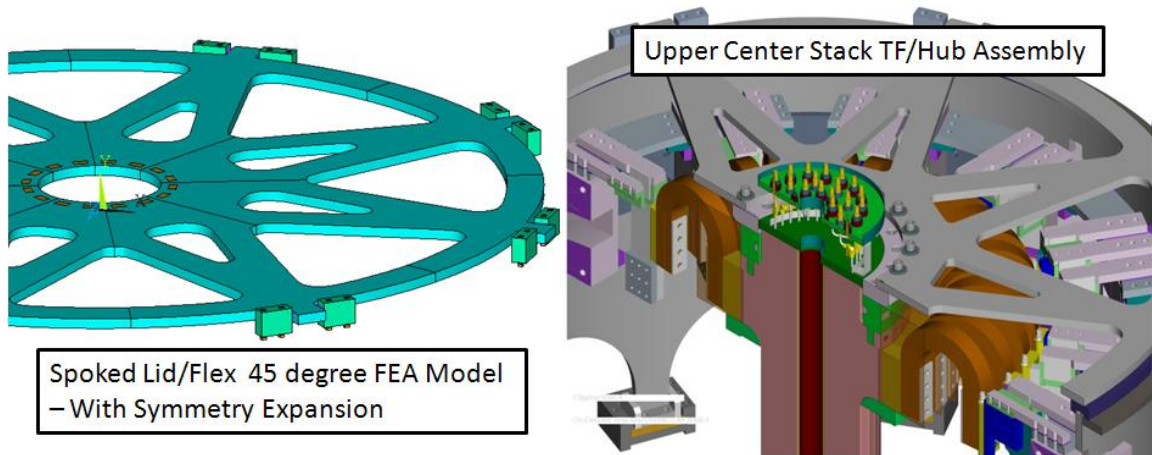
Figure 1.2-1 Upper Spoked Lid Model (left) and Machine Section (right)

The global machine torques is carried across the upper and lower lids, and also produces bending stresses in the spokes in an orthogonal plane. The torque load path is redundant.
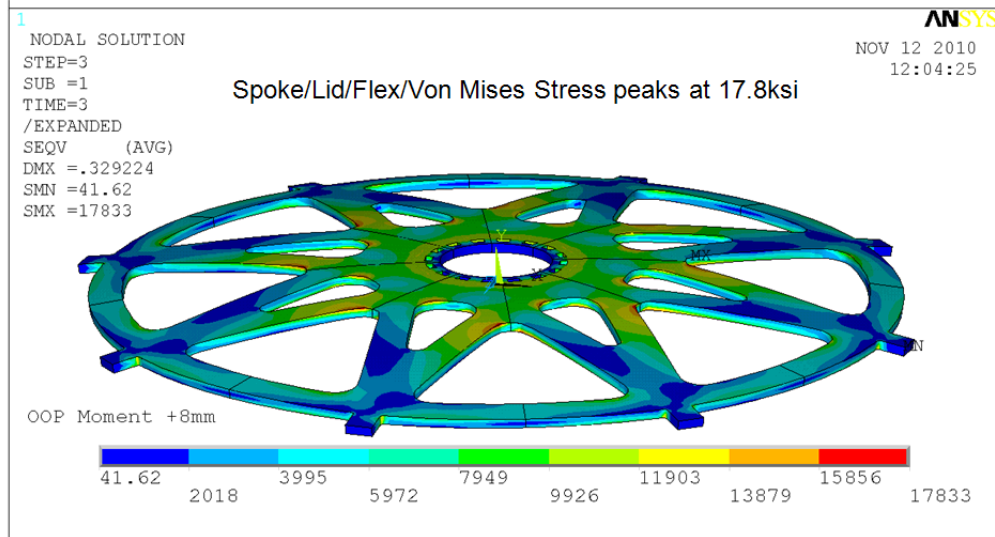
Figure 1.2-2 Upper Spoked Lid Stress with TF OOP Moment
and Centerstack Expansion Displacement Imposed.

The OOP torque load paths are similarly redundant on the bottom of the machine.
The upper lid lies in a plane and resists the machine torques with the small offset that results from the displacements of the TF. Stresses in the upper lid due to bake-out, normal operational heat up and extension of the TF, are also acceptable.

The stresses in the lower lid are also acceptable. The compliance of the bent spokes caused torques and lateral loads to be taken by other structures. There was a concern that having such a compliant member connecting the centerstack to the umbrella structure could introduce relative displacements and loads at the bellows. A flat concept was developed and it is the present FDR design approach.
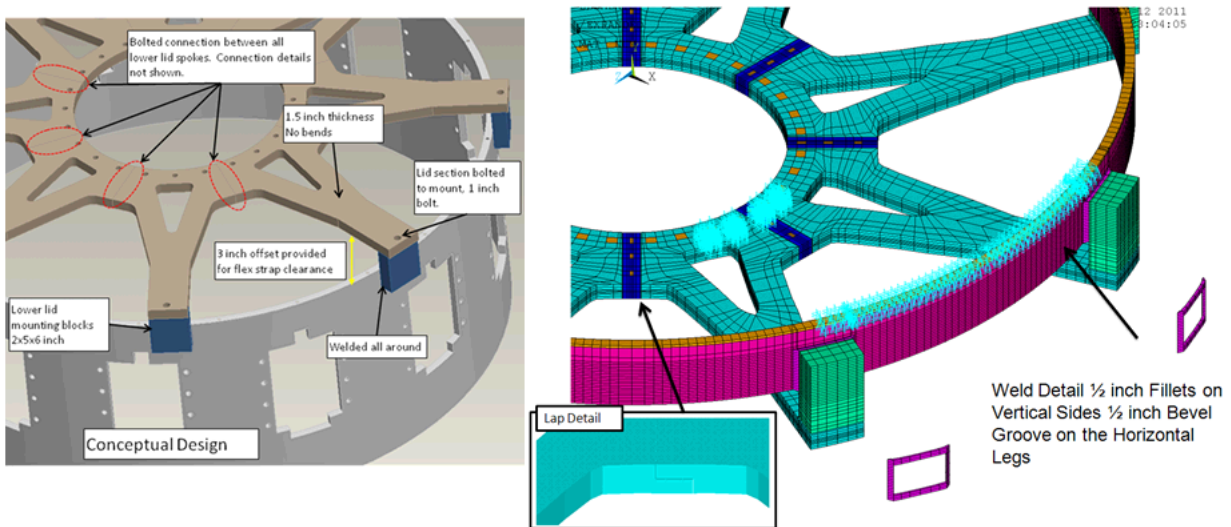
Figure 1.2-2 Flat Lower Spoked Lid Design Inverted for Clarity (Left) Analysis Model (Right)

Different design philosophies are used for the upper and lower lids. The upper lid is the primary torque transmission mechanism between the umbrella structure and the top of the TF flags. A secondary path of the machine OOP torque goes from the outer vessel, through the dome or dished head, through the ceramic break, then across the bellows [7] and into the centerstack casing.

The lower lid shares a part of three load paths that carry torque. The first is the spoked lid. The second is the bellows connection between vessel the centerstack casing. These are the load paths used for the upper structures, but the lower torque is also carried by a third load path through the pedestal to the floor and up through the braced vessel support columns to the vessel.

Designs have evolved from the CDR to the FDR. The lower torque load paths have shifted from the lid to the floor. This allows a significant increase in access from below the machine.

The interfaces at the ID connection to the TF flags is addressed by reference [6]. The OD interface with the umbrella structure rims is addressed in this calculation.
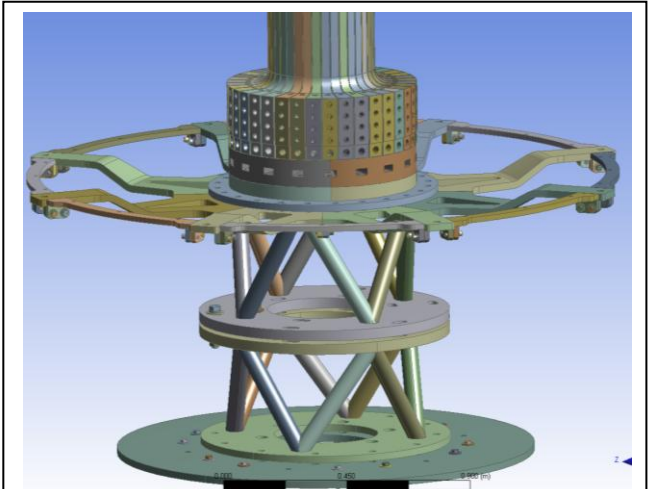
Figure 1.2-3 Lower Spoked Lid with Bent Spokes to Clear the TF Straps. The flat concept is preferred.

This calculation follows the torque being carried through the upper umbrella structure rim, across the lid assembly and to the upper TF flags [6]. The torque carried in this load path is quantified in the global model described in ref [1]. The inner TF flags and collar also carry this torque, and interface with the spoked lid. The lid also must allow the vertical growth of the TF inner legs.

The torsional moment for design of the lid/flex/Diaphragm bolting and the TF steps or keys from ref [1] is 0.3MN-m for the lower lid (Figure 3.2-1) and 0.25 MN-m for the upper lid from ref [1]). This is the torque being transmitted from the centerstack TF to the outer rim of the umbrella structure this was translated into a load per TF flag of about 7000 lbs.

Loads resulting from centerstack halo currents produce a lateral load and a moment at the lower connections to the pedestal. The bent spoked lid will transmit a minimal amount of this load to the umbrella structure because of the compliance of the bent spokes. The upper Halo current load inventory goes through the upper bellows to the vessel and not the spoked lid. This effect is addressed in bellows [7] and Centerstack casing calculations. This is included in the lid analysis via the 9000 lb load (the OOP torque load is around 7000 lbs). The lower centerstack Halo current load inventory goes through the skirt to the lower TF flag teeth/pins and splits between the pedestal and to the lower lid to the outer vessel leg supports. The lower TF G-10 collar must take the torques and centerstack halo loads - and (OH + PF1,abU&L) launching loads. Halo loads on the vessel and passive plates may go through the lower spoked lid being shared by the vessel support legs and the pedestal. The spoked lid bolts were checked for the full loading from the GRD specification of 700,000 amps across the face of the passive plates. This full load inventory is not expected to be applied to the lid - most will appear in the vessel support legs and reduced by the inertia of the tokamak.

The global model described in reference [1] was updated with the lower pedestal and spoked lid designs. This provides a means to qualify the stresses in the spoked lid, but the main purpose of including the lid in the global model is to address the need for torsional stiffness or compliance of the plate to ensure that the inner leg torsional shear stress is acceptable with the FDR configurations. The concern comes from the relative compliance of the bent spokes in the lower lid. Figure 4.0-2 shows the global model of the tokamak including the upper and lower spoked Lid

The hub/collar section is as Mark Smith, and Jim Chrzanowski has designed - with only preloaded bolts and friction connecting the spoke/lid to the collar in torsion. Since the moment caused by the 8mm expansion of the centerstack appears to impose minimal stresses on the collar, the outer lugs that connect to the umbrella structure flange can be pinned connections. The vertical growth can be absorbed by flexure of the spoked lid - and a little flexure of the collar. Ali preloaded the 18 bolts to 50000 lbs each.
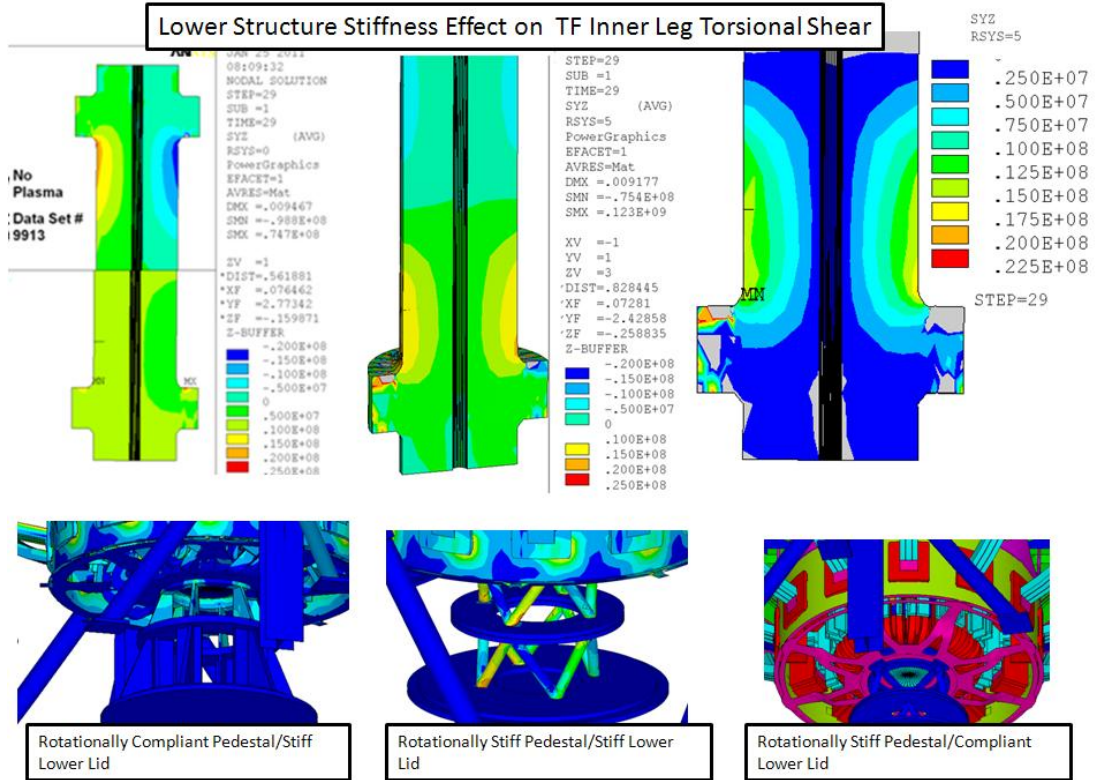
Figure 1.2-3 Effect of Pedestal and Lid Stiffness of TF torsional shear

The FDR chosen design for the lower lid is a flat, relatively stiff spoked "wheel" This was chosen over the bent spoke design which was too compliant to protect the bellows from relative motions and lateral loads from halo loading and from global machine TF OOP loading. Figure 1.2-4 shows the load path between inner and outer vessel structures that would result from a weak lower lid.
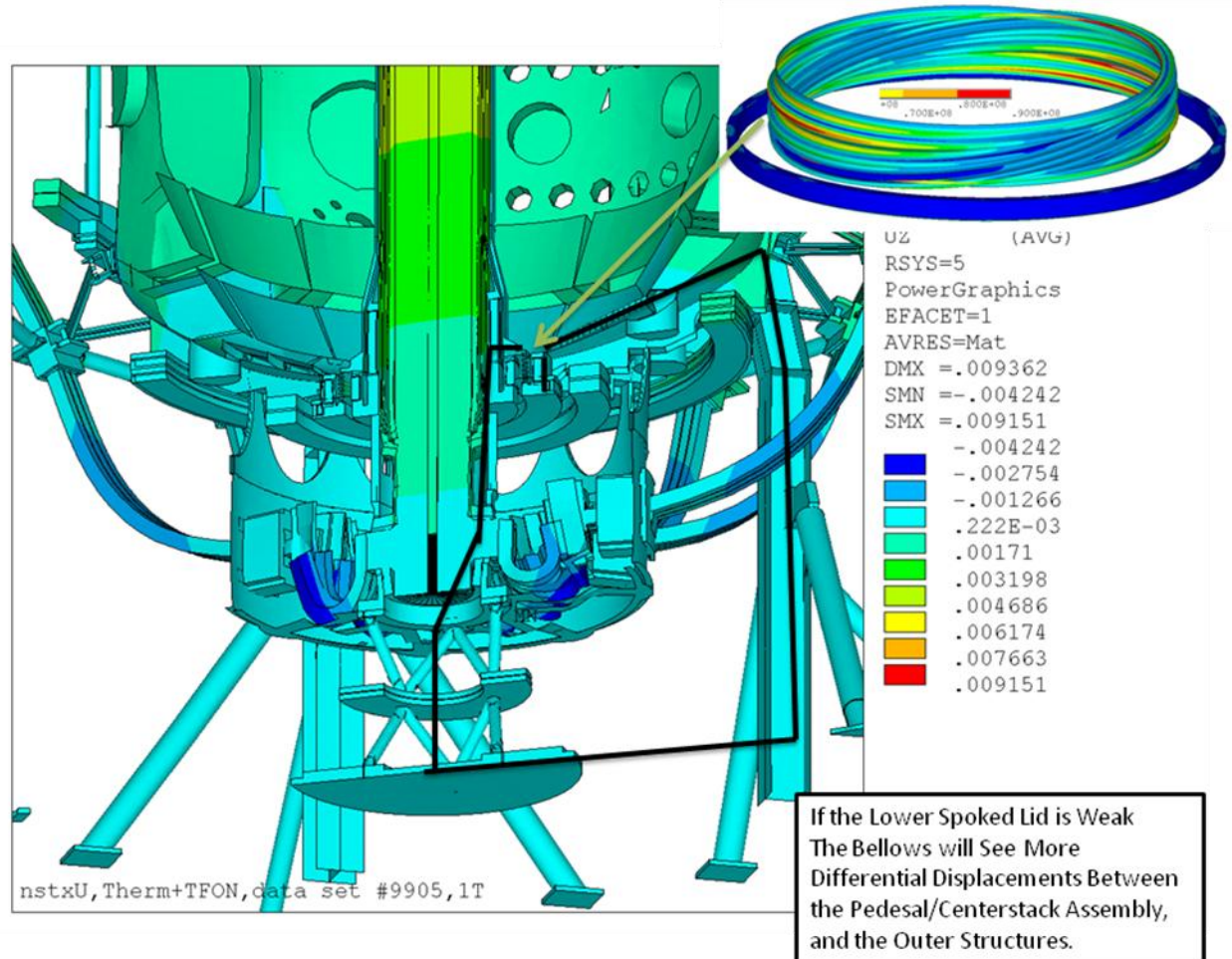
Figure 1.2-4 Structural Effect of a Laterally and Torsionally Compliant Lower Lid on the Bellows

Bend spoke lower lid analysis results were shown at the May 11, 2011, Wednesday project meeting based on models with the Vee pipe pedestal and the bent spoked lid. These two taken together behave differently than the CDR and PDR designs. The load path - exclusive of the spoked lid - for torsional and lateral loads - is shown with a dark line in the figure above. With the stiff pedestal and the softer lid, the bellows connection between the centerstack and the vessel will see more displacements. Jon Menard picked up on this and expressed a concern that this is a vacuum boundary and a problem here might affect the reliability of the machine. The net vacuum side load is included in the global model simulation. In the global model, the torsional stiffness's are reasonably represented. None of the bellows stresses were troublesome - The torsional shear is higher these would have required a revision to Pete Rogoff's bellows calc. - and Len Myatt's treatment of the ceramic break. The uncertain effect of the halo loading from the passive plates would require a more careful treatment if the lateral load path to the pedestal was compliant.

WBS 1.1.2 Analysis of the NSTX Upgrade Centerstack Support Pedestal
NSTXU-CALC-12-09-00 May 2011 Prepared By: Peter Titus
Reviewed By: Ali Zolfaghari, Cognizant Engineer: Mark Smith

3.0 Executive Summary:

The pedestal is a structure that provides gravity support for the centerstack and resists Coil Lorentz loads during operation. Because it is connected to ground, the lower lid assembly, and the TF flags, and the skirt which supports the centerstack casing, it also is a contributor to the torsional stiffness's that determine the distribution of the global torques in the machine. The pedestal must allow access to the service connections at the lower end of the centerstack. Provision must be made to allow passage of coolant lines, power leads and diagnostics. In order to service these lines, the pedestal may have to be able to be disassembled in pieces that do not capture the service connections. The current design for the FDR is shown in figure 3.0-1. The number of bolts at the mid flange is 6 pairs - but this was described as needing resolution in an email from Mark Smith [10]. The analysis model uses four bolts
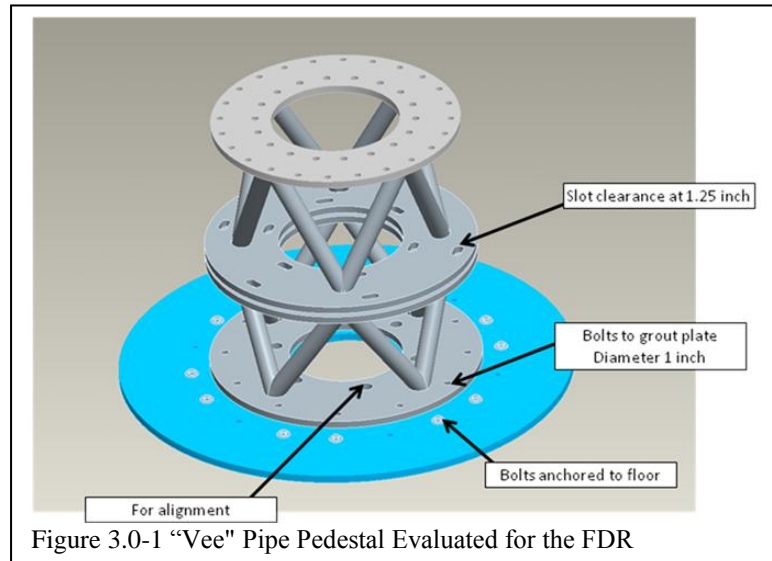
Figure 3.0-1 "Vee" Pipe Pedestal Evaluated for the FDR

in a pattern around the vertices of the trusses for a total of 8 pairs. Shimming of the mid flanges is assumed to also align with the vertices of the trusses. Use of high strength bolts at the flange connections (Mid height and at the base) allows these connections to be capable of resisting the worst case power supply loads. The limit to the upward loading is the concrete anchors or Hilties. Ninety four 3/4 inch Hilties are required to resist the worst case power supply loads. It is not likely that this number will be used. Only five 3/4 inch anchors are needed to react the normal operating net load on the centerstack. Many more than 5 are suggested. This number will set the limit that must be maintained by the DCPS.

There has been a couple of design concepts proposed for the pedestal. During the CDR, the pedestal was a bolted plate assembly. A number of analyses were performed based on this configuration, and the gusseted plate design was acceptable. Designers were concerned that a torsionally stiffer structure was needed, although the analyses (which also had a stiff lower lid structure) did not show this.
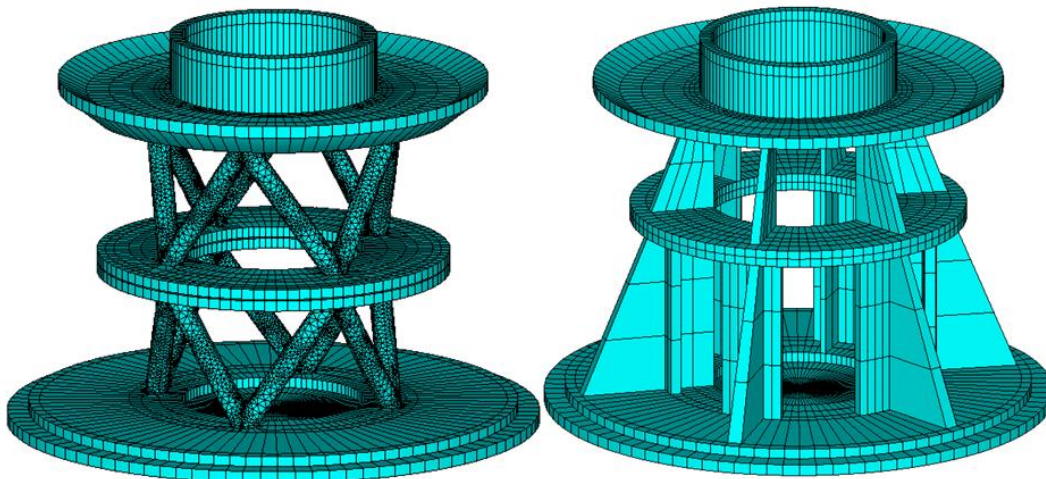
Figure 3.0-2 Two Concepts Proposed for the Pedestal; "Vee" Pipe (Left) and Gusseted Plate (Right)

Aside from qualifying the present Vee-tube structure, the global model used for the inner leg torsional shear calculation has been run with both the plate and Vee-tube structure.

Vee Pipe Pedestal

Plate Constructed Pedestal
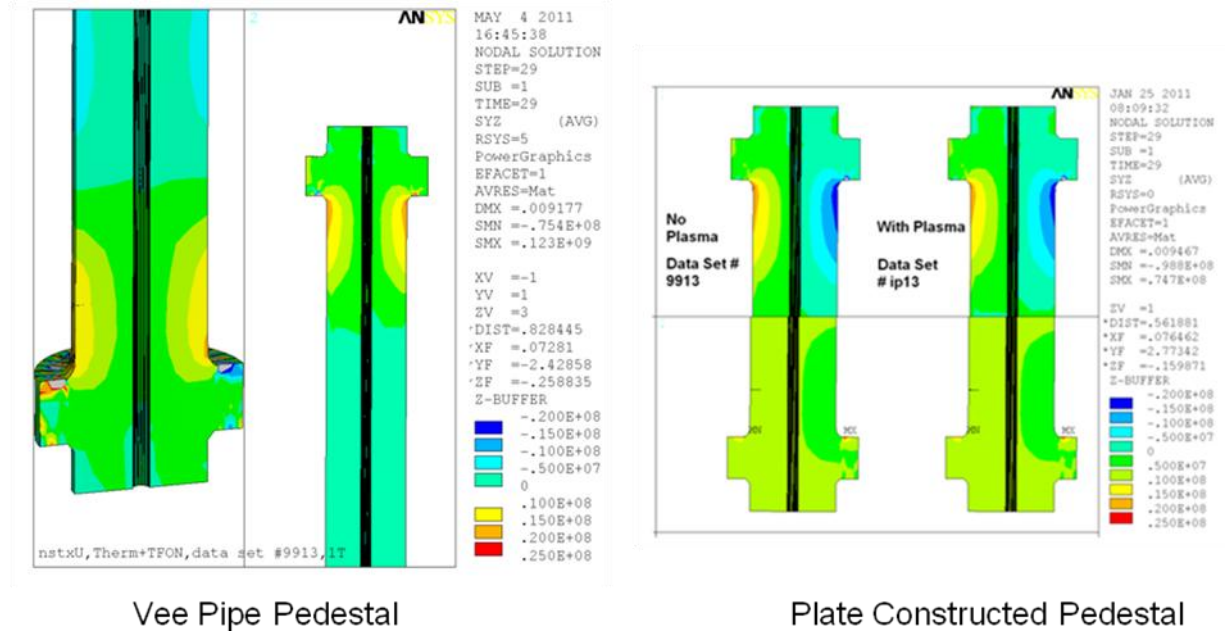
Figure 3.0-3 Inner Leg Torsional Shear for Two Pedestal Concepts

After reviewing a few scenarios, there is no differences in the max TF inner leg torsional shear of 25 MPa, but there is a difference in the shear in the lower end of the TF inner leg. This implies that there is a difference in torques transmitted via the TF flags and crown to the pedestal and lower spoked lid. For both these components, the torques has been based on an upper bound for the upper connections which have been found to be larger. So it is likely that the re-distribution of torque that is caused by the "Vee" Pipe pedestal will not be a problem, but rigorously, these should be re-investigated for the chosen pedestal design.
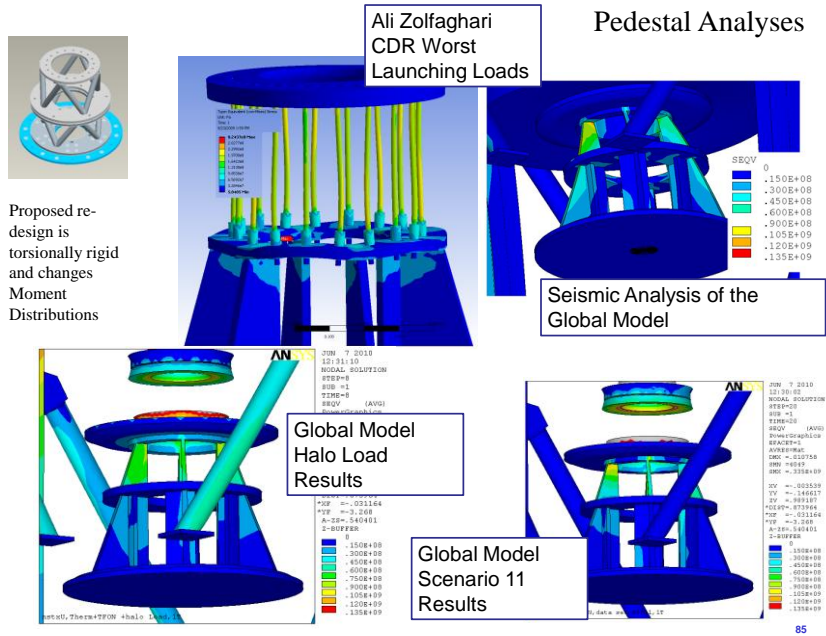
Figure 3.0-4 PDR Summary of Pedestal Designs

Figure 3.0-4 shows the work performed on the pedestal up to the PDR. The gusseted plate design has upper "vanes" that are torsionally weak and appear weak with respect to side loads from seismic and halo loads, but their stresses are well within allowables. Stresses in the "Vee" pipe truss pedestal design are slightly lower than for the gusseted plate design. Both are less than 20 MPa for normal loads and less than 200 MPa for the faulted loads. This provides a large margin. The bending allowable is 241 MPa for 316 weld material. Assuming full penetration welds producing no stress multiplier on the stress that is reported by the FEA analyses, the welds and structural elements have a large margin against normal loads and a normal design margin for faulted loads. . Connection to the TF flags is discussed, in Ali Zolfaghari's calculation [9]

The seismic analysis [6] was checked for the "Vee" pipe design - most of the modeling was with the plate design- and the seismic stress levels in the pedestal are acceptable.
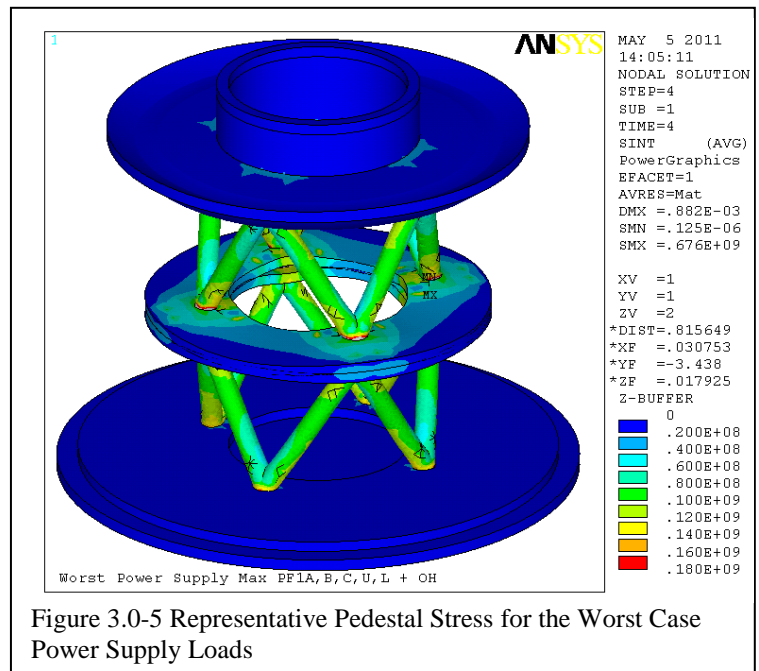
Figure 3.0-5 Representative Pedestal Stress for the Worst Case Power Supply Loads

Analysis of TF Outer Leg, NSTXU-CALC-132-04-00,
Prepared By: Han Zhang, **Reviewed by** Peter Titus
Cognizant Engineer: Phil Heitzenroeder

For the upgrade, the TF current will increase to 130 KA, resulting in 4 times the mechanical load, principally the out-of-plane (OOP) load. Consequently, various support structures will be over stressed, namely the umbrellas, and localized regions on the vacuum vessel (VV). To resolve these problems the load path will be modified. By adding structural support to transfer TF outer coil load to the VV at the clevis along with upgrading the clevis, maximum transfer of the OOP load can occur at this connection. This bypasses the umbrella. Furthermore, localized reinforcements will be added. Note, interference with auxiliary systems and supports was troublesome and limited the addition of trusses to help sustain the OOP load. Lastly, support rings will be added between the TF outer coils to reduce the pull-out (in-plane) loads.

A full model was built, including the umbrella reinforcement, new clevis, port and cover (NBI ports are reinforced) to replace the old vessel model in the TF truss analysis (Figure 1). But the centerstack, pedestal assembly and crown of umbrella structure are not included. TF truss is also modified to have coil reinforcement, modified clamp geometry and tie bar dimensions (Figure 2). The upgrade design replaces the turn buckles with a sturdy support ring which occupies the space of existing components. The support ring and tie bars transfer some of the in-plane and OOP load to the VV and is effective on both symmetric and asymmetric PF currents. The support ring reduces the pull-out (in-plane) load at the umbrella structure. Note, up-down asymmetric currents result in a net twist load which requires an attachment to the VV. The tie bars can take the net twist and also provided adequate OOP support for symmetric case.
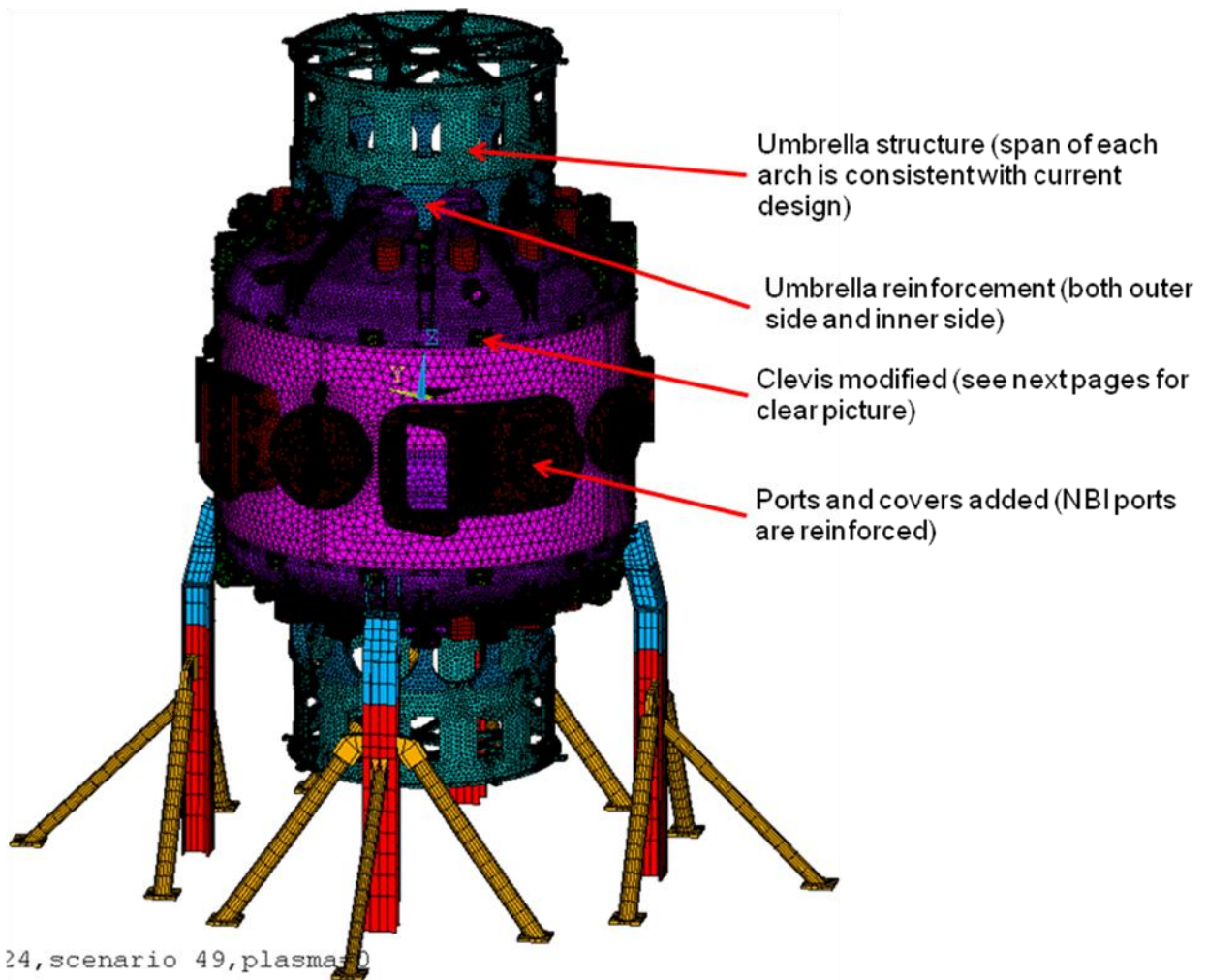
Figure 1: Changes made to vacuum vessel.
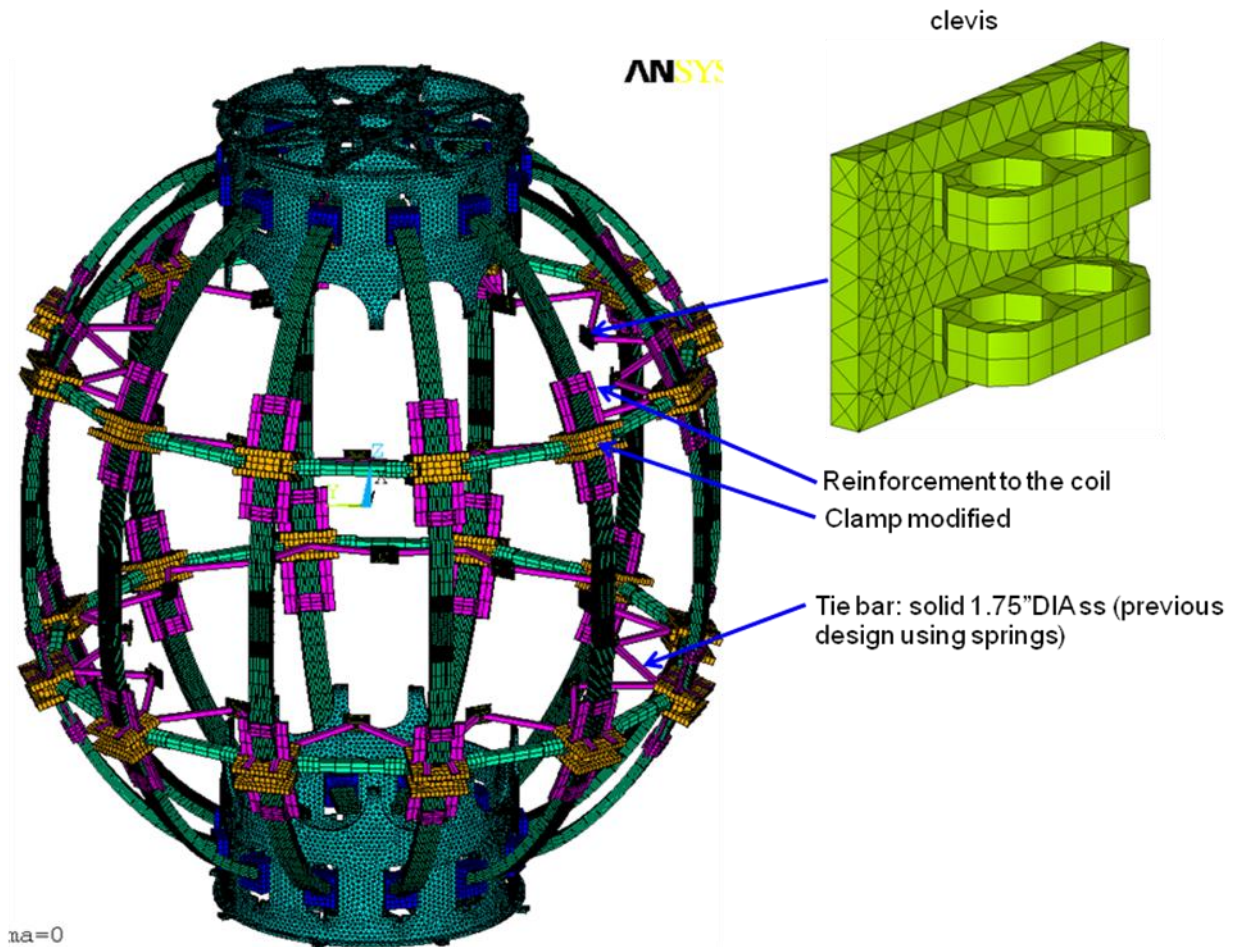
Figure 2: Changes made to TF truss.

Currently only two scenarios (49, 82) with larger OOP loads in TF outer coil are calculated, including symmetric (scenario 82) and asymmetric (scenario 49) PF current combinations. Total 96 scenarios will be run later to find out the worst load and stress in different components. From our calculation, without plasma current TF coil will have more OOP load and thus plasma current is set to be zero in these analyses. Also plasma disruption won't cause much load in TF coil and not analyzed too. With the new truss added, the displacement of the coil can be well restricted to be within 2 mm (Figure 3). Comparing to without the truss, the coil displacement is up to 27 mm. The maximal coil stress is 88 MPa (Figure 4), at the connection between TF clamp and ring. The model uses solid bond between coil and clamp. In reality, there is a thick epoxy layer between them that may further reduce the stress. The shear stress in the epoxy to bond the coils is within 7 MPa. The displacement and stresses are within allowable.

After reinforcement, the umbrella structure has max stress of 110 MPa (Figure 5), at the square hole to fix Aluminum block. Stress in umbrella arch area is too high before reinforcement (304 MPa) and drops down to 52 MPa. The stress in vessel is within 100 MPa. Stress level in the clevis is a little higher, 115 MPa. If it is bolted to the vessel, bolt load will be analyzed later. The ring should take 65 KN axial forces and 5000 N-m bending moment. These data has been transferred to a detailed model for further design and analysis of the ring. During vacuum vessel bake-out (150 °C), the truss will load TF coil and produced maximal stress is 151 MPa, which is within allowable and no need to disconnect the truss.
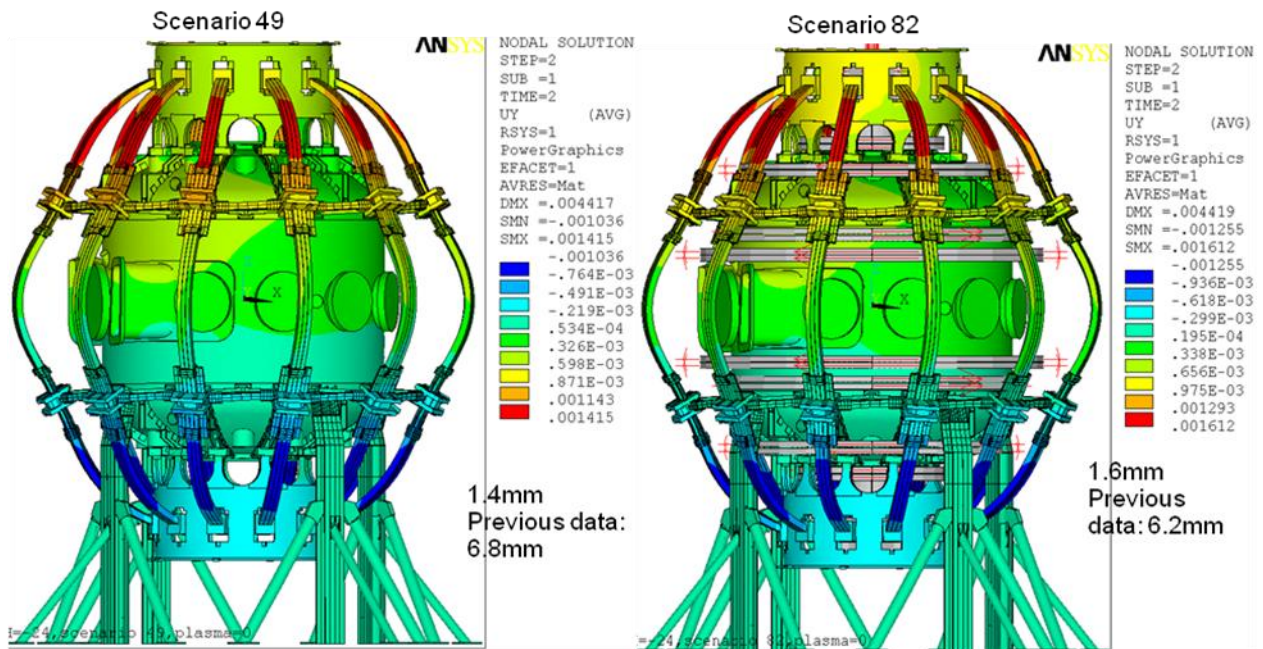
The coils are well restricted now because the tie bars are much stronger (solid, 1.75" DIA, comparing with the springs in previous design), which will result in lower stress in coil but much higher load in clevis.

Figure 3: Circumferential displacement (m).
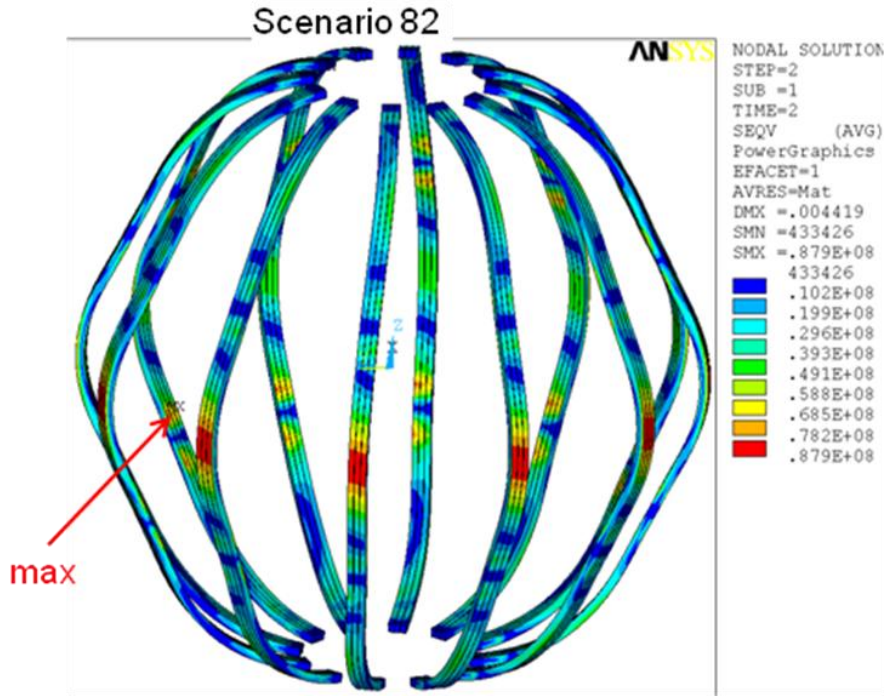
Figure 4: Coil Von Mises stress (Pa).
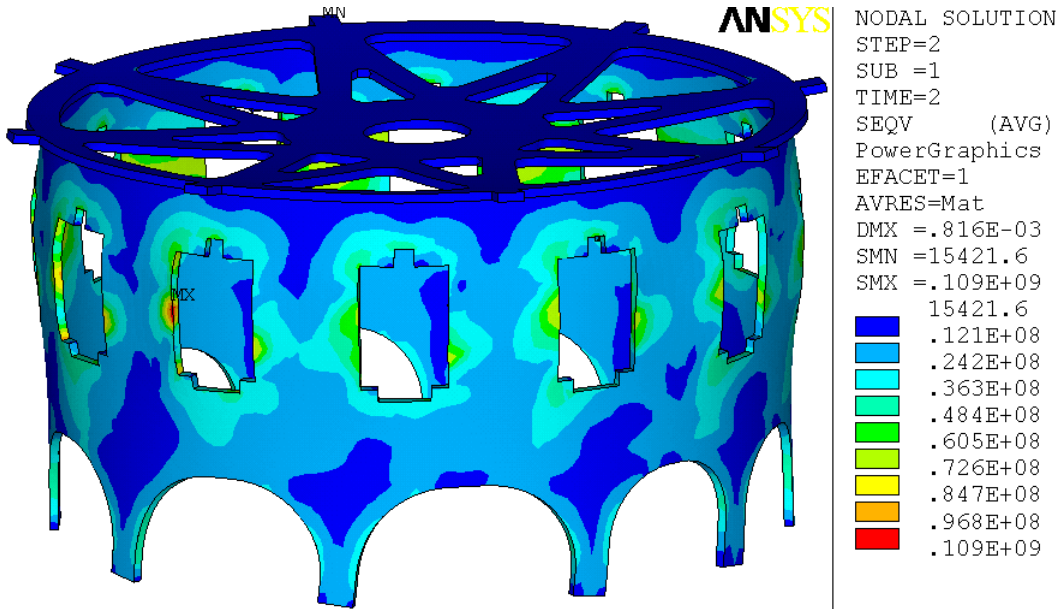
Figure 5: Umbrella structure Von Mises stress (Pa).

WBS 1.1.2 TF Strut to Vessel Knuckle Clevis Connection
NSTXU-CALC-132-09-00 Rev 0 March 2011, Prepared By: Peter Titus,
Reviewed by Han Zhang, Mark Smith, NSTX Cognizant Engineer

Executive Summary:

This is a qualification of a small part of the outer leg support system. The concept for this support has gone through a number of iterations. The chosen attachment has been sized and shaped to accept only shear loading and has been found acceptable for expected OOP loads that will be imposed on the vessel knuckle region by the TF outer leg support truss. Weld stresses are acceptable in terms of static and fatigue allowables, but inspections of the welds at the corners of the square pad are recommended.

The existing clevis attachment had a large offset to the pin centerline which produced a large prying moment in addition to the shear on the clevis. Concepts were developed that limited the load into the clevis, and concepts were developed to increase the load carrying capacity of the clevis. Loads at the attachment varied depending on the attachment and truss concept.

The existing clevis attachment bolting and 3/16 fillet welds are insufficient to support the upgrade truss/radius rod loads with the offset the present clevis design imposes. .

Figure 1 Existing Clevis Details

Welding the bolted clevis to the pad and increasing the weld size to 3/8 inch meets the static stress limits. Further analysis and possible re-enforcement was needed to satisfy fatigue limits. Once welding was considered, improvements in the clevis were also considered. One concern is that the existing bolts will gall when attempts are made to remove them. This is not expected (based on conversations with Eric Perry) but if they do gall than they can be ground off and the welded clevis welded over the bolts. In addition to the welded concept, another concept is evaluated here beginning on page 8. This is retained as a back-up in case access or interferences make welding difficult.

In the appendices, some of the calculations and presentation material are included to provide an understanding of the history that led to the present design choice. The weakness of the existing clevis produced a variety of design solutions that were more difficult and were not chosen. Prior to the CDR a diamond truss assembly was investigated, but only worked for up-down symmetric OOP loads and was impossible to install around the existing diagnostics, wave guides and service lines. At the PDR, a solution that employed compliant trusses to limit loading into the clevis was presented. This design used first, a coiled spring and then a Belleville spring stack. Off- loading the OOP loading from the vessel was

Figure 2 Photo of one of the Existing Clevises

| Diamond Truss | Pinned Ring Rigid Truss | Rigid Ring to Existing Clevis | Soft Springs to Existing Clevis |
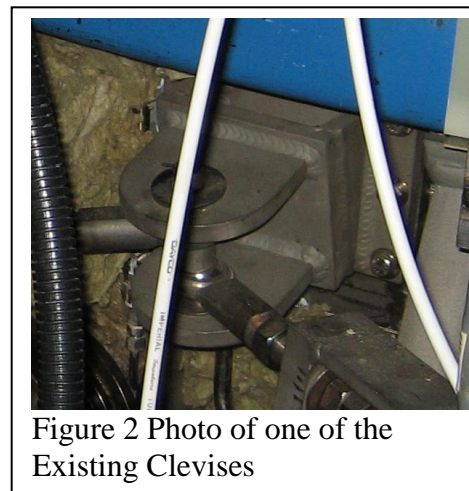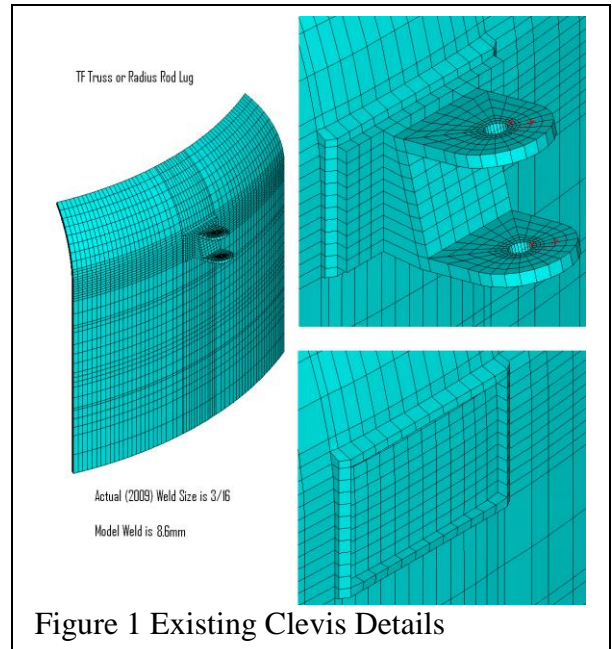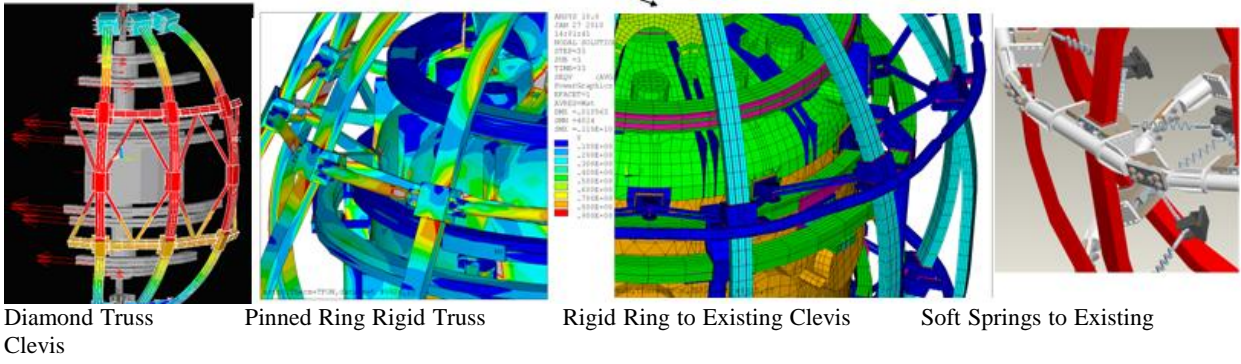
thought necessary to limit stresses at the mid-plane port ligaments. However more detailed analysis showed adequate capacity at the equatorial plane and the spring truss was dropped. Options that used the existing clevis pads as shear keys - with no tensile capacity were judged to have a precarious purchase on the pad, and this concept was never considered seriously. A concept which converted the PF 4 and 5 supports to take the TF OOP load was also considered and dropped. Some of the evaluations of this are included in Appendix B.
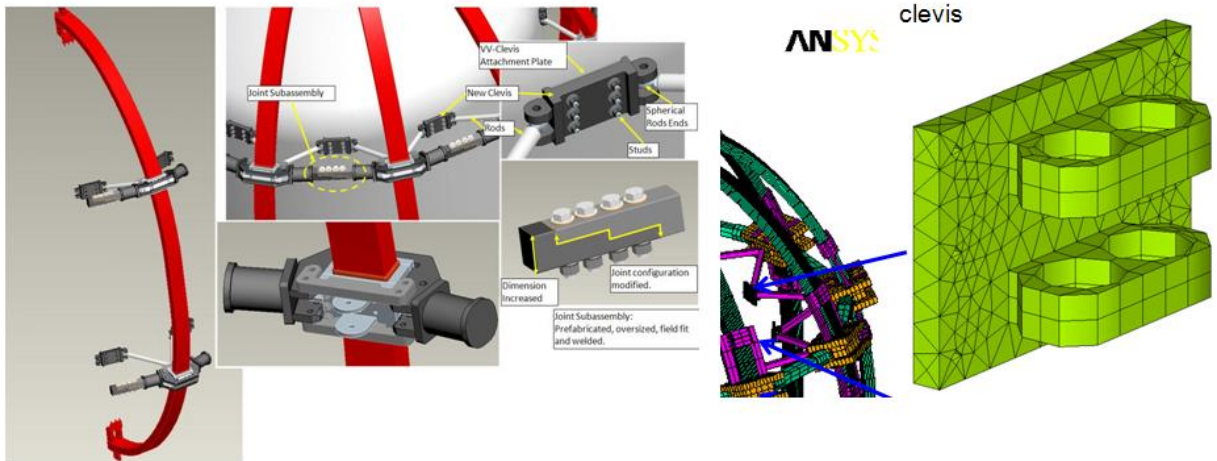
Elements of the Outer Leg Support System: An early version of the knuckle clevis is shown in the middle. Truss loads imposed a moment on this concept because of the width of separation to the "ears". The modeling employed in Ref 1 is shown at right. Preliminary results from this analysis show a truss shear load of 75 KN or 17,000 lbs

This Detail needs to be radiused
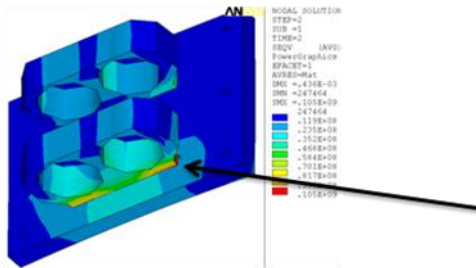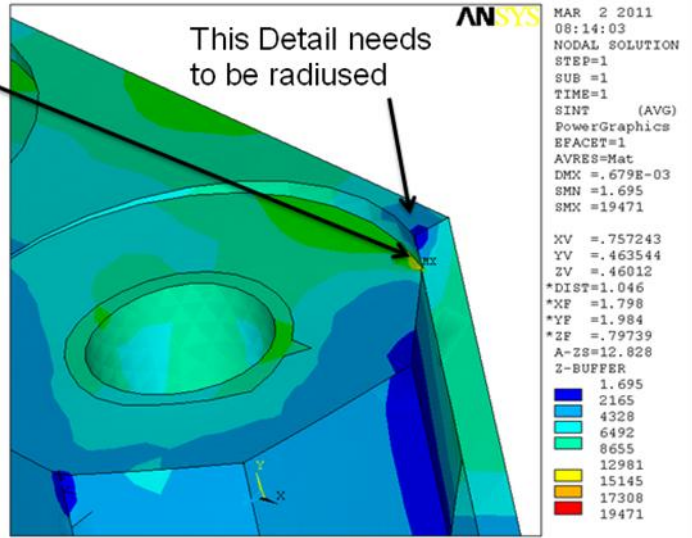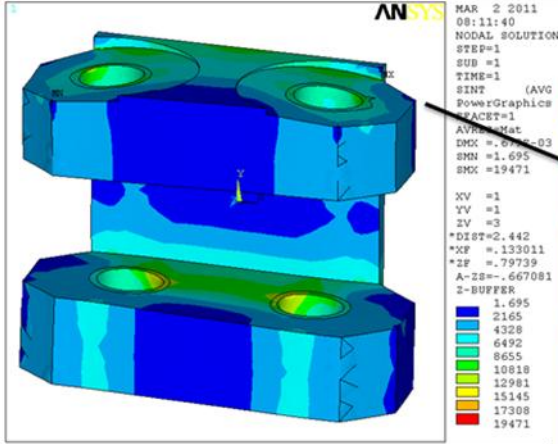
Ref [1] Preliminary Result from Wednesday Meeting. This Detail needs to be radiused

WBS 1.1.2 Ring Bolted Joint, NSTXU-CALC-132-11-00
Prepared By: Peter Rogoff, **Reviewed By** Irv Zatz,
Cognizant Engineer: Mark Smith

In order to support the principal magnetic coils of the NSTX device, two substantial rings are required to restrain the applied TF and PF forces. Each ring consists of twelve assemblies which are connected through a stepped lap joint with four stainless steel bolts. These bolts must provide sufficient compressive force, through combined preload, to resist the joint separation for all mechanical load applications.

This analysis is performed in order to check and design the joint integrity by selecting and specifying the necessary bolts. The actual joint geometry is presented in the calculation section.

NSTX   **Supported by**   **U.S. DEPARTMENT OF ENERGY** | Office of Science
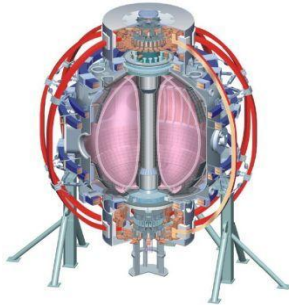
Update Ring Bolted Joint

Design and Recommend the Joint Geometry using bolts with necessary pre loads to keep the contact surfaces from sliding using the NSTX Global model extracted loads.

Ti=Fp(KD)- torque
K is the "nut factor" and dimensionless

This is done via Nastran FEA and hand calculations.

Fp=UTS x As – tension P.L.

As=.785(D-(.9743/n))^2

Explanation: Bolt preloads apply a compressive force "Fn" between the contact surfaces which must have a reasonable coefficient of friction in order to create a sufficient shear force "Fs" to resist the tensile force created by the applied loads.

n = # of threads per inch.

Selection of the Friction coefficient value "Mu" critical.

316 cold finished: Yield strength =100. ksi, Tensile (uts)= 125. ksi, Shear = 25. ksi

P. R.
3/9/2011

Complete Nastran Model

Nastran Node # 47431

Nastran Node #47432

ANSYS Node # 489653

Bolt Pre Load = 44,000. lbs

Coord 2R #21- Controls applied displacements

Total Distance between nodes #47432 and #47431 = 30.4 inches

ANSYS Node #489637
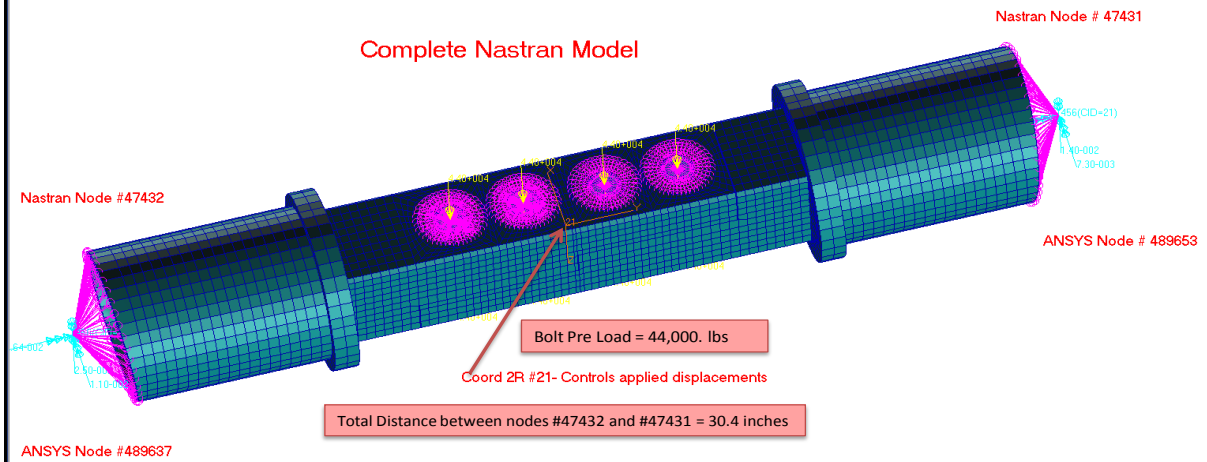
Calculations based on standard equations, See above

See next slide

Problem: 1.0 in. dia. Bolt , As= .663 in^2, Yield = 100.ksi, Based on 2/3 yield = 66.7 ksi.

Fp = 66.7ksi x .663in^2 = 44.22 Kips per bolt, If mu = .3, Fs = 44.22 Kips X .3 = 13,266 lbs/bolt
                                        Typical "nut factor"   see the torque equation
For two bolts Fs= 26532. lbs   And required torque = 44,220 lbs. x .2 x 1.0 in.= 8,844 lb-in

Scenario 49

Stresses from the global model

Node: 489637 Node: 489653 Node: 489637 Node: 489653

Pa
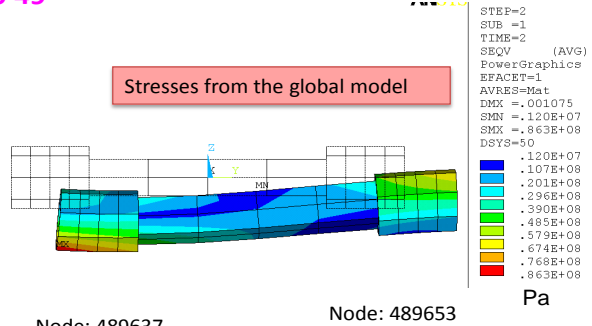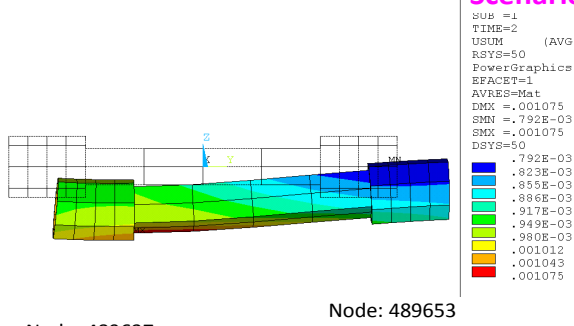
THE FOLLOWING DEGREE OF FREEDOM RESULTS ARE IN COORDINATE SYSTEM 50
unit: m

NODE	UX	UY	UZ	USUM
489637	0.29608E-03	0.68516E-03	-0.64286E-03	0.98507E-03
489653	0.18566E-03	0.74549E-03	-0.34586E-03	0.84252E-03

THE FOLLOWING DEGREE OF FREEDOM RESULTS ARE IN COORDINATE SYSTEM 50
unit: m

NODE	ROTX	ROTY	ROTZ	RSUM
489637	-0.54201E-03	-0.17193E-02	0.37961E-03	0.18423E-02
489653	0.21024E-03	-0.19470E-02	0.31508E-03	0.19835E-02

THE FOLLOWING X,Y,Z SOLUTIONS ARE IN COORDINATE SYSTEM 50
Unit: N

NODE	FX	FY	FZ
489637	-3440.5	-64444.	-8651.6
489653	3440.5	64444.	8651.6

THE FOLLOWING X,Y,Z SOLUTIONS ARE IN COORDINATE SYSTEM 50
Unit: N-m

NODE	MX	MY	MZ
489637	-4080.7	171.36	1405.3
489653	-2597.8	-171.36	1250.5

Data from the ANSYS Global model 3/19/2011

MSC FEA 2010.1.2 64-Bit 22-Mar-11 12:12:10
Fringe: Default, A3:Static Subcase, Stress Tensor, , von Mises, (NON-LAYERED)
Deform: Default, A3:Static Subcase, Displacements, Translational,

```
GRID        67232              23.2282 45.4854 -86.5923
$ Loads for Load Case : Default
SPCADD    2        1        3
$ Enforced Displacements for Load Set : Stretching2
SPCD      2        47432    1        .011     47432    2        .0264
SPCD      2        47432    3        -.025
$ Enforced Displacements for Load Set : Stretching
SPCD      2        47431    1        .0073    47431    2        .029
SPCD      2        47431    3        -.014
LOAD      2        1.       1.       1        1.       3        1.       4
          1.       5
$ Displacement Constraints of Load Set : Stretching2
SPC1      1        1235     47432
$ Displacement Constraints of Load Set : Stretching
SPC1      3        1235     47431
$ Nodal Forces of Load Set : UPPreLOAD
FORCE     3        47294    5        44000.   1.       0.       0.
FORCE     3        47307    5        44000.   1.       0.       0.
FORCE     3        47320    5        44000.   1.       0.       0.
FORCE     3        47333    5        44000.   1.       0.       0.
$ Nodal Forces of Load Set : DOWNPreLOAD
FORCE     1        47306    5        44000.   -1.      0.       0.
FORCE     1        47319    5        44000.   -1.      0.       0.
FORCE     1        47332    5        44000.   -1.      0.       0.
FORCE     1        47345    5        44000.   -1.      0.       0.
$ Nodal Forces of Load Set : Right Force
MOMENT    5        47431    21       25506.6  -.901061 0.       .433692
$ Nodal Forces of Load Set : Left Force
MOMENT    4        47432    21       38188.9  -.94551  0.       .325592
$ Referenced Coordinate Frames
CORD2R    5                29.8001 45.0852 -83.68784.01658 46.1807 12.5327
          29.5188 -54.5299-82.629
CORD2R    10               19.5362 44.76   -86.434419.8165 144.032 -87.4893
          -6.1586345.8515 9.4541
CORD2C    16               36.4143 45.0927 -81.916427.6557 145.057 -81.8895
          65.0164 47.6246 -178.068
CORD2C    17               9.42231 45.0925 -89.148116.9968 145.058 -84.7788
          32.724  47.5916 -186.72
CORD2R    21               22.9182 45.085  -85.531723.1987 144.445 -86.5875
          48.6339 43.9926 -181.506
ENDDATA 3359329b
```

default_Fringe :
Max 2.12+004 @Nd 59819
Min 2.10+001 @Nd 9761
default_Deformation :
Max 3.93-002 @Nd 3483

Loads with SPCDs and Moments
Total Load

MSC FEA 2010.1.2 64-Bit 22-Mar-11 12:30:10
Fringe: Default, A3:Static Subcase, Stress Tensor, , Max Principal, (NON-LAYERED)
Deform: Default, A3:Static Subcase, Displacements, Translational,

```
$ Loads for Load Case : Default
SPCADD    2        1        3
$ Enforced Displacements for Load Set : Stretching2
SPCD      2        47432    1        .011     47432    2        .0264
SPCD      2        47432    3        -.025
$ Enforced Displacements for Load Set : Stretching
SPCD      2        47431    1        .0073    47431    2        .029
SPCD      2        47431    3        -.014
LOAD      2        1.       1.       1        1.       3        1.       4
          1.       5
$ Displacement Constraints of Load Set : Stretching2
SPC1      1        1235     47432
$ Displacement Constraints of Load Set : Stretching
SPC1      3        1235     47431
$ Nodal Forces of Load Set : UPPreLOAD
FORCE     3        47294    5        44000.   1.       0.       0.
FORCE     3        47307    5        44000.   1.       0.       0.
FORCE     3        47320    5        44000.   1.       0.       0.
FORCE     3        47333    5        44000.   1.       0.       0.
$ Nodal Forces of Load Set : DOWNPreLOAD
FORCE     1        47306    5        44000.   -1.      0.       0.
FORCE     1        47319    5        44000.   -1.      0.       0.
FORCE     1        47332    5        44000.   -1.      0.       0.
FORCE     1        47345    5        44000.   -1.      0.       0.
$ Nodal Forces of Load Set : Right Force
MOMENT    5        47431    21       25506.6  -.901061 0.       .433692
$ Nodal Forces of Load Set : Left Force
MOMENT    4        47432    21       38188.9  -.94551  0.       .325592
$ Referenced Coordinate Frames
CORD2R    5                29.8001 45.0852 -83.68784.01658 46.1807 12.5327
          29.5188 -54.5299-82.629
CORD2R    10               19.5362 44.76   -86.434419.8165 144.032 -87.4893
          -6.1586345.8515 9.4541
CORD2C    16               36.4143 45.0927 -81.916427.6557 145.057 -81.8895
          65.0164 47.6246 -178.068
CORD2C    17               9.42231 45.0925 -89.148116.9968 145.058 -84.7788
          32.724  47.5916 -186.72
CORD2R    21               22.9182 45.085  -85.531723.1987 144.445 -86.5875
          48.6339 43.9926 -181.506
ENDDATA 3359329b
```

default_Fringe :
Max 1.73+004 @Nd 59594
Min -5.16+003 @Nd 59807
default_Deformation :
Max 3.93-002 @Nd 3483

Loads with SPCDs and Moments
Total Loads

TF Coupled Thermal Electromagnetic Diffusion Analysis,
NSTXU-CALC-132-05-01,
Prepared By: Han Zhang, **Reviewed by** Yuhu Zhai,
Cognizant Engineer: Jim Chrzanowski

The objective of this analysis is to calculate the temperature and stresses during TF coil ramp up, flat top and ramp down, using normal operation waveform. PF field is not considered. The distribution of current in TF coil depends on the resistance, inductance and contact pressure in the contact area. Coil temperature reaches highest, 117ºC, at the end of the pulse, i.e., 10.136s. Comparing with C. Neumeyer's result (101 ºC temperature rise) this analysis with current diffusion effect results in a little higher temperature. Max coil temperature is 47 ºC in TF outer coil. But the temperature at the end of the coil can reach 65 ºC because it connects to the arch which has higher temperature.

Using high strength copper (80% IACS) in the flag extension increases the temperature only by < 1ºC. Thus high strength copper can be used if required to increase the pressure of joint bolt insert over the capacity of pure copper.

The central beam has maximal hoop tension stress of 72.7MPa at 9.512s (i.e. the end of flat top) and 58.5MPa at 10.136s (i.e. the end of pulse), similar to Titus's result.

To avoid bending of TF inner leg, some structural supports will be added to the upper flags and the fillet radius of upper flag is modified to be bigger, which will help to reduce the temperature at the corner. Thus the model was modified and ran again to know how much temperature reduction. To avoid the work of re-mesh, only the positions of the nodes at fillet are modified and the radius may not be accurate. Also active water cooling is added with changeable parameters. With active water cooling (0.25" diameter tube, 3 m/s coolant velocity and inlet temperature of 12 ºC), the maximal temperature of lower flag drops to 113.4 ºC (117ºC without cooling) and that of upper flag becomes 110.8 ºC (Figure 1)
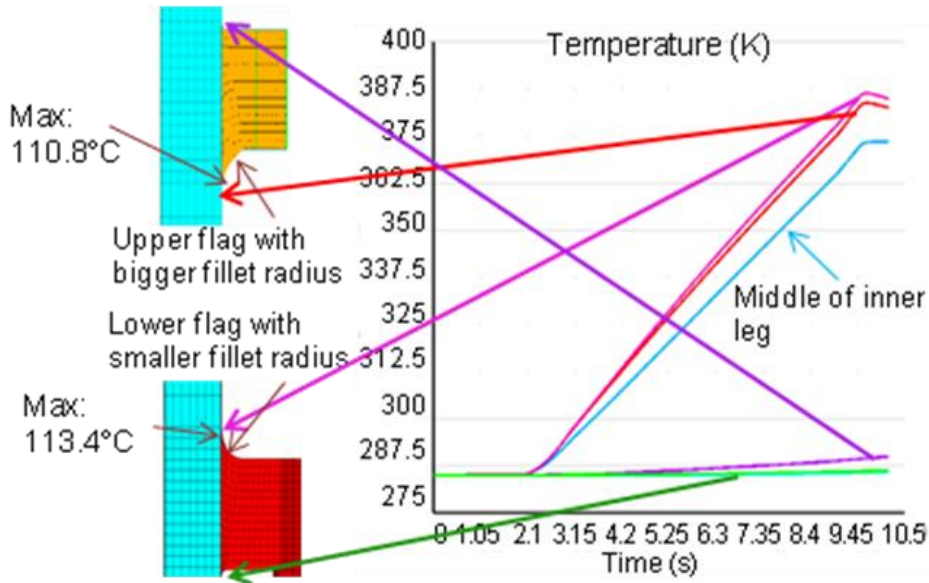
Figure 1: Temperature rise in TF inner coil with water cooling (0.25" diameter tube, 3 m/s coolant velocity and inlet temperature of 12 ℃).

The epoxy to bond TF coils has thermal expansion coefficient of 1.362E-5 /°C. The thermal expansion coefficient of copper is 1.54E-5 /°C at 0 °C and 1.6E-5 /°C at 100 °C. Different thermal expansion between copper and epoxy may cause delamination. Currently there are two ideas to place the cooling line, in the middle or at the side of the coil. Both are evaluated. Figure 2 show that putting cooling line at side produces lower Stheta (i.e. stress component that can cause delamination) of 90 MPa than putting cooling lines in the middle, because latter will cool the coil down faster and result in more shrinkage. In these analyses, 0.3" tube is used with 3 m/s velocity and it takes 5 minutes to cool the inner coil down to room temperature. If the cooling process can be slower, for example, by using a 0.25" tube and the same velocity, the stress Stheta can be reduced to 48 MPa. Total cooling time of using 0.25" tube hasn't been calculated yet. It is still unknown to us how much stress will cause delamination but we are trying to reduce it as much as possible. To reduce Stheta, it is better to cool down slowly. Using thinner tubes, lower coolant speed and different cooling line positions are all options.

The max temperature in outer coil reaches only 47 ℃ at the end of pulse. But to avoid further temperature rise upon following pulses, active cooling is simulated. With cooling line of 0.5" tube diameter, 3 m/s velocity and tube attached to the surface of outer coil, the coil can be cooled down to 25 ℃ in 5 minutes.
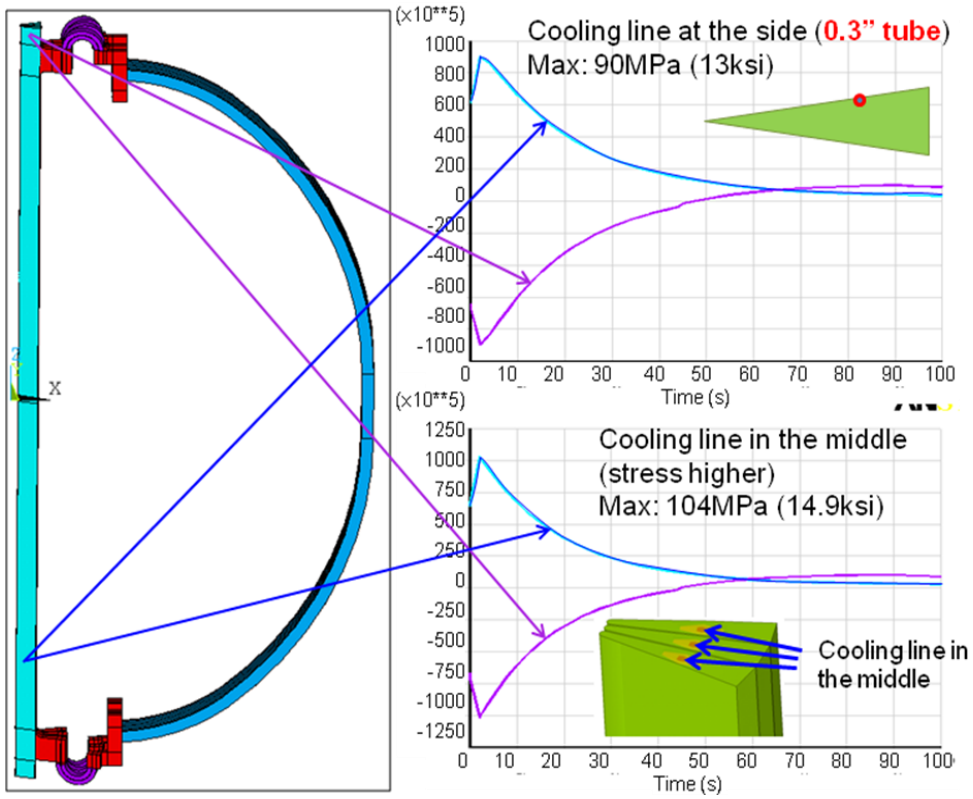
Figure 2: History plot of stress Stheta (Pa) in TF coil with water cooling (0.3" tube, 3 m/s).

TF Flex Joint and TF Bundle Stub NSTXU-CALC-132-06-00
Prepared By: Tom Willard, **Reviewed by**: Ali Zolfaghari
Cognizant Engineer: Jim Chrzanowski

The objectives of this analysis of the NSTX Upgrade TF Flex Strap and TF Bundle Stub design were: 1.) to determine if the design is adequate to meet the requirements specified in the NSTX Structural Design Criteria, specifically, if the flex strap lamination stresses and the copper lead extension thread stresses meet the requirements for fatigue, yield, and buckling, under worst-case/ power supply-limit load conditions: 130,000 amps/ strap, 0.3 T poloidal field, and 2.0 T toroidal field; and 2.) to verify that the local contact pressure in the bolted electrical joints is a minimum of 1500 psi, sufficient to maintain the joint contact electrical conductance above the design goal, based on the current-design development tests, of 1.0E06 siemens/in^2.

The results of the ANSYS multiphysics finite element analysis - electric, transient thermal, magnetostatic, and static structural - show that: 1.) the maximum equivalent stress in the laminations is 27.5 ksi, which is 25.5 ksi below the fatigue allowable for the full-hard C15100 copper-zirconium strip; 2.) the maximum equivalent stress in the copper threads is 29.1 ksi, which is 32.9 ksi below the fatigue allowable for the full-hard C18150 copper-chromium-zirconium plate; 3.) the minimum average contact pressure is >6500 psi, and the minimum local contact pressure is >2500 psi, which is 1000 psi above the design goal; and 4.) the lamination minimum linear buckling load multiplier factor (LMF) is > 58, which is approximately 10x the minimum allowable specified in the NSTX Design Criteria document.
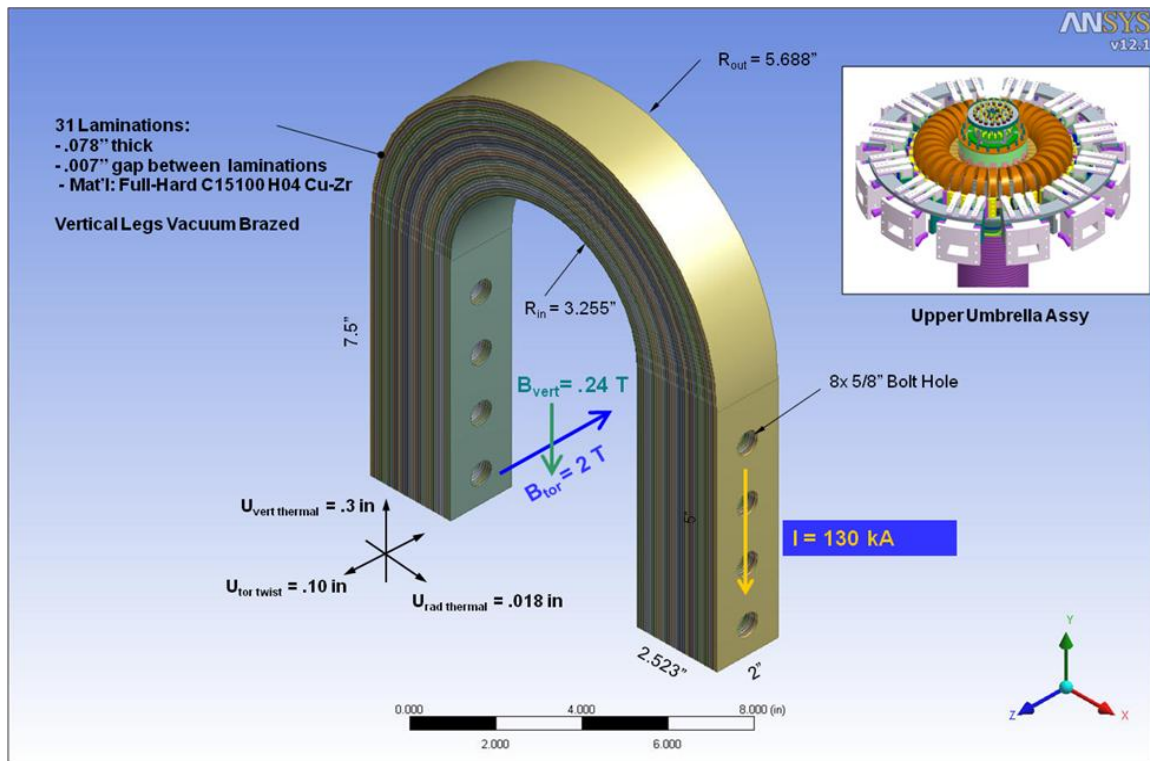
Figure 1 NSTX flex strap assembly and applied boundary conditions

Plymetal Shim Size:

Thickness = 0.010"
Width = 2.00"
Length = 7.50"
Quantity/assembly = 60

Or

Plymetal Roll
Length/assy = 37.5 ft

Plymetal Silver Braze Alloy = A50N (AWS BAg-24)

Silver	50.0 wt %
Copper	20.0 wt %
Zinc	28.0 wt %
Nickel	2.0 wt %
Total other elements	0.15 wt %
Solidus	1220 F (660 C)
Liquidus	1305 F (707 C)
Brazing Range	1305-1550 F (707-843 C)

Figure 2 Flex strap wolverine ply-metal Silver braze alloy
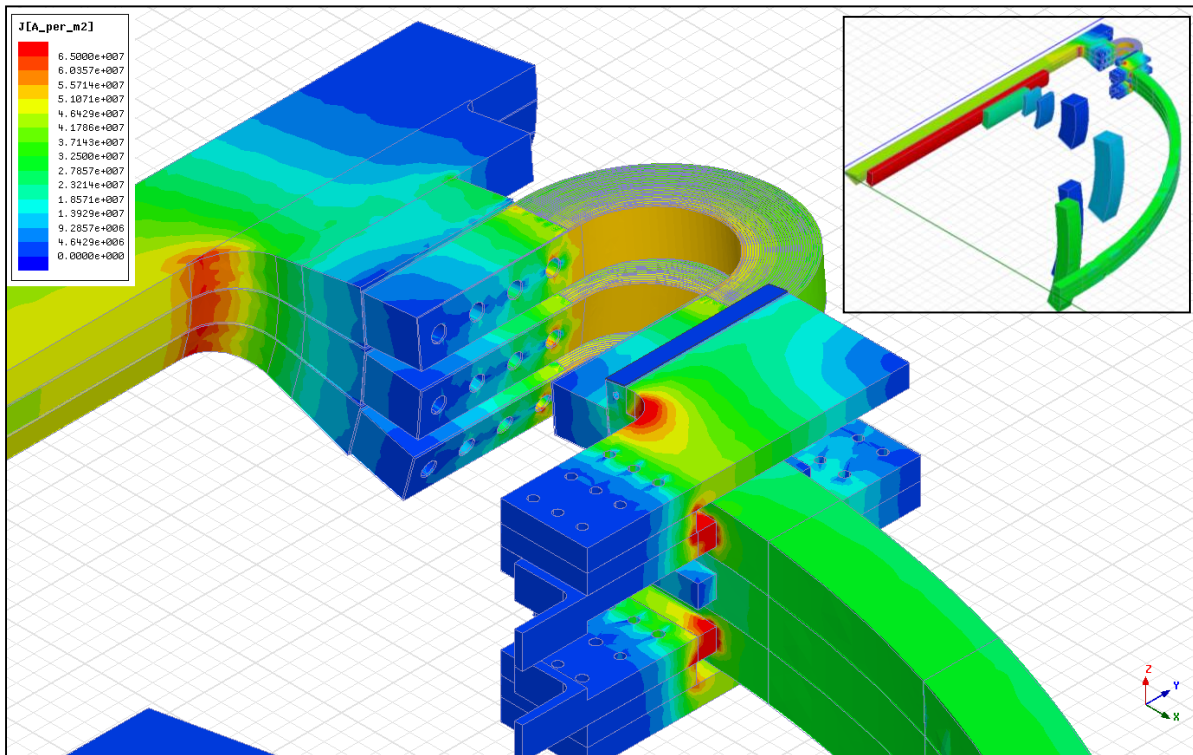
Figure 3 – Static current density for current scenario #82
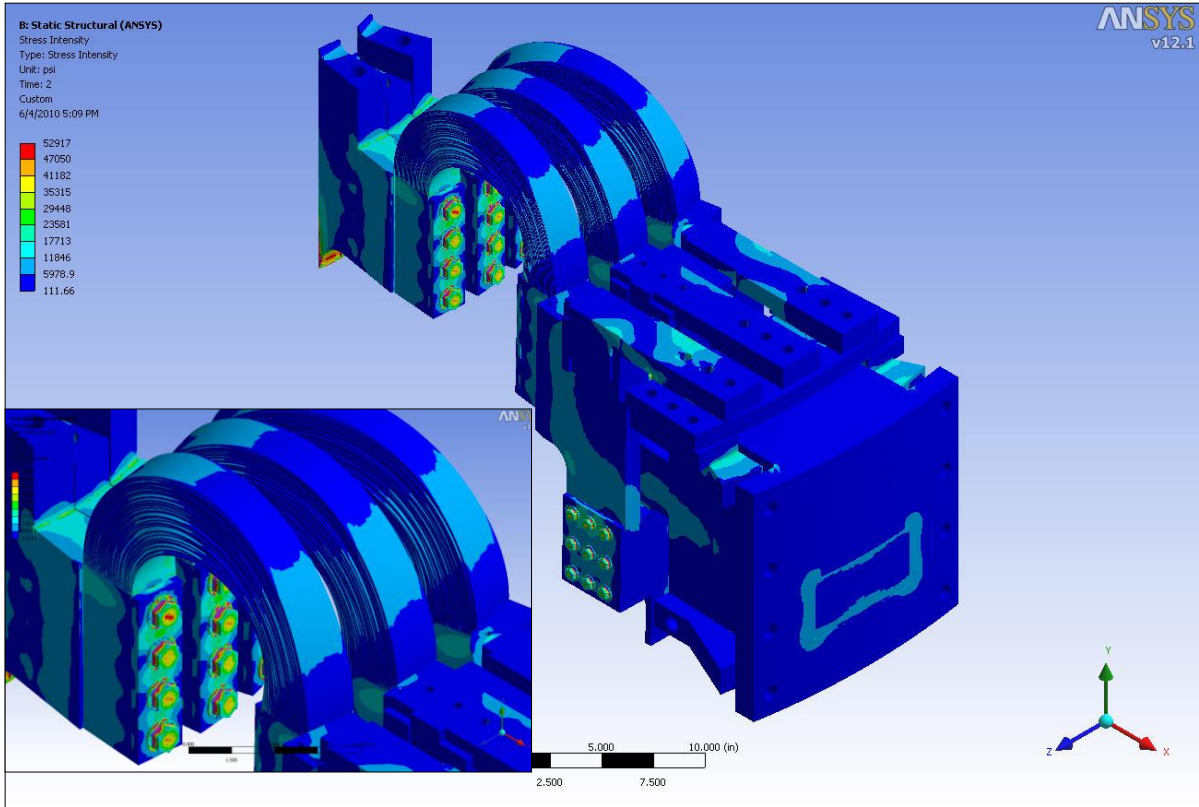
Figure 4 – Tresca stress distribution in flex joint for current scenario #82
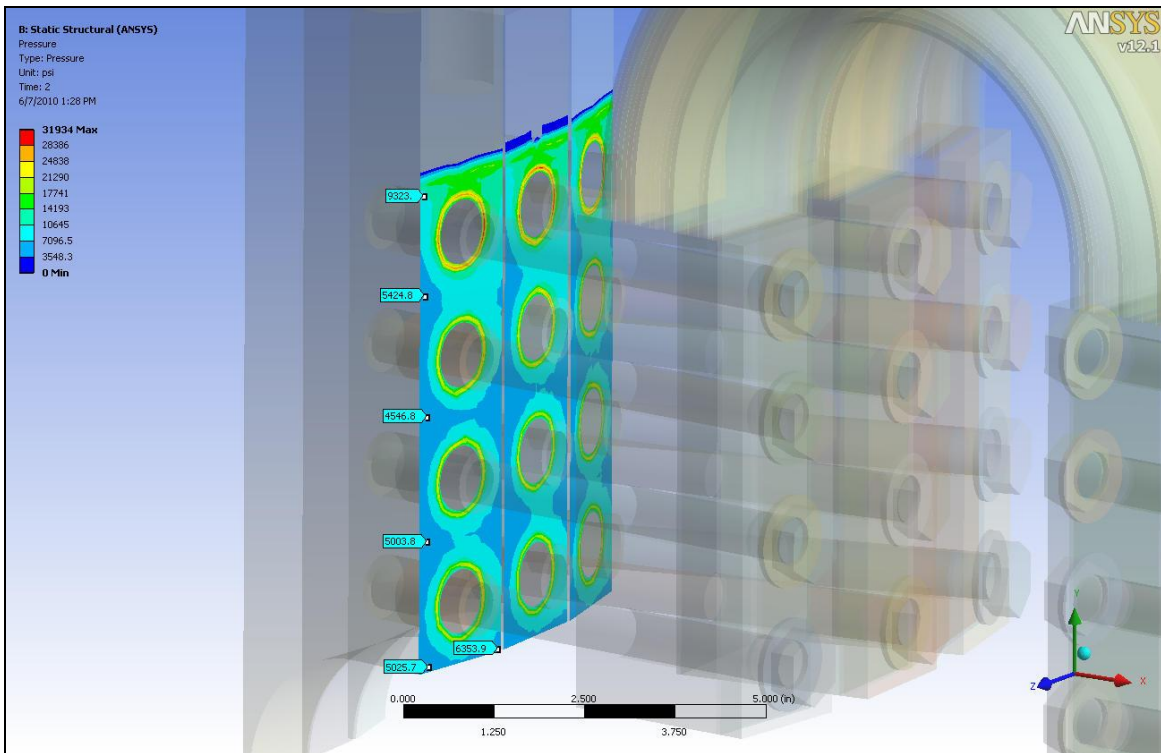
Figure 5 – Bolted contact pressure for current scenario #82; the minimum local contact pressure is >2500 psi (1000 psi above the minimum requirement)

Estimated C15100 H04 CuZr Fatigue S-N Curve
Olin Brass: Room Temperature; 40% CW; Reverse Bending (R-1)

S_u = 58 ksi
S_y = 57.6 ksi

20x Cycles

2x Stress

Ctr Flex Peak Stress

S - Strength (ksi)

N - Number of Cycles
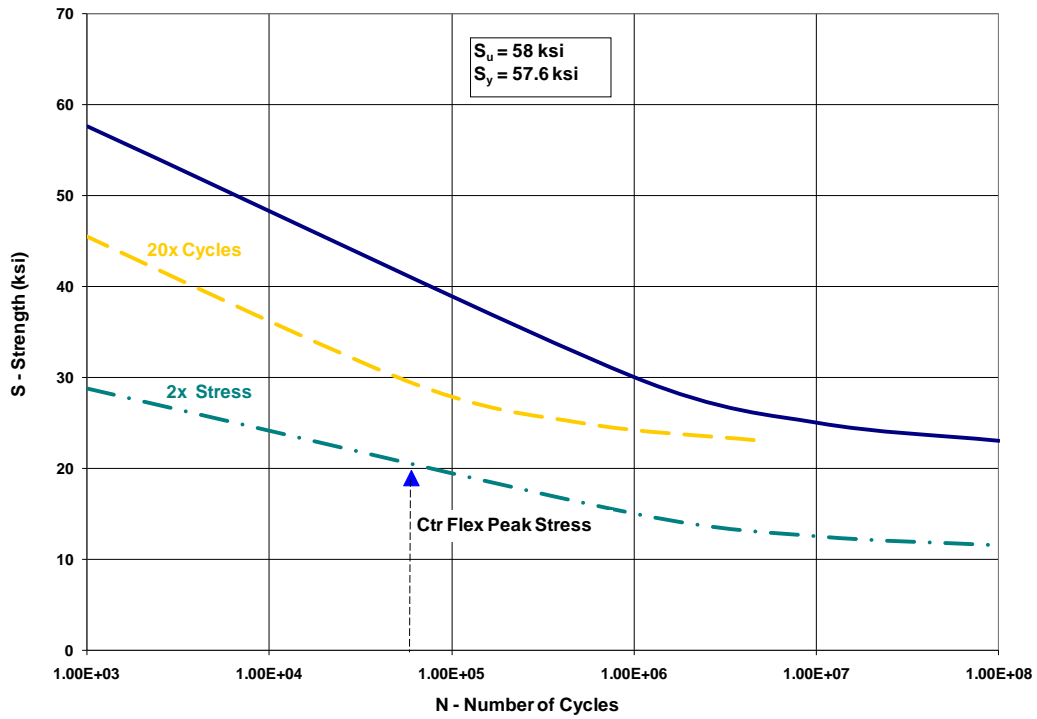
Figure 6 – Fatigue S-N curve for C15100 copper-zirconium; the lamination stress is slightly below 2x stress level and meets all the design requirements
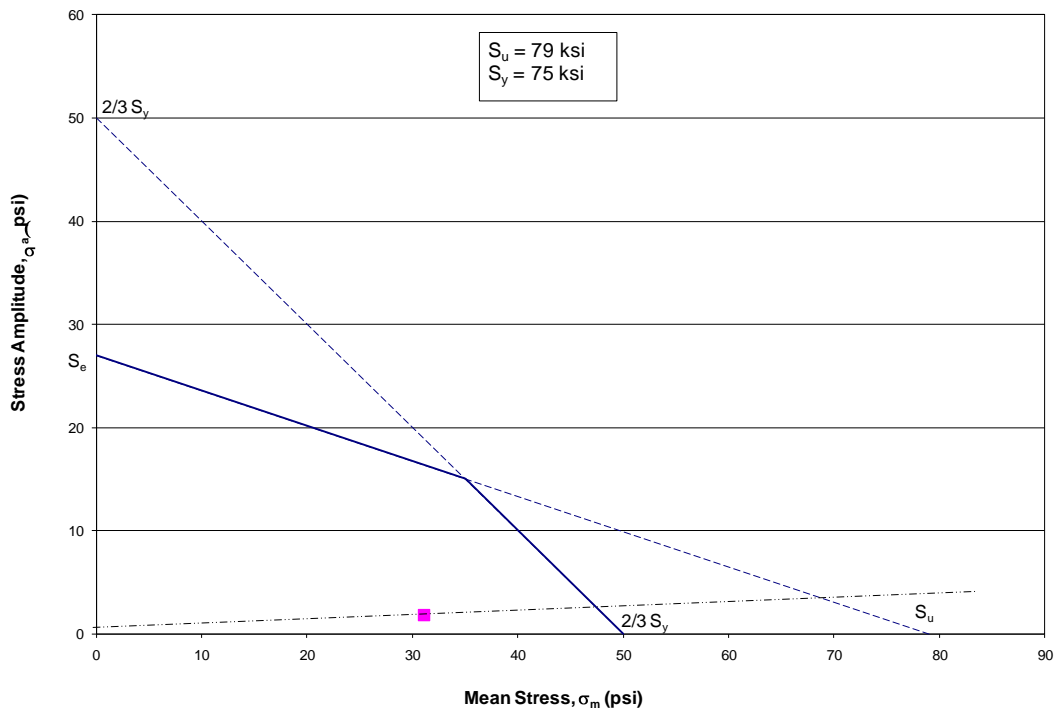
Figure 7 – Modified Goodman diagram for C18150 TL04 CuCrZr: thread Tresca stress meets all the design requirements
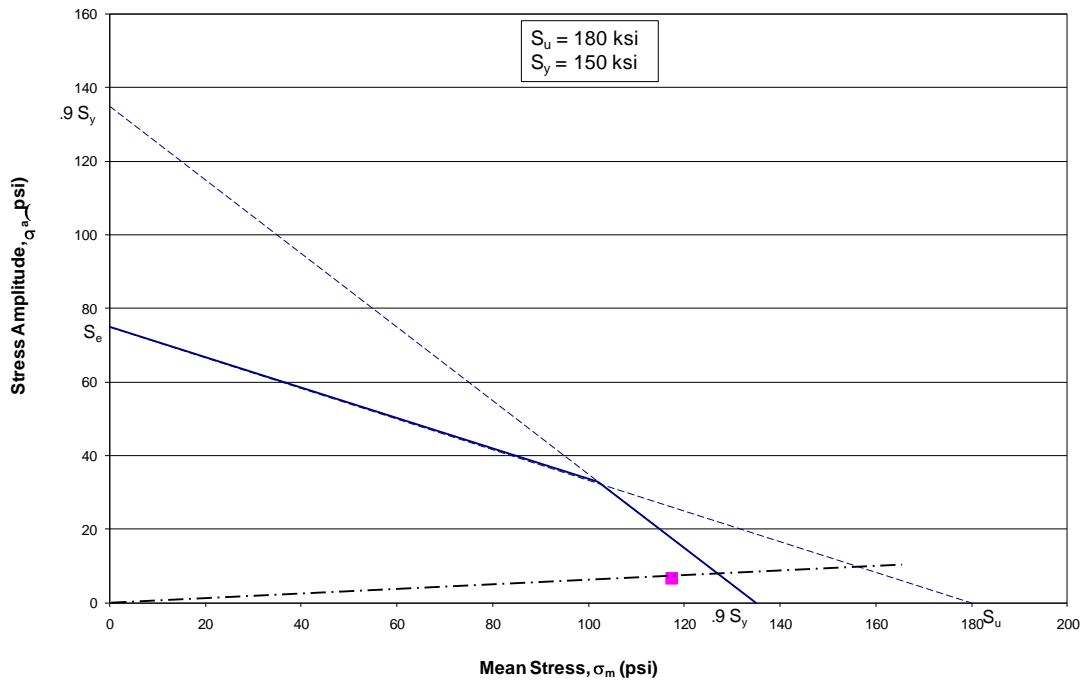
Figure 8 – Modified Goodman diagram: Inconel 718 AMS 5663 bolt tension stress

WBS 1.1.3 TF Inner Leg Torsional Shear, Including Input to the DCPS
NSTXU-CALC-132-07-00,
Prepared By: Peter Titus, Reviewed by Bob Woolley
Cognizant Engineer: Jim Chrzanowski

Executive Summary:

This calculation is intended to qualify the inner leg torsional shear stress and provide an appropriate algorithm for calculation of these stresses in the digital coil protection system (DCPS). The corners of the inner leg experience some current "bunching" due to the resistive and inductive behavior of the currents turning the corner at the flag extension. This produces some higher temperatures than the Design Point calculates [13] and the shear capacity of the epoxy bond degrades with higher temperature. From the global model simulations, the local Peak Shear stresses are below 24 MPa in the inner leg corners near the friction stir welded flags. The global model load files are based on the earlier +/-24ka OH scenarios and the use of the influence coefficients allows computation of the TF torsional shear for the latest set of scenarios.
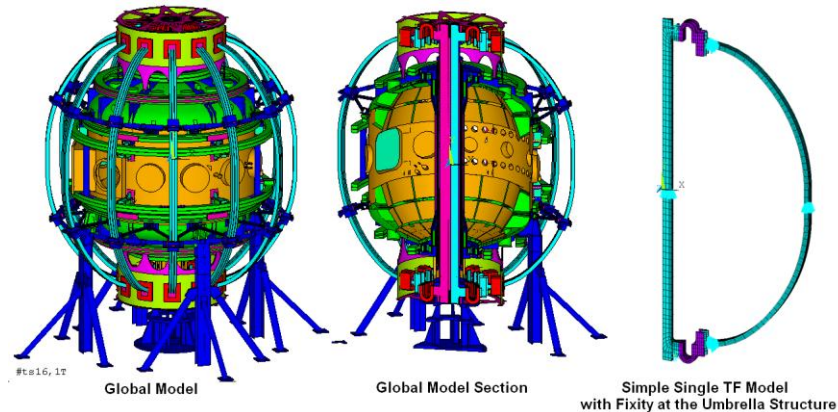
Figure 1 FEA Models Used for the Calculation if TF Inner Leg Shear Stress Influence Coefficients. The version of the global model has the overlaid plate reinforcements and the older pedestal and knuckle clevis

Based on the DCPS influence coefficient TF inner leg upper corner torsional shear, for all 96 June 3 2010 scenarios are all below 20 MPa with and without plasma. Rigorously these should have the 10% headroom applied (the coefficients do not include this) - So the torsional shear stress to compare with the allowable is 22 MPa. Pending acceptable results from testing the CTD-101K/Cynate ester primer system [14], the torsional shear is acceptable. Influence coefficients for the DCPS algorithm have been generated based on the global model [2]

For the worst PF loads considered in the global model, the peak torsional shear stress is 20 MPa – just below the allowable of 21.7 MPa. This analysis utilizes the global model described in ref [2]. The global model requires extensive set-up and run times and it has been difficult to maintain the model consistent with the design changes in the outboard structures. There have been some changes in the PF scenario as well between the CDR and FDR. The influence coefficient approach not only has utility for the DCPS, but also allows 16 load files, - 15 from the PF's and 1 from the plasma to be used in spreadsheet evaluations of the 96 scenarios with and without plasma. This replaces 192 load cases with 16load cases and spreadsheet calculations of the torsional shear.

Out-of-Plane (OOP) loads on a toroidal field (TF) coil system result from the cross product of the poloidal field and toroidal field coil current. Support of OOP loads is statically in-determinant, or multiply redundant, requiring an understanding of the flexibility of the outboard structures and the inboard stiffness of the central column. There are a number of ways in which the torsional shear stress in the inner leg of the TF can be calculated. The global model is the primary tool for this computation. A single TF model was

investigated to see if the inner leg OOP forces alone dominate and if the outer structures could be ignored. This turned out to be not the case. This means that the global torsional stiffness's of the umbrella structure, its proposed upgrade reinforcement, the port region stiffness, the top and bottom spoke assembly stiffness, and the pedestal stiffness all will have some effect on the inner leg torsional shear
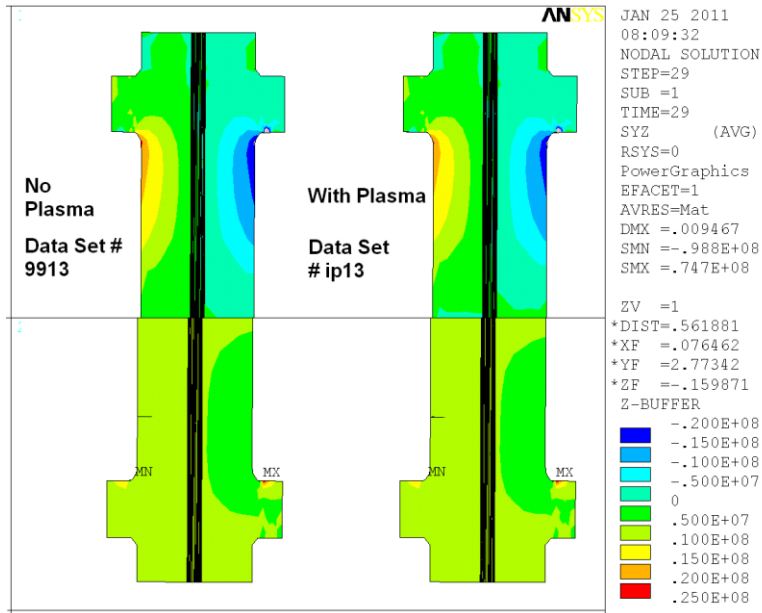
Figure 2. This shows one current set from the global model analysis, in which the plasma current effect on the torsional shear is difficult to discern. From the influence coefficient calculations it is about a 1 MPa effect (see Figure 6). The magnitude is close to 20 MPa.

Torsional shear stresses in the inner leg have been found to be slightly lower with the inclusion of the plasma in the load calculations; this has been found when applying loads calculated with and without the plasma on the global model, and also in the influence coefficient calculations.
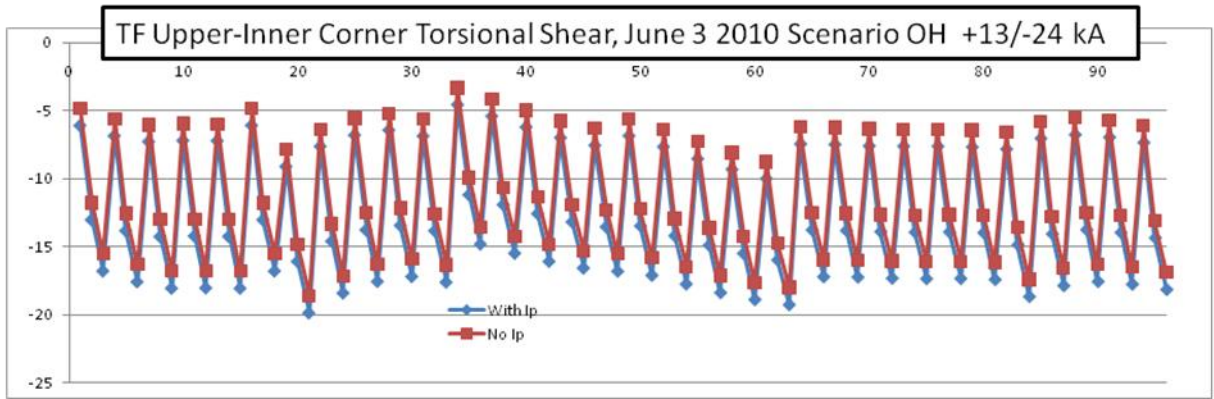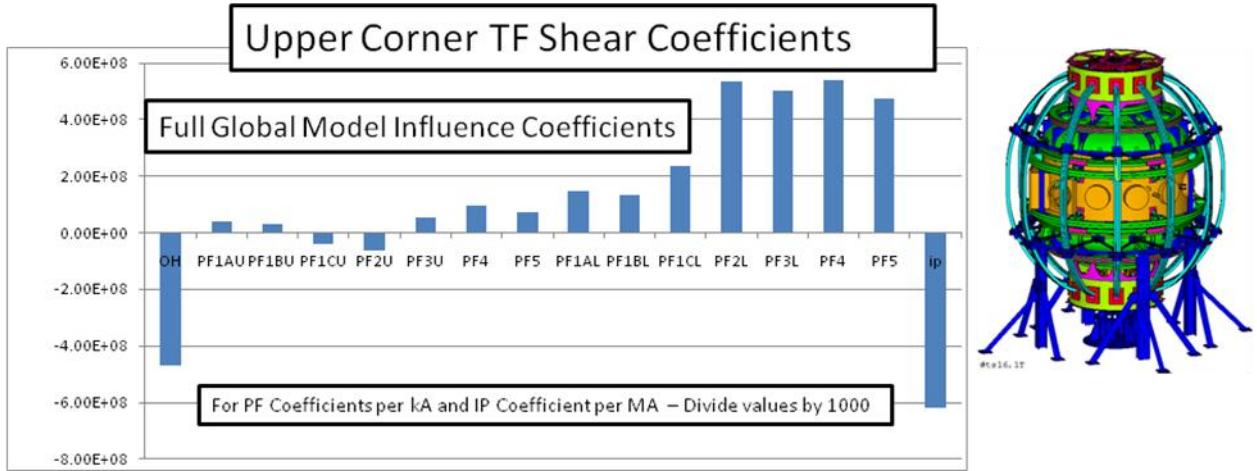
Torsional Shear Stresses from the influence coefficients multiplied by the Design Point Scenarios

Determination of Shear Forces between the TF Conductors NSTX-CALC-132-08-00
Prepared by: Ali Zolfaghari, **Reviewed by:** Tom Willard
Cognizant Engineering: Jim Chrzanowski

Executive Summary

The NSTX upgrade center stack TF conductors need to engage the G-10 insulating crown and exchange out of plane torques between the TF inner leg bundle and umbrella structure/vacuum vessel. A locking mechanism was designed which uses radial pins that engage the crown, the flags and the TF conductors. Expected torques and forces were obtained from the global FEA model for the worst case out-of-plane twisting loads. The forces and moments were exerted on a 20-degree cyclic symmetry FEA model of the mechanism. The simulations show manageable stresses in the G-10 and the epoxy insulation.
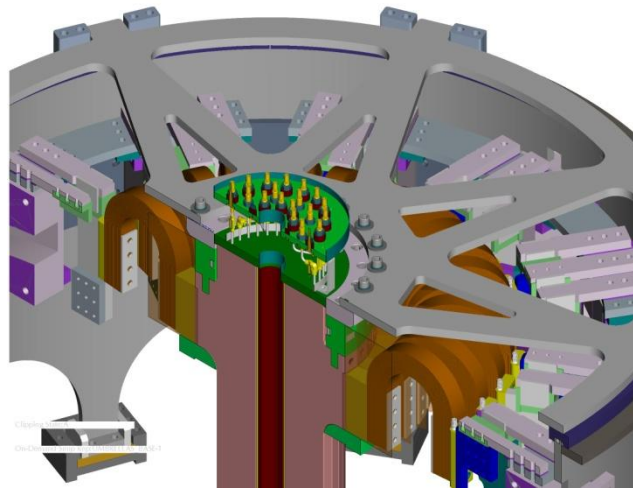
Upper Center Stack Design
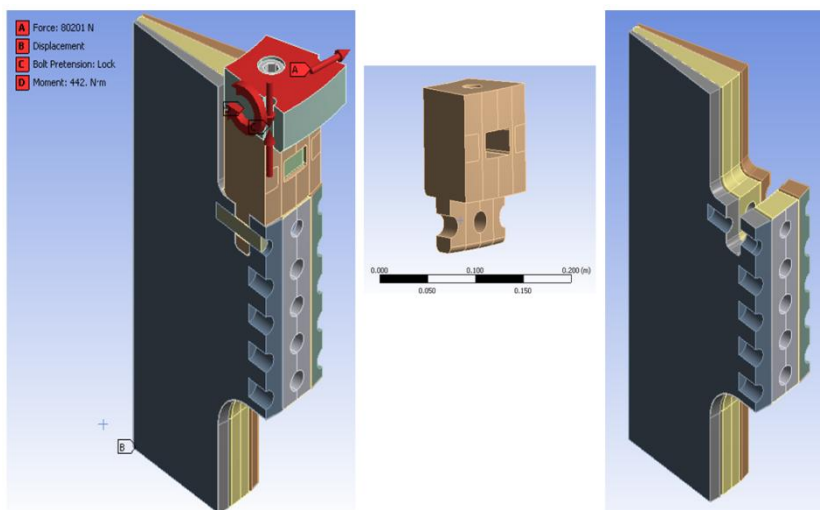
20 Degree Cyclic Symmetry Model
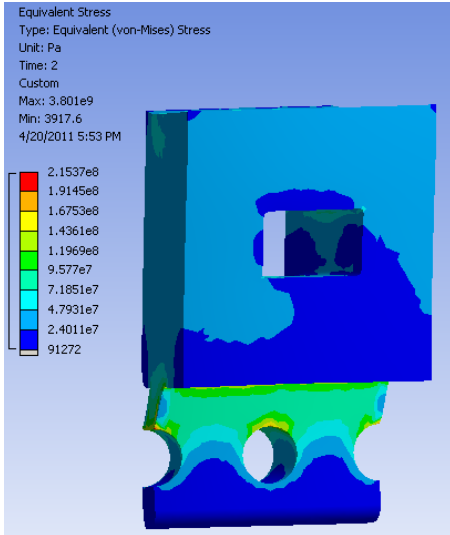
Equivalent Stress in G-10 Crown
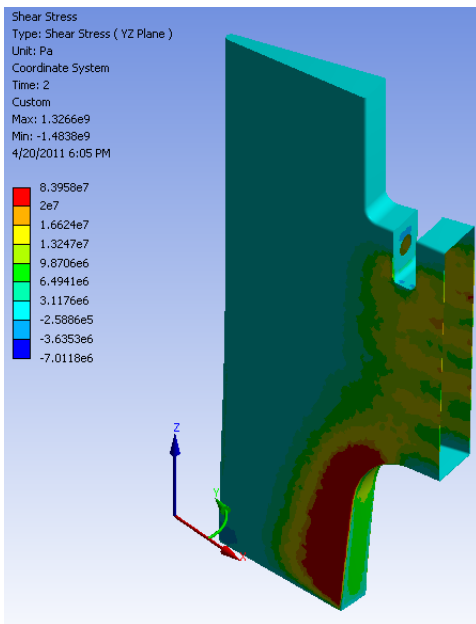
Shear Stress in the Insulation

TF Cool-down using FCOOL CALC-132-10-00
Prepared by: Ali Zolfaghari, **Reviewed by**: Mike Kalish
Cognizant Engineer: Jim Chrzanowski

Executive Summary

The objective of this analysis was to estimate the cooling time and temperature of the TF inner leg during the cooling period between discharges. The TF inner legs are cooled by water flowing in the coolant channels in each of the 36 TF conductors. 1D Finite-section transient simulations of flow and cooling parameters were performed using the Fcool code developed by Fred Dahlgren and the PPPL team. We have calculated that for 135,000A flowing in each TF inner leg conductor for a pulse width (equivalent square wave) of 8.5 seconds, the cooling takes 600-700 seconds.
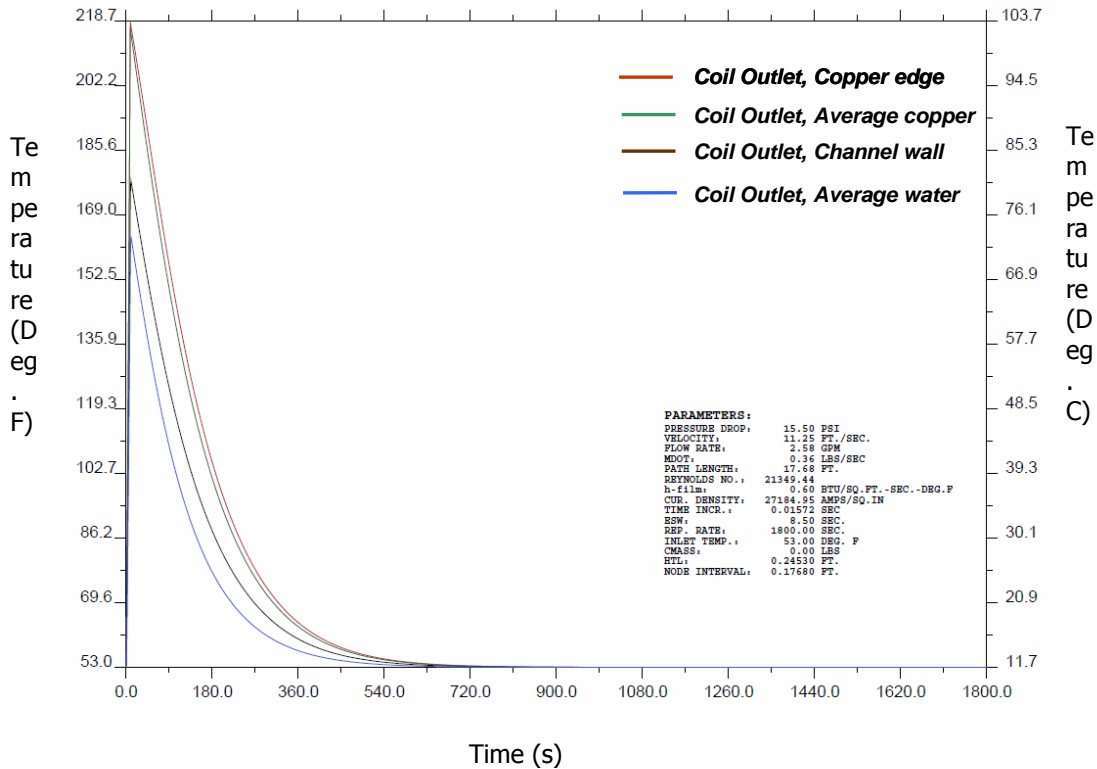
Figure 1: Temperature vs. time at the coil outlet

WBS 1.1.3 OH Preload System & Belleville Spring Design
NSTXU-CALC-133-04-00, Prepared By: Peter Rogoff, Tested by T. Kozub, Cognizant Engineer: Jim Chrzanowski

NSTX update requires the center column OH coil assembly to remain steady in its proper position during the applications of the TF and OH coils currents. The OH should remain steady since the cooling mechanisms could experience the unnecessary stresses. To accomplish this, a compressive force (pre load) on the upper surface of the OH coil is necessary. For these analyses a force of about 20,000 lbs. total, was estimated to accomplish this task. It was also calculated that during the maximum currents applications, the involved coils grow due to the following thermal expansions: TF coil expands 8.4 mm, while the OH coil 6.0 mm, and, may not occur at the same time. Therefore, a mechanical OH coil pre load system is required to regulate these variations? This is best accomplished by creating a disk springs stacks regulating system as is shown in the enclosed analyses.

OH Coil Pre Load System
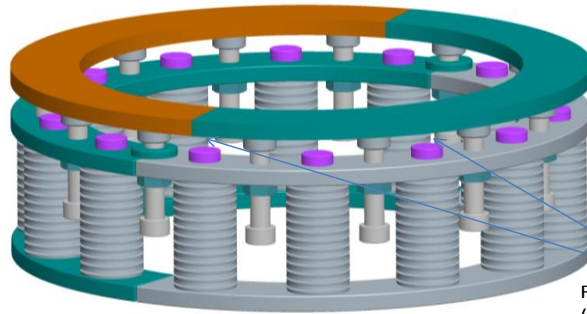
Spring dimensions:
26 disk springs/stack
Di = 30.5 mm
De =60.0 mm
t = 3.5 mm
Lo =5.0 mm
E = 206,000. Mpa
mu = 0.3

Required 14 stack to maintain a minimum of 20,000. lbs. total load on the OH coil

Note: Spring should be made from SS 301 material Depending on Stainless Steel conditions modulus of elasticity may be slightly different. In this case, minimum load on the OH coil may decrease by a small percentage (say 3 to 4 %) while everything else will stay the same.

Required gap = 23.87 mm (maximum permitted compression on the stack. Protects overloading of permitted spring stresses.)

Supporting calculations:

"TFhot OHcold26_14.ppt"
"TFcoldOHhot26_14.ppt"
"TFhotOHhot26_14.ppt"
"Spring Calculations in mm.xls"

System scenario	Compression mm	Force on OH N	Force on OH lbs.*	Tensile Stress N/mm	Fatigue Cycles
Pre Load	17.87	162,512	36,520.	849.	-----
TF hot OH hot	15.47	142,268.	31,970.	731.	2 Mil. +
TF hot OH cold	9.47	89,698.	20,157.	459.	high
TF cold OH hot	23.87	211,582.	47,546.	1185.	500,000

Thermal expansions:
  FT = 8.4 mm
  OH= 6.0 mm

  * Allowable OH launching loads.
Note: For supporting calculation see power point files for full details.

Bellville Washer Stack
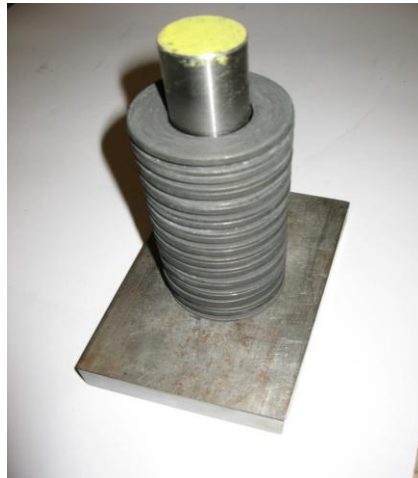
TEST SETUP

Bellville Washer Stack

SET 1 - CYCLE 1 -- K = 3922 lb/in
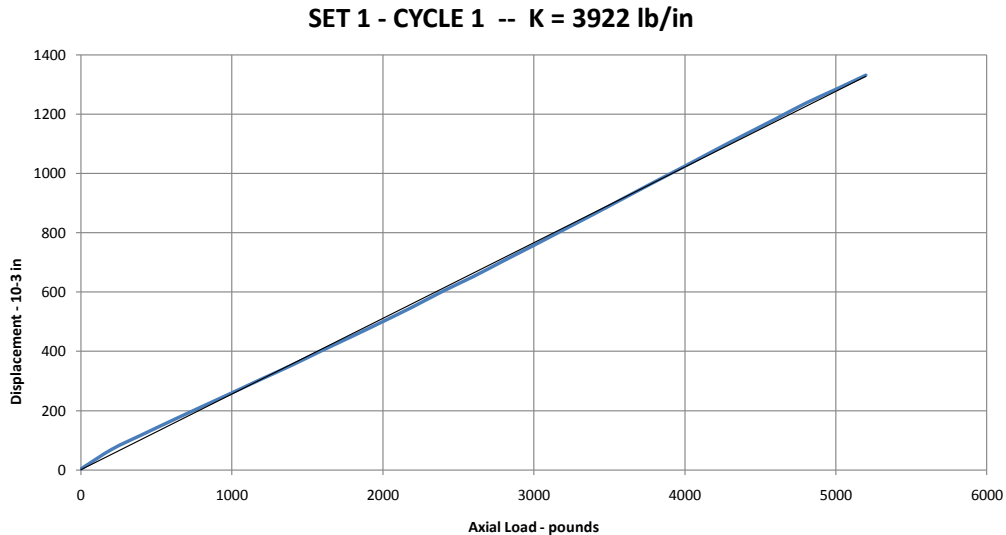
Comparison of the Calculated to Test data for a single washer stack

Test data Spring Rate = 3,922. lb/in

Calculated from the required minimum load on the OH coil,
Total Load = 20,157.0 lbs. at 9.47 mm displacement or = .373 in.
There are 14 Stacks, with 26 Bellville spring each.

Therefore: 20,157/14 = 2,128.5 lbs/mm,
        2,128.5 X 25.4 mm/in =54,064 lbs/in for 14 stacks,
       Than K = 54,064/14 = 3,862. lb/in

Calculated K = 3,862 lb/in

Spring rate check, at .373 in disp. is: 3,862. X .373 = 1,440 lb per stack
therefore, total load for 14 stacks = 1,440. X 14 = 20160. lb

WBS 1.1.3 Magnet Systems, Halo Current Analysis of Center Stack
NSTXU-CALC-133-05-00
Prepared By: Art Brooks**, Reviewed by:** Peter Titus**,**
Cognizant Engineer: Jim Chrzanowski

Executive Summary:

An analysis was done to estimate the inductive effects during a halo current strike. Previous analyses and guidance have assumed the flow of halo current thru structures is resistively distributed. The halo currents were modeled as a current source entering at one poloidal location and leaving at another. This assumed resistive distribution results in a potentially non conservative prediction of EM loads on the structures. Results presented herein show that the time constant for establishing the halo current flow is fairly long relative to the disruption timescale.
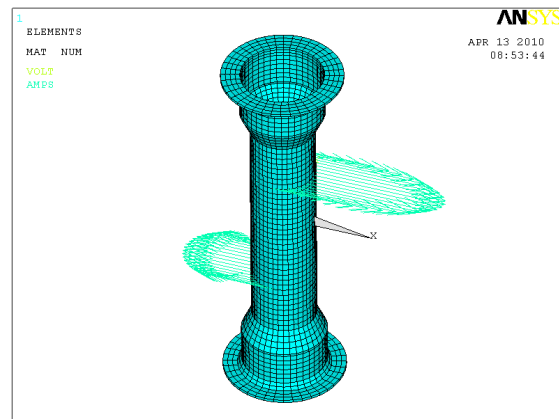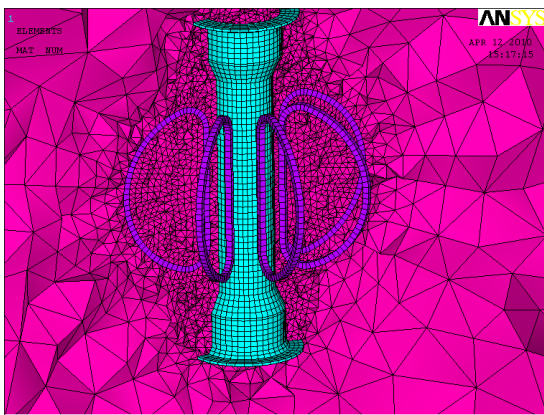
The coils representing the plasma halo are assumed to carry an initial current distribution totaling 400 kA but modulated to provided a (1+cos(phi)) distribution. The halo current strike is assumed to occur very quickly (a finite value 0.1 ms was used in the analysis) by ramping the current in the straight legs of the coils representing the plasma halo to zero while at the same time injecting equal current into the neighboring CS structure at z=+/- 0.6m

The injected halo current is assumed to persist (which could be argued, perhaps a waveform would be more appropriate) while the eddy currents in the CS redistribute over time.
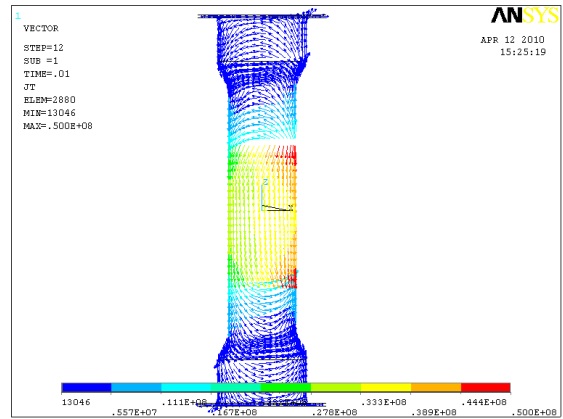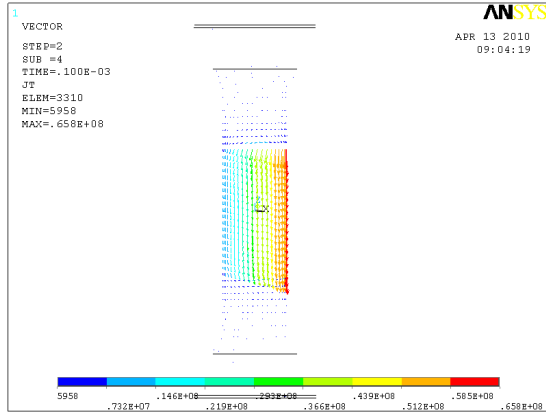
The left figures above show the Inductive Distribution immediately following the halo current strike on the CS. Distribution mirror initial assumed plasma distribution. The right figure shows the Resistive distribution 10 ms after halo current strike.

OH Coolant Hole Optimization, NSTXU-CALC-133-06-00
Prepared by: Ali Zolfaghari, **Cognizant Engineering:** Jim Chrzanowski

Executive Summary

The objective of this analysis is to estimate temperature rise in the upgraded NSTX OH coil during a discharge with 24 kA current and equivalent square wave time, Tesw, of 1.473 seconds. The objective also included estimating the cooling time between OH discharges as a function of pressure drop in the cooling pump. Based on these analyses the coolant channel size was to be checked in order to ensure that the maximum temperature of the coil remains below 100° C. The pump pressure required to keep the cooling time less than 20 minutes were to be estimated.

The analysis using in-house Fcool code showed that a coolant channel diameter of 0.225 in. is sufficient for achieving the required Tesw in the coil without exceeding 100° C. The results also show that a 430 PSI pump pressure (i.e. the existing NSTX pump system) can provide cooling times less than the 20 minutes required.

OH Inner Radius (Copper)	0.2074 m
OH Outer Radius (Copper)	0.2768 m
OH Ground & turn insulation	0.004 m
OH Height	4.2416 m
OH #turns	884
OH #layers	4
OH Conductor width	0.0155 m
OH Conductor height	0.0168 m
OH Cooling hole diameter	0.0057 m
OH Packing fraction	0.7013
OH Voltage	6077 V
OH Current Base	24000 A
OH Inlet Coolant Temp	12 °C
OH Maximum temp	100 °C
OH Copper Mass	2800 kg

OH Coil Design Parameters
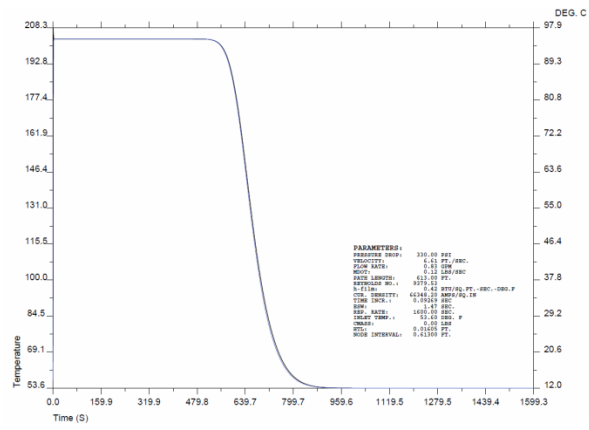
OH coil cooling with 430 PSI pump.

- OH coil can withstand hoop stress and shear stress at I=24kA.
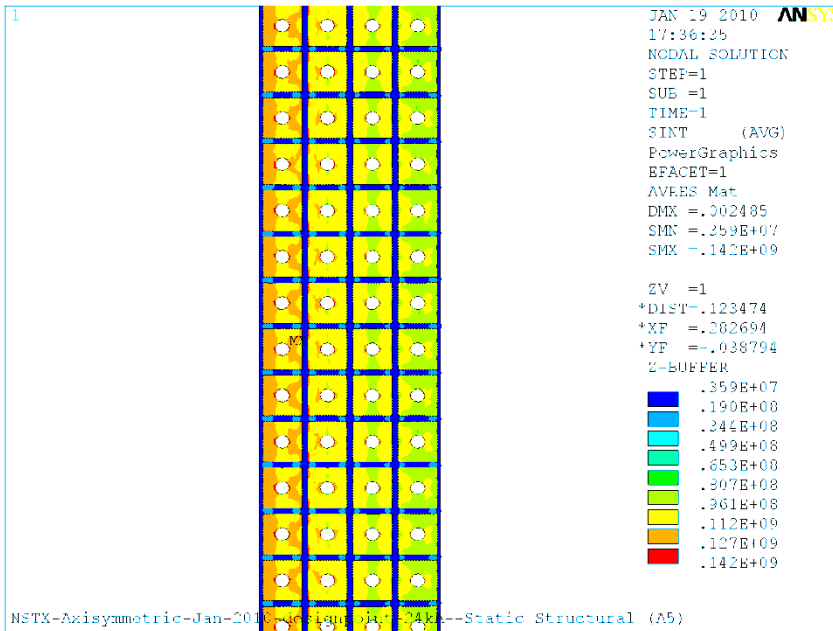
- In order to run the PF1A coil at 16.6 kA concurrently with the OH coil, the current in the OH will need to be limited to 13kA.
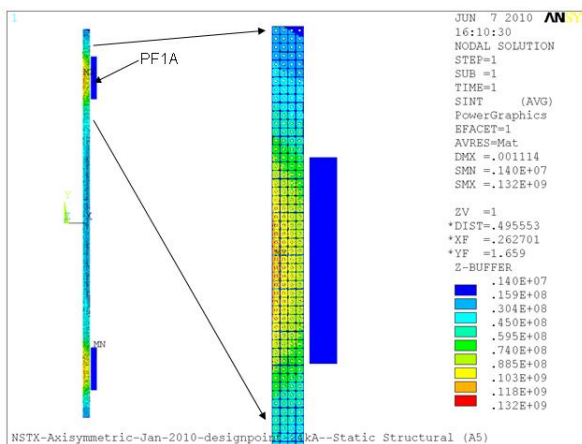
- Need to equalize flow velocity in the inside and outside OH turns in order to avoid large thermal stresses in the OH coil winding.
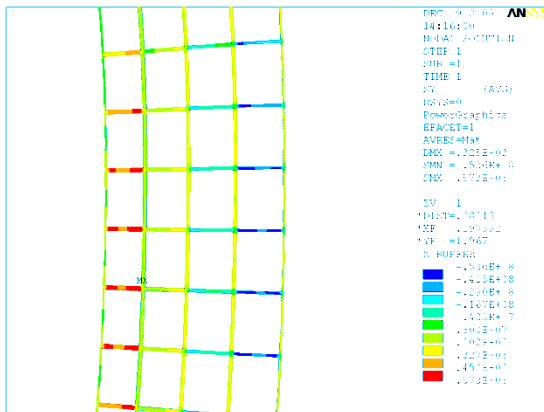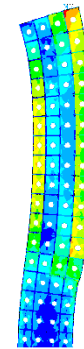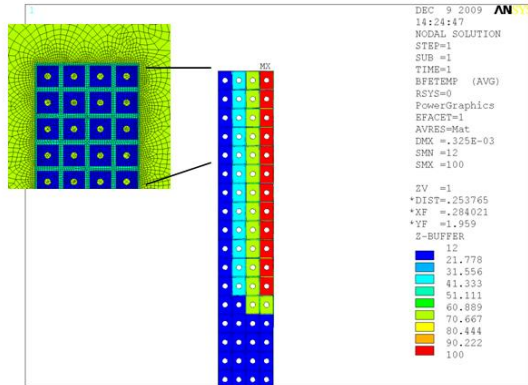
- In the bottom of the coil where cold water enters the hot coil and where the coil is attached to a cold G-10 base, stress in small localized regions in the insulation exceeds the limit. It is recommended to put a slip plane at the interface of the base and the outside layer of the coil.
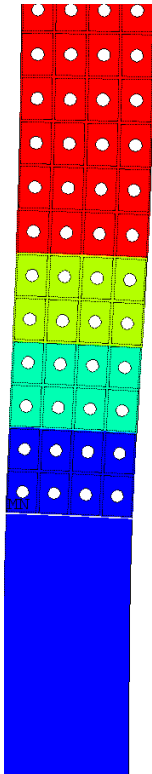
APR 29 2011
16:59:27
NODAL SOLUTION
STEP=1
SUB =1
TIME=1
BFETEMP (AVG)
RSYS=0
PowerGraphics
EFACET=1
AVRES=Mat
DMX =.005317
SMN =30
SMX =100

ZV =1
*DIST=.226133
*XF =.17986
*YF =-2.04767
Z-BUFFER

    30
    37.7778
    45.5556
    53.3333
    61.1111
    68.8889
    76.6667
    84.4444
    92.2222
    100
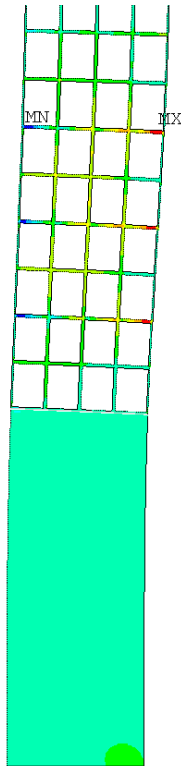
16:49:26
NODAL SOLUTION
STEP=1
SUB =1
TIME=1
SXY   (AVG)
RSYS=0
PowerGraphics
EFACET=1
AVRES=Mat
DMX =.005317
SMN =-.705E+07
SMX =.929E+07

ZV =1
*DIST=.226133
*XF =.17986
*YF =-2.11551
Z-BUFFER

    -.705E+07
    -.524E+07
    -.342E+07
    -.161E+07
    210591
    .203E+07
    .384E+07
    .566E+07
    .748E+07
    .929E+07
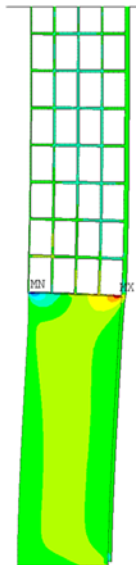
MAR 31 2011
11:39:59
NODAL SOLUTION
STEP=1
SUB =10
TIME=1
SXY   (AVG)
RSYS=0
PowerGraphics
EFACET=1
AVRES=Mat
DMX =.005414
SMN =-.129E+08
SMX =.139E+08

ZV =1
*DIST=.206876
*XF =.247872
*YF =-2.12832
Z-BUFFER

    -.129E+08
    -.996E+07
    -.698E+07
    -.400E+07
    -.101E+07
    .197E+07
    .495E+07
    .793E+07
    .109E+08
    .139E+08
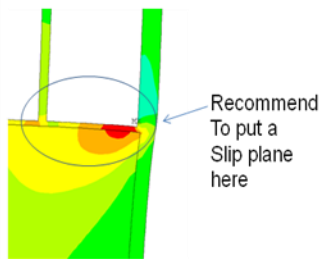
Recommend
To put a
Slip plane
here

Executive Summary as in the report:

Analysis shows that the OH coil can withstand hoop stress and shear stress at I=24kA. The analysis also revealed that in order to run the PF1A coil at 16.6 kA concurrently with the OH coil, the current in the OH will need to be limited to 13kA. The stress in the OH coil due to hot-OH cold-TF scenario was found to be acceptable but the frictional shear along the length of the TF-OH interface produces unacceptable vertical tension in the OH coil. Mechanical solutions such as low friction interface and removable interface layer as well as electrical solutions in the coil protection system need to be considered for this problem.

In analyzing the cooling stresses, we also pointed out the need to equalize flow velocity in the inside and outside OH turns in order to avoid large thermal stresses in the OH coil winding. In the bottom of the coil where cold water enters the coil that has been heated to near 100 Deg C due to the current and where the coil is attached to a cold G-10 base, stress in small localized regions in the insulation exceeds the limit. It is recommended to put a slip plane at the interface of the base and the outside layer of the coil.

There are two bellows used on the NSTX center stack, upper and lower. These form a vacuum connection between the center stack casing and the insulated ceramic break and the rest of the vacuum vessel structure. The bellows must maintain the normal vacuum conditions for the necessary operation of the NSTX device under various load conditions, which include the bake-out and other thermal scenarios. This calculation is intended to justify and recommend convolution geometry and acceptable thickness of the bellows as an initial sizing exercise, and then provide the design specifications for the purchase of the bellows. Ultimately, the bellows manufacturer shall provide the qualification of the bellows. To ensure an adequate initial design, this calculation provides qualification of the acceptable stress state and performance for the various load conditions.

- Halo Current Loads (upper bellows only). Reference calculation #NSTX CALC 133-04-00.

- The upper bellows must allow thermal motion due to the bake-out and the normal operation where heat from the plasma is transferred to the CS casing through the insulating tiles. Reference calculation # NSTX CALC 11-01-00.

- The upper bellows must support the seismic loads, Reference calculation #NSTX CALC 10-01-02.

- The upper and lower bellows transmit some portion of the torsional moment from the upper vessel structure to the center stack casing. This moment comes through the umbrella structure, Reference calculation # NSTX CALC 10-01-02.

- Pressure due to vacuum condition which is always present during any operations of the machine.

These calculations were performed using:
- EJMA (Expansion Joint Manufacturers Association) Basic equations presented in section 4.13 of the manual.

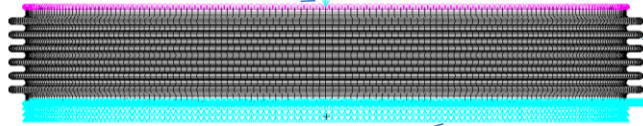- NASTRAN Version MSC FEA x64 2010.1.2 finite element code.
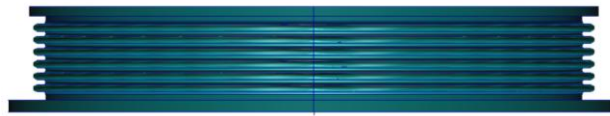
Modulus of Elasticity = 29,000,000.
stainless steel (FEA and EJMA)
t = variable (.02, .025, .03) in.

Di = 38.0 inches
Do =40.25 inches

w = 1.095 in. convolution height
q = 1.0 in. convolution pitch

COMPLETE FEM MODEL

Node #49436 – central, RBE2 independent
Deformations and loads applied through it.

Fixed : x, y, z, Rx ,Ry, Rz

```
M O D E L   S U M M A R Y

NUMBER OF GRID    POINTS   =   45301

NUMBER OF CQUAD4  ELEMENTS =   45000

NUMBER OF RBE2    ELEMENTS =       2
```

Note: All stresses reported are for cquad4 surface "Z2" . This is the bellows inside surface.

Design justification for the NSTX Update Bellows

FEM model simulation: Quad4 NASTRAN element with various convolution thicknesses.
For present analyses, .020, .025 and .030 in.

Load conditions:
1) 8 mm - Axial compression due to the CS expansion.
2) Static Pressure = 14.5 psi.
3) TORSIONAL deformation = .00315 in. (Applied as pure moment values.
which were calculated from P. Titus inputs).
4) Halo Loads Reactions at the bellows (variable as per bellows thickness
as calculated from A. Brooks inputs).
Note: Conditions #3 and #4 change, based on the selected material thickness.

EJMA equations and related constants were used to test and justify the validity of the
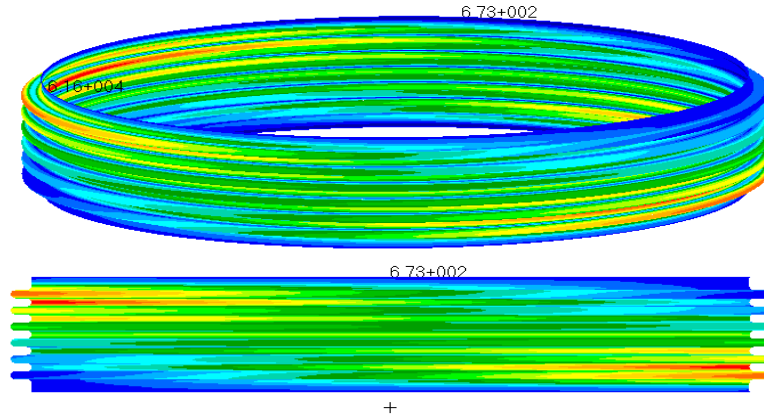FEM simulation using axial deformation and pressure loads:
Eq. 4-30, 4-31, 4-32, 4-33 and 4-37.
EJMA constants: Cp, Cf and Cd.
Figures 4.16, 4.17, 4.18.
Figure 4-20 for fatigue life estimates.

COMPLETE FEM MODEL with combined loads

Delta Y = -.315 in = 8 mm (CS thermal expansion)

Delta X = .02 in = .508 mm (from 204,200. shear rate) Halo load

tn = .03 in, w = 1.095 in, q= 1.0 in.

Torque = 147,400. in-lbs (.00315 in torsion)

Spring Rate, X-Dir = 204,200 lbs/inch

STATIC PRESSURE 14.5 psi

	6.16+004
	5.75+004
	5.35+004
	4.94+004
	4.53+004
	4.13+004
	3.72+004
	3.32+004
	2.91+004
	2.50+004
	2.10+004
	1.69+004
	1.29+004
	8.79+003
	4.73+003
	6.73+002
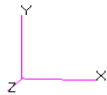
default_Fringe :
Max 6.16+004 @Nd 24937

Summary of stresses for total loads combination

Thickness		von Misses	Max Shear	delta Y	Delta X	Pressure	Torque	X-Spring Rate
inches		psi	psi	inch	inch	psi	in-lbs	lbs/inch
0.02		66,800.0	36,700.0	-0.315	0.0374	14.5	98,211.0	71,200.0
0.025		64,500.0	35,700.0	-0.315	0.0284	14.5	122,800.0	128,200.0
0.03		61,600.00	34,200.0	-0.315	0.02	14.5	147,400.0	204,200.0

Notes: For INCONEL, say, Sy=95,000 psi, 2/3Sy = 63,300 psi, Bellows thickness of .030 in can be selected

X-Spring Rate is based on 1 .0 mm (.0394 inch) shear deformation and for selected bellows thickness,
Delta X is calculated using this spring rate.

Torgue is based on the toroidal deformation (.8e-4 m) of the selected bellows thickness
Applied at Node # 49436 as "Moment Y" (d.o.f. "Ry" through Nastran "Coord 0")

Delta Y due to the CS thermal expansion

Pressure always present

WBS 1.1.3 OH & PF1 & 2 Electromagnetic Stability Analyses
NSTXU-CALC-133-11-00 Rev 0 March 2 2010
Prepared By: Peter Titus, Ali Zolfaghari, Reviewed By: H.M.Fan,
### Cognizant Engineer: Jim Chrzanowski

Executive Summary:

The possibility of magnetic instabilities of the various poloidal coils was raised at the CDR and PDR. All the coils are well supported off the vacuum vessel or centerstack casing. There are no coils supported by light, flexible supports. PF 1a and 1b upper and lower are mounted on the centerstack casing. The radial connection between the centerstack casing and the rest of the NSTX structure is rigid and strong at the lower casing connections. A "skirt" connects the lower casing flange to the lower TF flag structures. PF1 (a) and (b) lower are aligned stiffly with respect to the OH. At the upper end there is no connection between the centerstack and the TF or the OH. Alignment is maintained by the upper bellows. The OH is also well positioned with respect to the TF at the lower end through the "skirt", but at the upper end, alignment is maintained by the lateral stiffness's of the Belleville preload mechanism. The centerstack TF components are well centered by the spoked lid and collar. This calculation addresses the magnetic stability of the centerstack assembly with respect to the OH coil; Magnetic loads that result from a unit offset of the centers of the coils are computed in MAXWELL. This establishes a Magnetic "stiffness". This is then compared with a structural stiffness. The structural stiffness must exceed the magnetic stiffness for the coils to be stable. The magnetic stiffness was calculated to be .637 MN/m and the structural stiffness was calculated to be 425 MN/m

Magnetic Stability of PF's and OH

The Centerstack Stability with Respect to the Rest of the Poloidal Coil System relies on the stiffness of the Upper and Lower Lid – and some centering system of the OH with Respect to the TF (Bumpers in the Gap? Lateral Stiffness of the Belleville Spring Stacks?)

Other Stabilities Need to Be Addressed
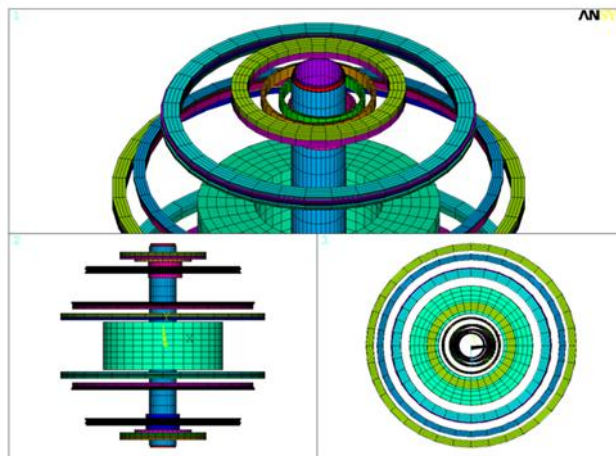
Stability of PF1a,b with Respect to the OH

Magnetic Stability of PF1a With Respect to the OH
## A Zolfaghari MAXWELL Results

PF1a is supported off the centerstack casing which is stabilized laterally by the bellows/ceramic break assembly. The stiffness of the supports must be sufficient to overcome the magnetic stiffness. To quantify the magnetic stiffness the Lorentz force between the OH and PF1a coils was calculated for different lateral offsets.

Pf1a and Oh coils dimensions and arrangement were used from the latest design point.

Coil	Current (kA)	Turns
OH	24	884
PF1a	18.3	64
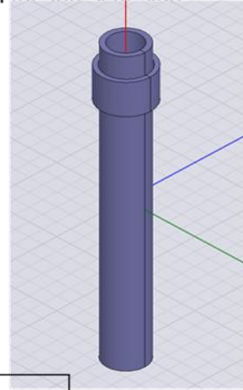
The PF1a is moved 2mm and 5mm in the positive Y direction.
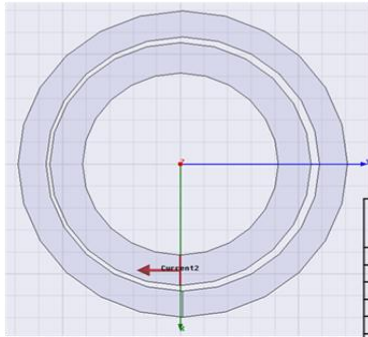
Magnetic Stiffness=
3189/.005 N/m =
.637MN/m

Orientation of currents	PF1a Offset (mm) in +Y direction	Force on PF1a (N) in +Y Direction
Parallel	2	1191
Opposite	2	-1255
Parallel	5	3167
Opposite	5	-3189
Parallel	0	-141
Opposite	0	125

NTFTM Calculation of Shifted Coil Loads
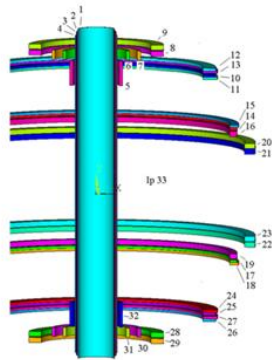
PF Model Consistent with J. Menard's
33 coil set Equilibria
Used as a starting point to create the model at right.
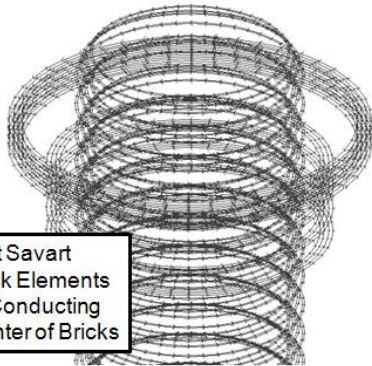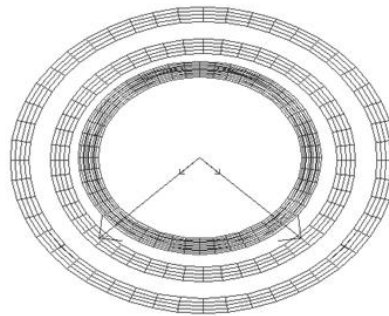
Biot Savart Stick Elements at Conducting Center of Bricks
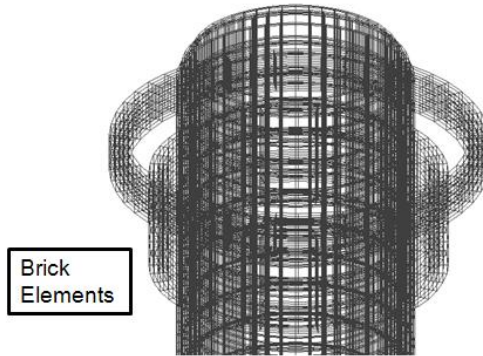
Brick Elements

PF 1a,b (real 5, and 6) shifted 1 cm with respect to the OH (real 1 through 4)

WBS 1.1.2 Vessel Rework for the Neutral Beam and Thomson Scattering Port
NSTXU-CALC-24-01-00
Prepared By: T. Willard **Reviewed by:** A. Zolfaghari
**Cognizant Engineers:** M. Smith, G. Labik, C. Priniski

The purpose of this calculation was to qualify the NSTX upgrade changes to the vacuum vessel (VV) midsection required to accommodate the addition of a second Neutral Beam (NB) at Port J and the larger diameter port at Port L. Specifically, the goal was to determine the maximum stress in the VV midsection and port extensions under the worst-case simultaneously applied load conditions. The applied loads include: vacuum/ atmospheric pressure, magnetostatic Toroidal Field (TF) coil torsion load, and the electromagnetic transient plasma disruption, with a dynamic load factor of 1.8. Refer to figure 1 for the Maxwell current density plot and figure 2 for the Ansys WB loads and constraints.

The results of the one-way coupled electromagnetic-static structural analysis show the maximum stress occurs at the intersection of vessel wall and the J-K port cap extension, along the perimeter weld seam, and is below the maximum allowed by the NSTX Structural Design Criteria. Refer to figure 3. A detailed fatigue analysis of the weld, submodeled from the global model with the full inventory of loads for the worst-case current scenario, is required to fully qualify the NSTX upgrade changes.

Update 5-13-2011
Prepared by: M. Smith
In order to reduce the stress, various reinforcement schemes have been proposed and analyzed. Several approaches show significant reduction in stress. The current approach uses localized thickening of the VV wall in conjunction with reinforcing gussets and plates. However, there is concern the thicker VV wall will adversely affect various diagnostic coils. While this adverse affect is being quantified, other reinforcement designs are being evaluated.
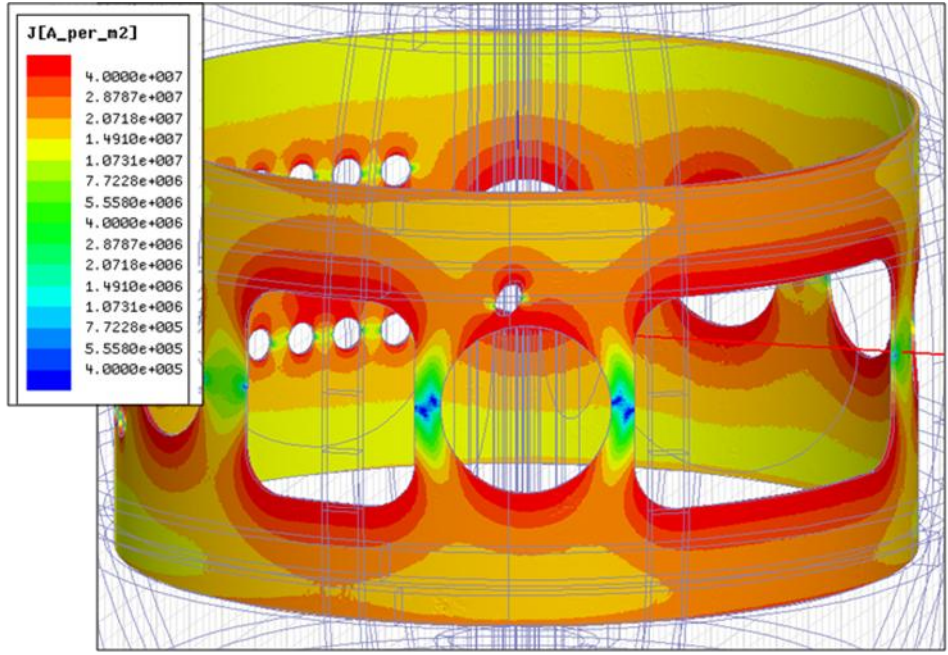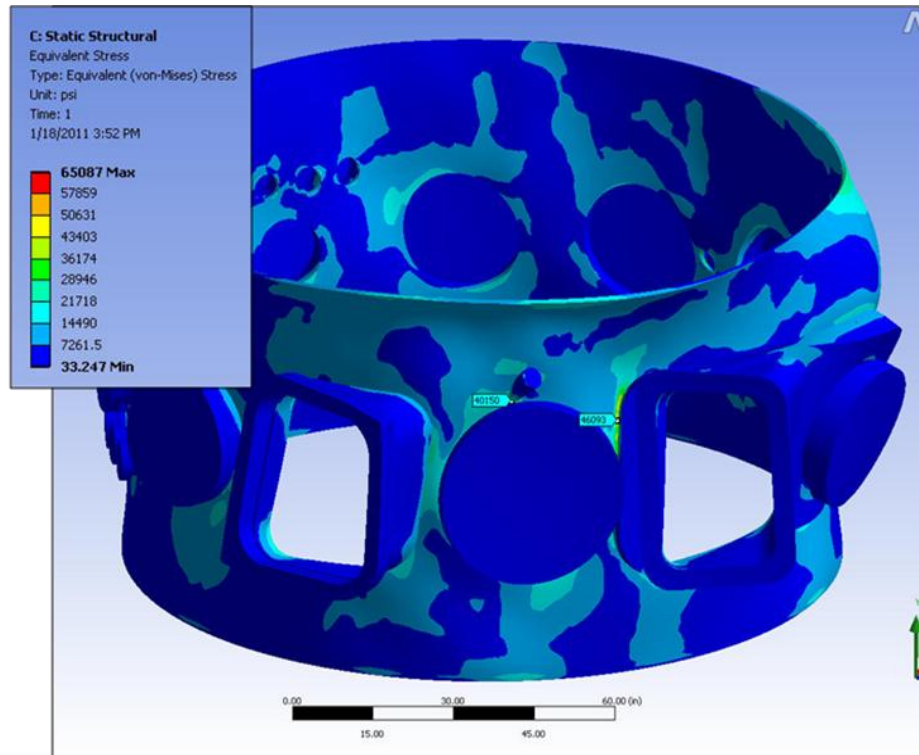
Eddy Current Density on Vacuum Vessel w/o Ports: End of Quench
1ms Centered-Plasma Disruption: Current Scenario #79 w/ Headroom Background Field

Figure 1: Maxwell Results: Disruption Eddy Currents
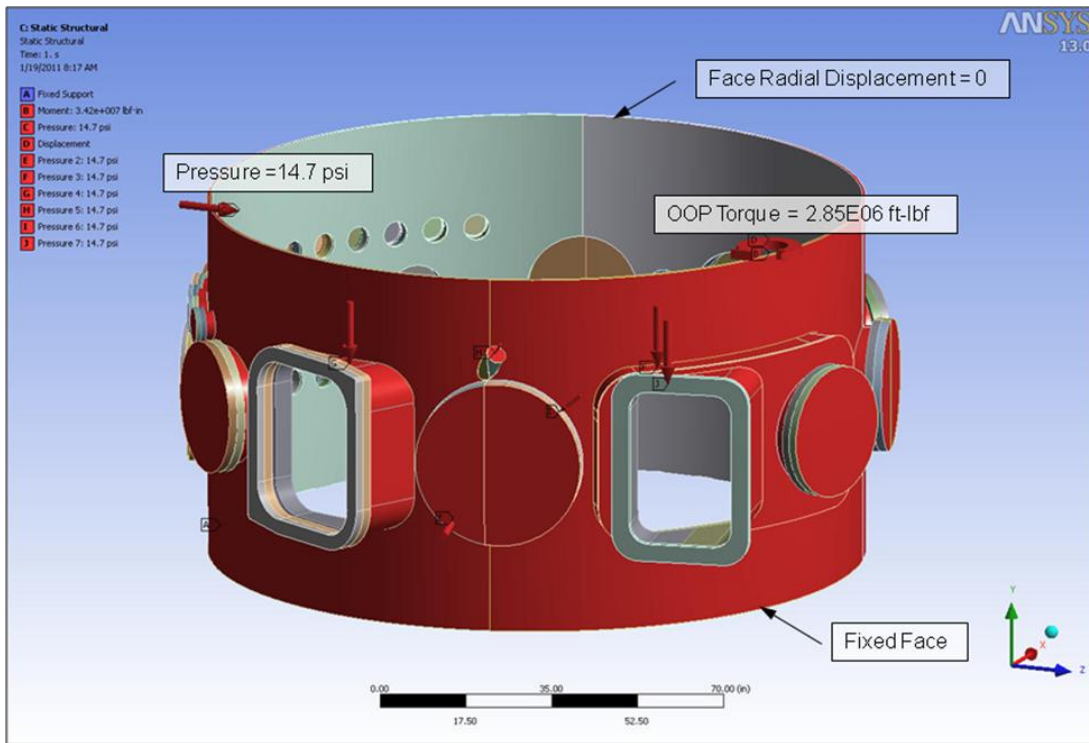
Figure 2. ANSYS Static Structural Model: Loads and Boundary Conditions

Static Structural Results, Ports Excluded from EM Solution: von Mises Stress
1 ms Centered-Plasma Disruption: Current Scenario #79 w/ Headroom Background Field

Figure 3: Ansys WB Static Structural Results Von Mises Stress (psi)

Diagnostics Analysis Summary

The purpose of this analysis is to predict any unintended effects that the NSTX-CSU may have on the diagnostic systems, including mechanical failure of the shutters, material degradation from radiation, and any other perceived threats to the diagnostic. record any analysis concerning the diagnostics. A sample entry in this database can be seen on the right. The database is a living document that is updated as more information is discovered or becomes available.

Table 1, below, lists the diagnostics and the most likely cause(s) for concern for each diagnostic if there are any. The information in A sample entry in this database can be seen on the right. The database is a living document that is updated as more information is discovered or becomes available.

Table 1 was taken from a database that is used to record any analysis concerning the diagnostics. A sample entry in this database can be seen on the right. The database is a living document that is updated as more information is discovered or becomes available.

Table 1. *List of diagnostics and the most likely cause for concern and relevant comments for each diagnostic.*

Diagnostic	Causes for Concern/Comments
"Optical" soft x-ray array	None. Diagnostic is being replaced.
1-D CCD Hα cameras (divertor, midplane)	See General Concerns for Cameras
2-D divertor fast visible camera	See General Concerns for Cameras
Beam Emission Spectroscopy (BES) (32 ch)	Uses forced air cooling for optics during bakeout. If heating becomes a problem, cooling could be used constantly. Glass for optics could be darkened by radiation.
Biased Electrode and Probe	Should be unaffected. Will also be modified before

(BEAP)	upgrade.
Charge-Exchange Recombination Spectroscopy (CHERS): Ti(R) and VΦ(r) (51 ch)	Optics could be darkened by radiation.
Diamagnetic flux measurement	None. If loop is installed, it will be designed with upgrade in mind.
Divertor bolometer (20 ch)	See General Concerns for Cameras
Edge deposition monitors	Window could be darkened by radiation.
Edge Neutral Density Diagnostic (ENDD)	See General Concerns for Cameras
Edge neutral pressure gauges	None.
Edge Rotation Diagnostics (Ti, VΦ, Vppol)	Optics could darken from radiation.
Fast camera view of RF antennas	See General Concerns for Cameras
Fast ion D-alpha diagnostic	Should check supports for vibrations during disruption.
Fast IR Camera	Already becomes activated. Higher radiation dose will be worse. Also, increase in noise.
Fast lost-ion probe (energy/pitch angle resolving)	Radiation could darken glass.
Fast visible camera	See General Concerns for Cameras
Fission chamber neutron measurement	None.
Gas-puff Imaging (2msec)- midplane and divertor	Shielding for electronics may need to be increased. Fiber optics may darken.
Halo Tile current detectors	Thermally isolated. Could be a problem.
High-n and high-frequency Mirnov arrays	Saturation of digitizers.
Interferometry/forward scattering (1 mm, 1ch)	G10 base could become activated.
IR cameras (30 Hz) (3)	None. Also used on high radiation machines such as DIII-D.
Langmuir probe array-inter- LLD	Designed for 10 MW/m2 for 1 second. May need to be replaced anyway.
Langmuir probes-outboard edge	May need to be replaced when CS is taken out.
Langmuir probes-PFC tiles	On CS. Being replaced.
Langmuir probes-RF antenna	May need to be replaced when CS is taken out.
LLNL EUV spectrometer LoWEUS	None.
LLNL EUV spectrometer XEUS	Being relocated. No other concerns.
Locked-mode detectors	Possible saturation of digitizers. Detectors need to be relocated. Extra PF supports may interact with

	sensors.
Magnetics for equilibrium reconstruction	High heat fluxes may make diagnostics more difficult. Would be a nuisance, but not a problem. Mounting techniques may need to be modified because of high heat fluxes.
Microwave reflectometers (65 GHz backscattering, correlation, FM/CW, fixed frequency)	Window could darken. Copper pipes could bend from larger eddy currents (has happened before). Teflon connector cables could degrade.
Midplane tangential bolometer array	See General Concerns
Motional Stark Effect based on Collisionally-Induced Fluorescence	May need to clean window more often because of longer run time. Noise problems could worsen. Fibers could darken.
Motional Stark Effect based on Laser-Induced Fluorescence	Noise problems may worsen. Sightlines blocked by extension of beam armor.
Multi-pulse Thomson scattering (30 ch, 60 Hz)	May not be able to take measurement at 10 keV at higher temperatures. More noise and saturation problems. G10 components become activated. Vinyl and PVC could degrade.
Neutron detectors (2 uranium and 4 fast scintillator)	Will need to add another channel to accommodate higher neutron flux.
P-CHERS: Vθ(r) (75 ch)	Optics could be darkened.
Plasma TV	See General Concerns for Cameras
RF Antenna (ECH Launcher)	Most of the heat is taken by the boron nitride section.
RF edge magnetic probe	Shielded by tiles. Can be adjusted if they are too close to plasma.
RWM Coils	Should be checked for effects of eddy currents and vibrations.
RWM sensors (n = 1, 2, and 3)	Could be bent by forces induced by halo currents. May saturate digitizers.
Sample probe	Samples may become activated. Can be a nuisance, but not a problem.
Scrape-off layer reflectometer	Similar problems to microwave reflectometer.
SWIFT 2-D flow diagnostic	See General Concerns for Cameras
Tile temperature thermocouple array	Array on center stack will be replaced. Should be designed with upgrade in mind.
Ultra-soft x-ray arrays - tomography	Eddy currents could present a problem. May need stronger supports that can take a larger load. Noise from SPA's is an issue. Adding more will make it worse.
UV survey spectrometer (SPRED)	To be relocated.
Vertical x-ray crystal spectrometer	None.
Visible (VIPS) survey	Fiber optics could darken.

spectrometer	
Visible bremsstrahlung detector (1 ch)	Window could be darkened. New beam dump needed (geometrical reasons).
Visible filterscopes	Fiber optics could darken.
VUV transmission grating spectrometer	Currently well-supported, though more supports may be desired. Fast cameras may be added.
Wall coupon analysis	Wall supports should be checked. Activation would be a nuisance.

General Concerns for Diagnostics
Several of the diagnosticians expressed concerns that could affect many of the diagnostics. They are listed below:

- The spa's (fast switching power supplies) create noise for the diagnostics. If more are needed, there will be more noise.
- Wire fatigue could be a problem for vessel-mounted diagnostics from more vibration.
- Saturation of digitizers could occur because of larger magnetic fields.
- More deposition (lithium, carbon, etc.) on glass from longer shots could cause problems for diagnostics.

There was also a concern that does not directly affect diagnostics, but may be important to correct since the radiation levels are expected to rise by a factor of 50. The test cell wall penetrations are drilled straight through (line of sight) the wall, allowing radiation to directly penetrate the wall. The holes should be drilled at angles to prevent radiation from penetrating.

General Concerns for Cameras
There are also concerns that will mostly affect cameras. First, any glass fiber optics or windows may darken much more quickly. If the darkening occurs too quickly, they should be replaced with quartz. Also, any cameras that use a silicon chip may need better shielding to prevent additional noise.

Diagnostic Shutters
The diagnostic shutters are being analyzed for the stresses that develop from eddy currents as well as their deflections due to these stresses. Thermal analyses may also be done to check for deflection. The eddy current analyses are being done in ANSYS using the resistive solution, since this is the worst-case solution. One such analysis can be seen on the left. If the stresses that develop due to the resistive solution are too large, the inductive solution will also be checked for a more realistic comparison. The thermal analysis will be done using ANSYS and using a simple script to model the ratcheting of the temperature. The stresses due to thermal expansion are expected to be small, since the shutters are very thin.
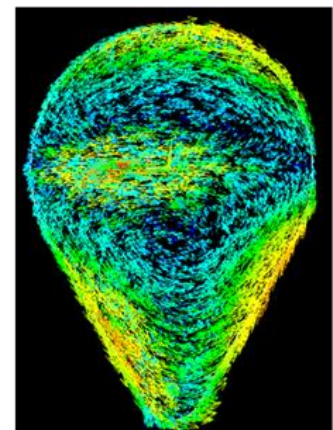
ARMOR BACKING PLATE NSTX-CALC-24-02-00
Prepared by: Larry Bryant, **Reviewed by** Irv Zatz, Pete Titus,
Cognizant Engineer: Craig Prinski

Purpose of Calculation:
  1.) To qualify the Armor backing plate calculation
  2.) Build and evaluate a Finite Element Model for The Armor Eddy Current Analysis
  3.) Apply Disruption Case of Magnetic Vector Potential from Opera Data Tables
  4.) To evaluate Static and Transient dynamic structural stress results

  APPENDIX 1: Show the foundations of the applied equations in the scripts used in the analysis
  APPENDIX 2: Demonstrate that the Applied Electromagnetic Loads Applied is Conservative
  APPENDIX 3: Demonstrate that applying the changes described results in an excellent match in the B field and flux rate data between ANSYS and OPERA.
  APPENDIX 4: Principal Stress Plots, Modal analysis, Conference paper with improved procedures and methods NSTX Disruption Simulations of Detailed Divertor and Passive Plate Models by Vector Potential Transfer from OPERA Global Analysis Results P. H. Titus[a], S. Avasarala, A. Brooks, R. Hatcher 2010 SOFT Conference, Porto Portugal October 2011

The Neutral beam armor plate is designed to react the mechanical disruption loads from the plasma. This analysis evaluates this armor plate for the structural loads and stresses using a very conservative methodology. Static and transient dynamic analysis is compared at several key locations on the structure to show that these are significantly below the material capacity of the structure.

The analysis also identifies that the applied disruption loads are much higher that the values provided by the electromagnetic program, OPERA when compared to ANSYS. The theoretical flux field differences were evaluated between the OPERA and ANSYS. The differences in the disruption flux field predictions between these programs were explained along with corrections to the methodology. The final result did show close correlation between both programs.

This work was followed by independent development work by others that resulted in a complete re-work of the electromagnetic analysis procedure.

Conclusions

  1.) The Armor Electromagnetic, Transient Dynamic and Static Structural analysis is complete based on the best OPERA information available as of May 7, 2010 and the assumptions of the merged solids.
  2.) The max static stresses (10,993psi at loadstep17) for the identical transient loads show that this disruption profile is not significant and that the effective

time constant is lower resulting in similar load reaction magnitudes between transient and static load cases.

3.) The reaction loads are very small at the armor attachment points to the vessel hoop loads and the vessel boundary. This demonstrates that the longer time duration of the disruption event does not necessarily imply that reaction load magnitudes will be greater.

4.) Revisions to the analysis script were determined to be necessary for the best correlation in the electromagnetic loads.

5.) After applying a number of corrections, we were able to get a very close correlation between the OPERA program and ANSYS values of Flux rate.

6.) This work was the motivation for further development by others that led to a conference paper described in Appendix 4.

7.) Given that the revised electromagnetic procedure completed after this calculation would provide lower loads the calculation was not repeated.
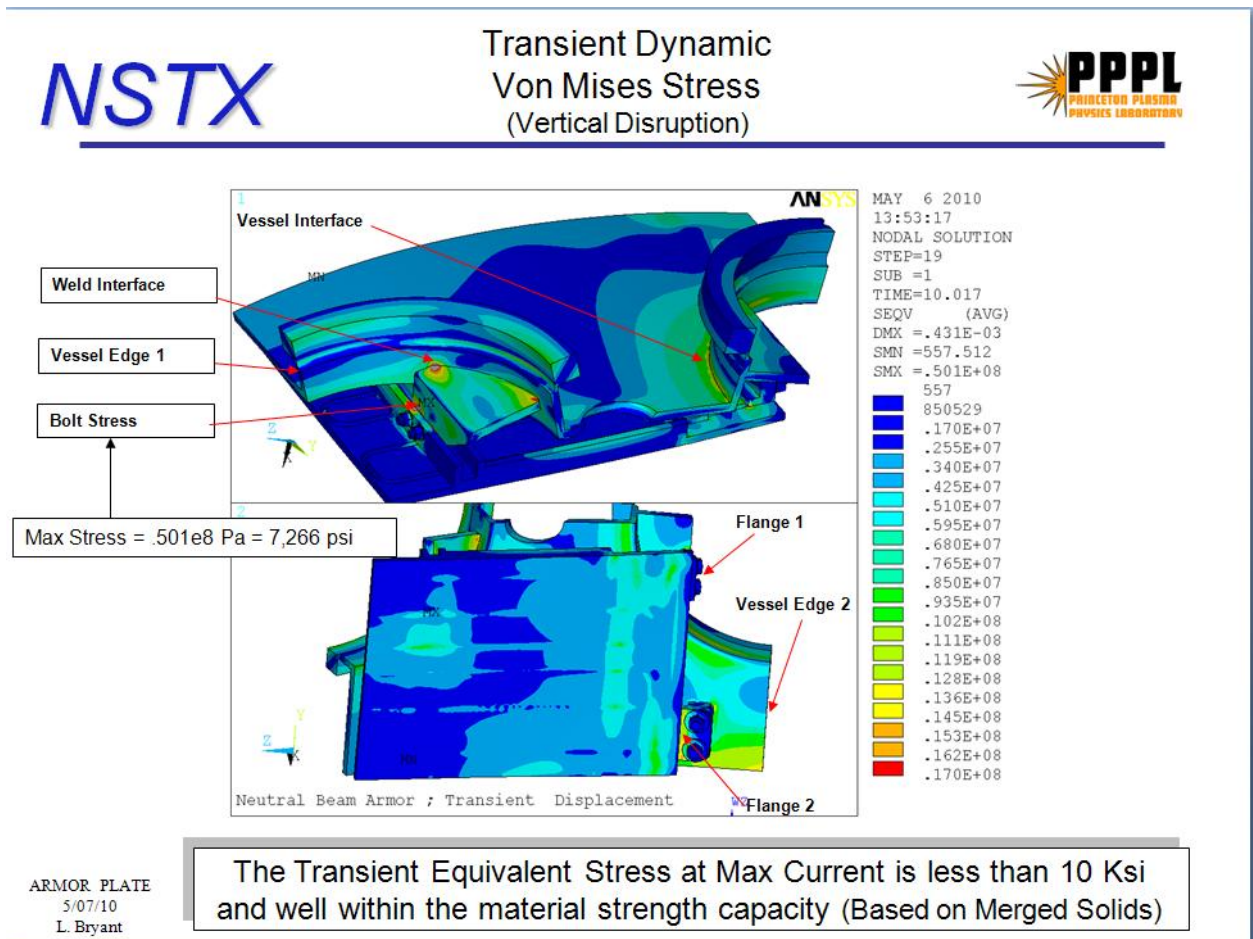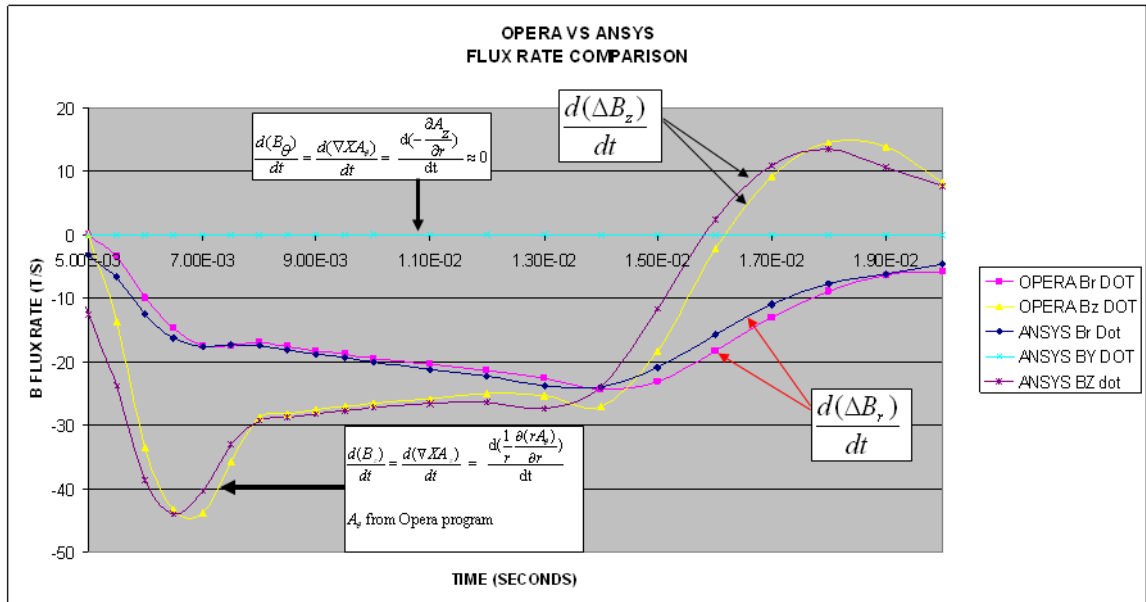

Figure #1 Transient Dynamic Stresses at Max Current for Armor Backing Plate
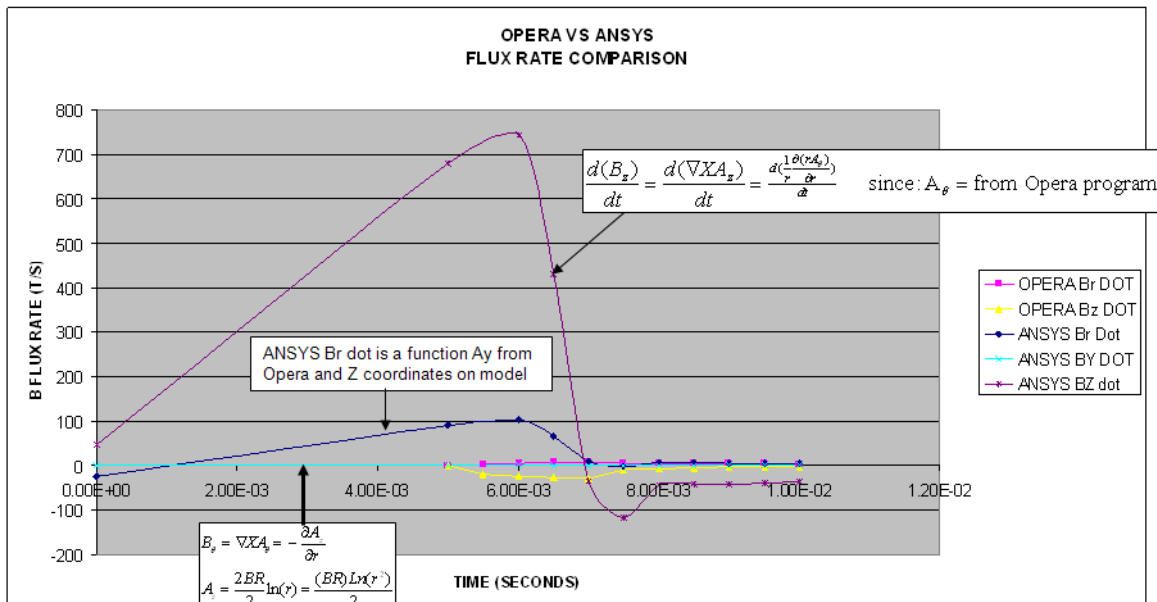
**Figure #2 B Flux Data comparison from OPERA Program to
ANSYS before corrections was applied.**

**Figure #3 B Flux Data comparison from OPERA Program to
ANSYS after corrections applied.**

Turbo Pump Magnetic Shielding Analysis NSTXU-CALC-24-04-00
Prepared By: Yuhu Zhai **Reviewed by:** Ali Zolfaghari
Cognizant Engineer: Bill Blanchard

The objectives of this analysis were: 1) to design magnetic shield using low carbon steels to reduce the maximum fringe field from NSTX coils at the turbo pump location (initially 3.5 m away from NSTX and ~3.45 m below the NSTX mid-plane but later on moved 20 inches further down the mid-plane to be closer to ground) to below 50 gauss on the pump within the shield. Specifically, NSTX coils generate about 350 gauss fringe field at the initial pump location (3.5 m in radial direction and 3.45 m down the NSTX mid-plane) where the fringe field consists of ~300 gauss radial field, 110 gauss vertical field and 145 gauss toroidal field; and 2) to extract Lorentz forces on the magnetic shield to ensure the shield is adequately supported.

OPERA and Maxwell 3d magnetic shielding models with current carrying conductors such as PF, OH inner TF and outer TF coils are developed for the nonlinear magneto-static analysis using BH property of M19 steel. M19 is considered the most effective in our preliminary 2D analysis. The coil magnetic fields from 3D models are benchmarked against the Design Point Spreadsheets and the Woolley Design Sheet. The fringe field from PF 4 and 5 are dominant and thus current scenarios #49 and #79 with the combined largest net negative current in these coils are investigated without plasma current to be conservative. The plasma current (in positive direction) will reduce the coil generated fringe fields.

The results for the half inch thick cylindrical shield show that: 1) the maximum field in the shield is ~1.5 T, which is below the saturation value for the M19 steel; 2) the fringe field inside shield is below 50 G and the net Lorentz force on the pump is below 50 pounds. 3) Although the magnetic field with shielding at the mid-plane inside the shield is below 20 gauss, the shield, however, needs to be at least 12 inches longer than the pump (6 inches above the top and below the bottom of the turbo pump) for the fringe field to be within 50 gauss at the pump top and bottom of the pump.

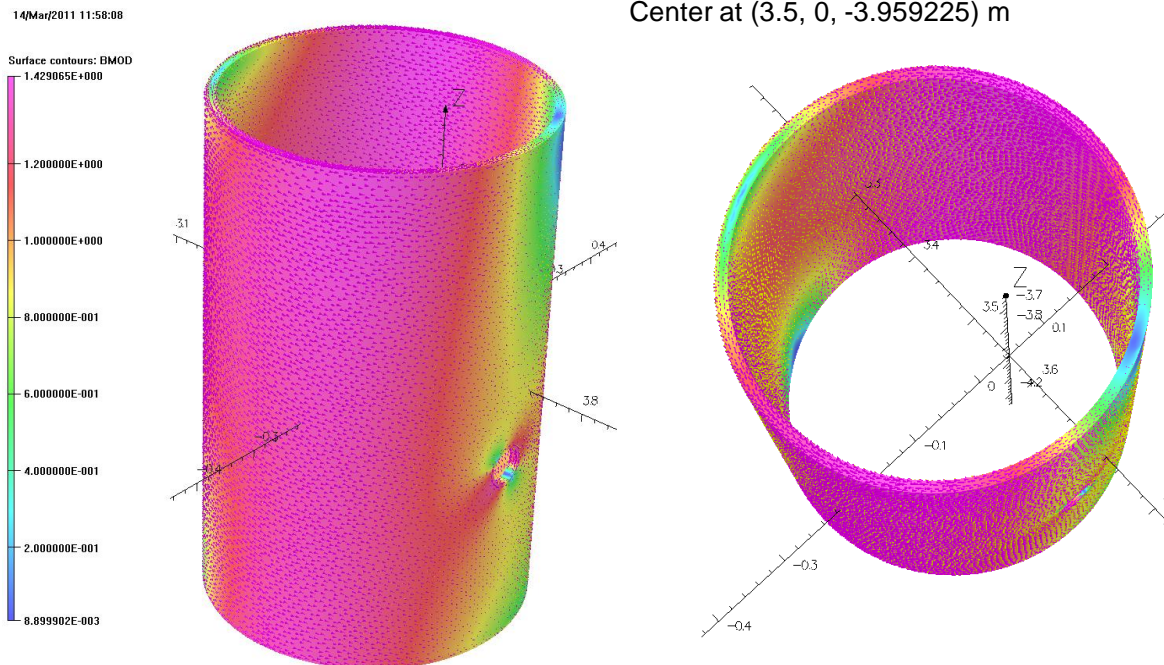The total volume of the cylindrical shield is 0.01228 m^3 and its weight is about 100 kg (220 lbs) for an iron mass density of ~8000 kg/m^3.

Table 1 – Force and Torque on the Shield due to Magnetization

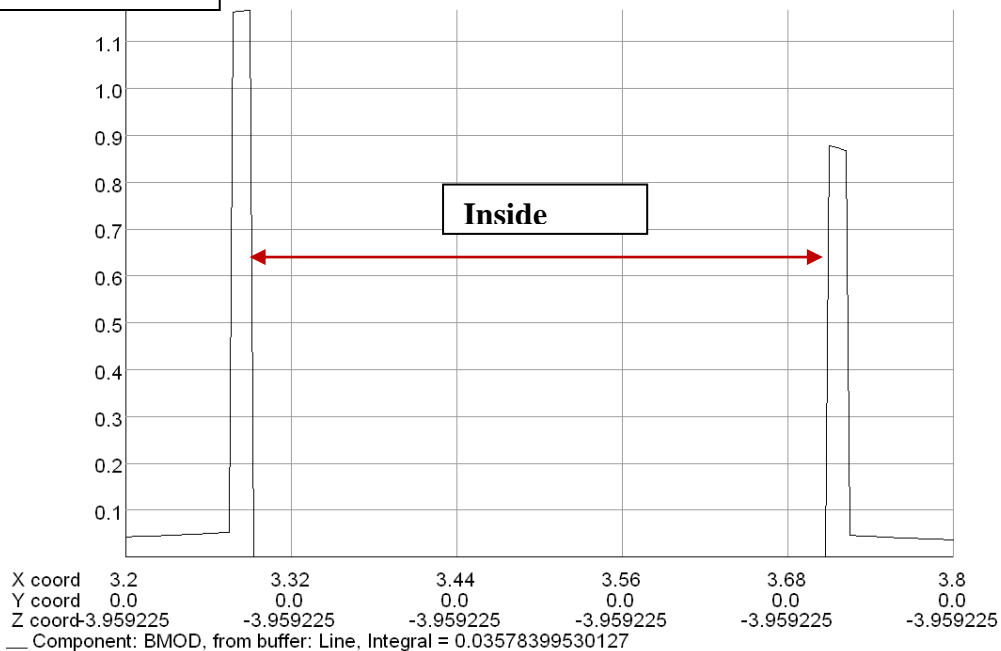|	Radial	Toroidal	Vertical	Total
Force (N)	-166.8	-31.0	86.6	190.5
Force (lb)	-33.1	-6.15	18.3	42.8
Torque (Nm)	32.0	-64.5	113.3	134.2
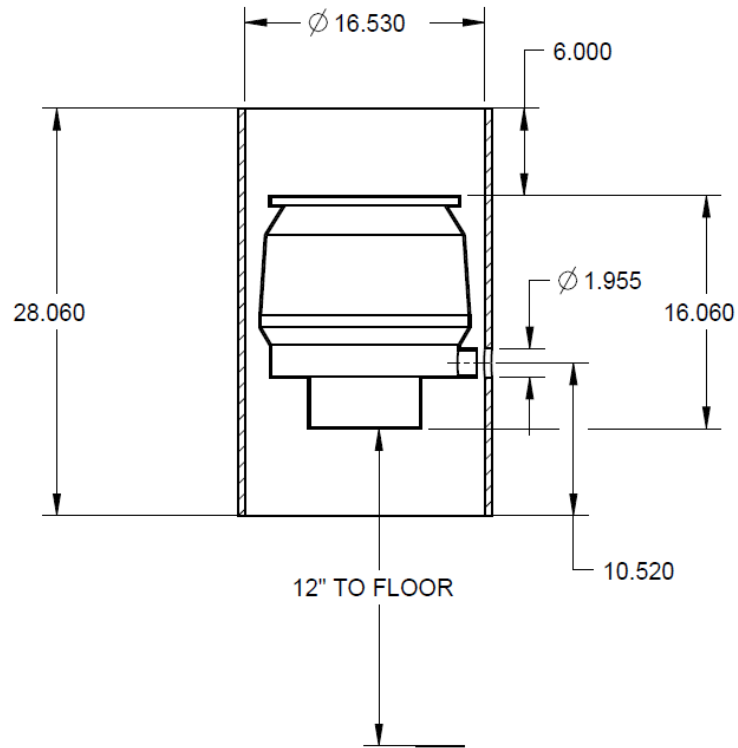
Figure 1 Magnetic shield for the NSTX vacuum turbo-pump

Figure 2 OPERA 3D: Flux density distribution (Tesla) on the magnetic shield

Figure 3 – Magnetic Field along Radial Direction in Shield Mid-Plane (Field drops significantly inside shield)

Magnetic Shielding Calculation, NSTXU_CALC-24-04-00
Prepared by: Larry Bryant, **Reviewed by** Ali Zolfaghari**,** Pete Titus**,**
Cognizant Engineer: Bill Blanchard

Purpose of Calculation:
  1.) To design the selection of materials and thicknesses for shielding the magnetic flux field for a pump
  2.) Build and evaluate a parametric finite element model for magnetic flux shielding.
  3.) Locate and Plot Non linear (Typical) shielding B –Vs H material data curves for 4 common materials.
  4.) Complete a parametric evaluation and sensitivity study on the max fields with various thicknesses
  5.) Develop ANSYS APDL scripts and apply a constant uniform field (0.0317 Tesla)
  6.) Generate vector plots of the field and complete hand calculations for these cases.
  7.) Plot graphs to illustrate trends in the data for a 12 inch and 8 inch shield diameter.
  8.) Provide Conclusions and Recommendations that will allow for an internal target field of 25 Gauss (0.0025 Tesla) or a maximum field of 50 Gauss.

A two dimensional parametric finite element study was completed to evaluate a variety of different materials and thicknesses in order to shield out the flux field for an ion pump. The analysis is based on ANSYS parametric script language (APDL). The results demonstrated that a silicon based material was the clear choice based on cost, and effectiveness of the material for shielding the pump. A range of thicknesses from 0.352 to 0.409 inches was determined to meet the requirements.

Conclusions
1.) A parametric magnetic shielding analysis has been completed that shows Magnetic Shielding behavior for a simplified two dimensional case for four different metals:
2.) The M19 Silicon Based Electric Steel provides;
   a. The best shield with the best sensitivity closer to the lower operating target of 25 Gauss.
   b. Virtually the same shielding properties per thickness as the low carbon steel.
   c. The highest sensitivity of all metals for the 8 inch diameter region inside the 12 inch diameter shell.
3.) The SA120 provides results that are similar to the low carbon steel with a lower sensitivity near the 25 gauss operating range.
   a. This option is not as robust of a solution in comparison to the low carbon steel.
4.) If the Pump (Shielded Item) can fit within the 8 inch diameter limit of the 12 inch diameter shield - a reduction on shield thickness of:

a. 13.0%   can be used for the low carbon steel at 50 gauss.
b. 13.9%   for the M19 Silicon based steel at 50 gauss

5.) Mu metal has:
   a. Almost at full saturation and would not be tolerant to manufacturing issues
   b. A higher and almost constant sensitivity (Tesla / Meter) in the 8 inch diameter operating range.
   c. Requires 2.5 times the thickness as that of the low carbon steel to achieve the same shielding

Recommendations:
   1.) Use the Non Oriented M19 Silicon Electric Steel with the standard C-O coating.
   2.) Design the magnetically sensitive items on the pump to be positioned within the 8 inch diameter region of the 12 inch diameter shield to avoid the localized flux leakage.
   3.) Complete a 3-D evaluation of this shielding to eliminate and end effect concerns from the non symmetrical fields.
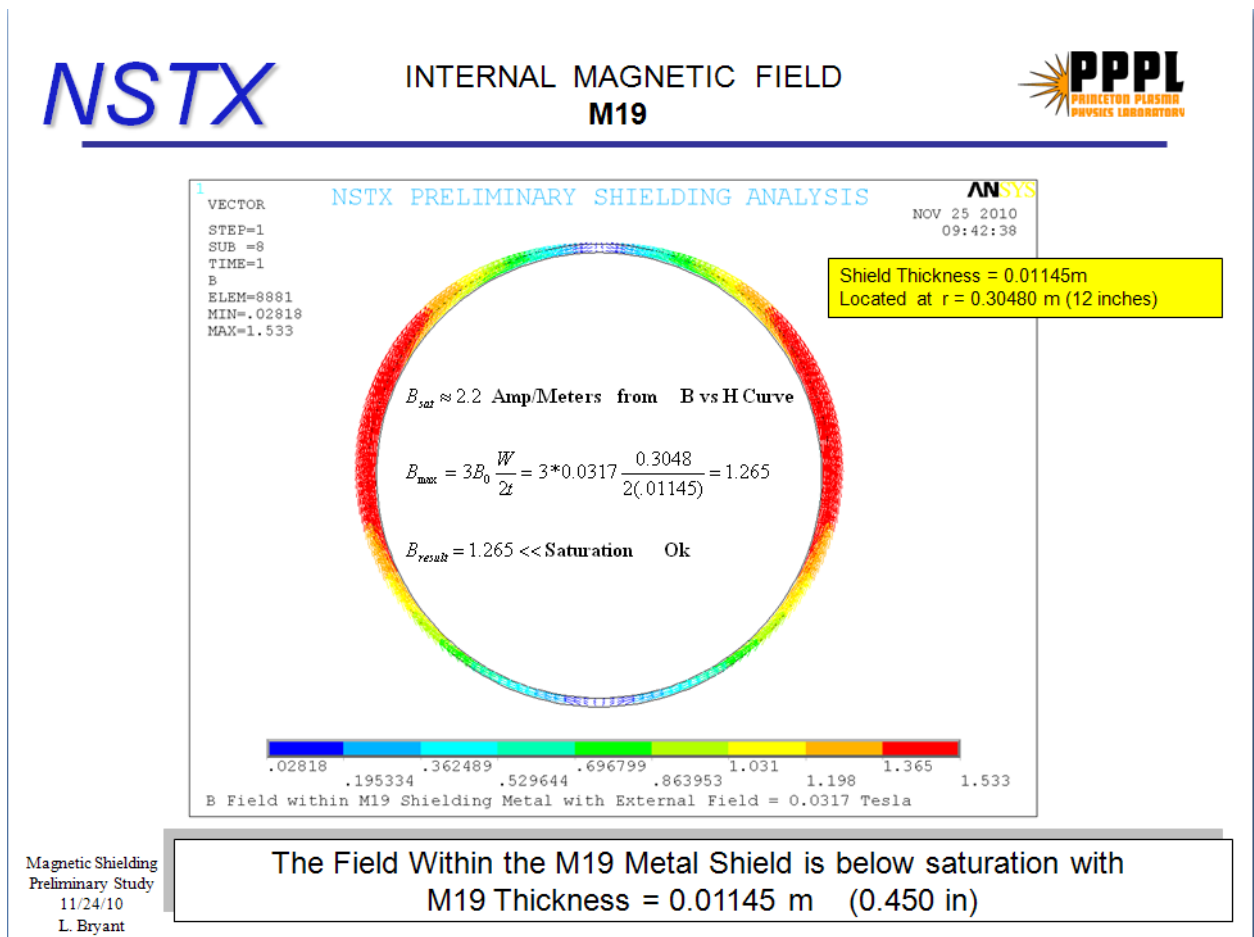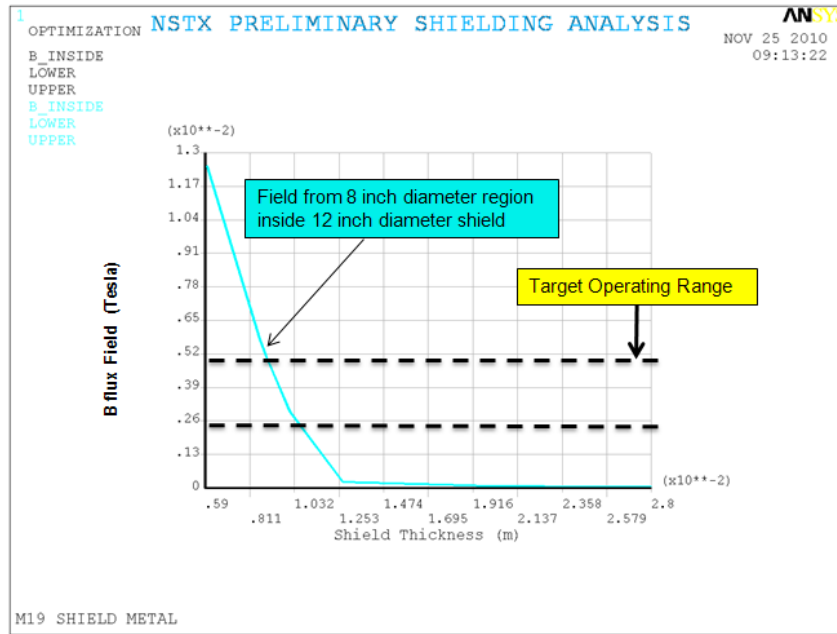

NSTX INTERNAL MAGNETIC FIELD M19 PPPL

NSTX PRELIMINARY SHIELDING ANALYSIS

VECTOR
STEP=1
SUB =8
TIME=1
B
ELEM=8881
MIN=.02818
MAX=1.533

NOV 25 2010
09:42:38

Shield Thickness = 0.01145m
Located at r = 0.30480 m (12 inches)

$B_{sat} \approx 2.2$ Amp/Meters from   B vs H Curve

$$B_{max} = 3B_0 \frac{W}{2t} = 3*0.0317 \frac{0.3048}{2(.01145)} = 1.265$$

$B_{result} = 1.265 << $ Saturation   Ok

.02818   .362489   .696799   1.031   1.365
   .195334   .529644   .863953   1.198   1.533
B Field within M19 Shielding Metal with External Field = 0.0317 Tesla

Magnetic Shielding
Preliminary Study
11/24/10
L. Bryant

The Field Within the M19 Metal Shield is below saturation with M19 Thickness = 0.01145 m   (0.450 in)

Figure #1 Flux Field within the M19 Material to show results are below saturation.

Figure #2 Flux Field results as a function of shield thickness for M19 material

NSTX

B Field Variation versus Shield Thickness
M19

PPPL
PRINCETON PLASMA
PHYSICS LABORATORY

M19 METAL

SHIELD THK (M)	B Field Inside (Tesla)	B Field External (Tesla)	B Field Shield (Tesla)
6.00E-03	1.25E-02	4.83E-02	1.78494
8.60E-03	5.80E-03	5.13E-02	1.7012
8.70E-03	5.59E-03	5.14E-02	1.69593
8.90E-03	5.17E-03	5.16E-02	1.68636
8.95E-03	5.07E-03	5.16E-02	1.6834
1.01E-02	2.96E-03	5.25E-02	1.62271
1.02E-02	2.80E-03	5.26E-02	1.61641
1.03E-02	2.65E-03	5.26E-02	1.61001
1.04E-02	2.50E-03	5.27E-02	1.60361
1.27E-02	2.49E-04	5.36E-02	1.42854
1.88E-02	9.88E-05	5.36E-02	0.97559
1.89E-02	9.79E-05	5.36E-02	0.970654
1.97E-02	9.13E-05	5.36E-02	0.933221
1.98E-02	9.05E-05	5.36E-02	0.928328
2.15E-02	7.96E-05	5.36E-02	0.857946
2.16E-02	7.91E-05	5.36E-02	0.854108
2.38E-02	6.89E-05	5.36E-02	0.778254

Operating Target Range
0.0025 Tesla
0.0050 Tesla

Note: External field in table is a max sorted value and not a representation of far field variations

Magnetic Shielding
Preliminary Study
11/24/10
L. Bryant

M19 Shielding for the operating target range
Is acceptable between 0.00895 m (0.352 in) – 0.0104 m (0.409 in)

**Figure #3 the table shows a range of M19 thicknesses that would be acceptable.**

WBS 1.5.2 Force Influence Matrix Coefficients NSTXU-CALC-13-03-01
Prepared by Ron Hatcher, Review by: Peter Titus, Cognizant Engineer: Ron Hatcher

Force influence coefficients between are calculated for the PF coil system and the plasma. The coils, plasma, and other conducting structures are modeled using Opera. The conductors (coils and plasma) are energized with unit current (1 kA) and a static electromagnetic analysis is run to determine the resulting forces. The analysis is performed for each conductor singly and for all possible pairs of conductors. Output data from the Opera analysis is used in a Matlab™ code that produces the force influence matrices for the contracted coil set.

The influence matrices can be used to quickly calculate force vectors for a given current vector and are used in other project calculations. One such use is in the project configuration spreadsheet where the influence matrices from both the circular and shaped plasma models are used to bracket the post-disruption coil currents and forces.
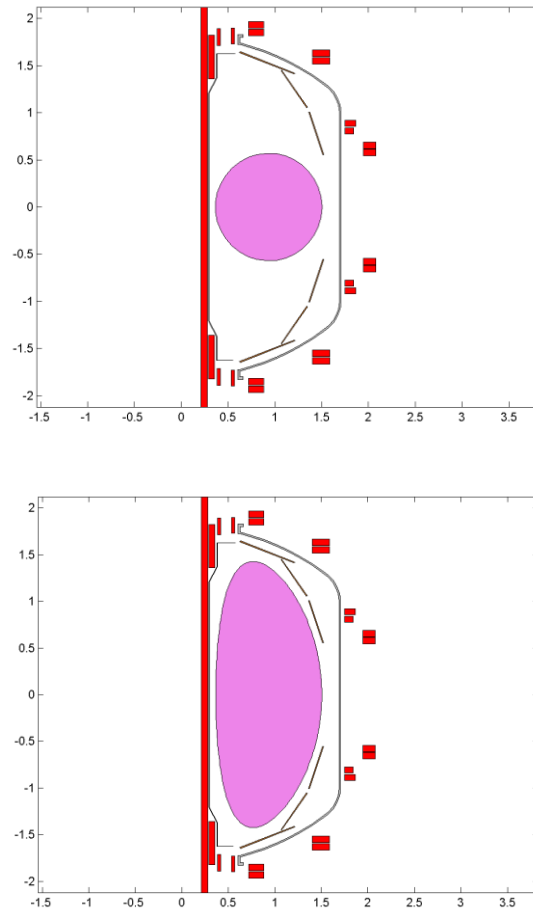
Figure 5 – Configuration with two plasma models for NSTX CSU Influence Matrix Calculation

System	Current [kA]	Fr [lbf]	Fz [lbf]
PF1aU	1.43	2.21E+04	7979.3
PF1bU	11.75	9.10E+04	-38575.5
PF1cU	10.39	-4.19E+04	-23976.4
PF2U	-0.16	1.37E+03	608.8
PF3U	-6.13	6.07E+04	-2480.0
PF4U	4.39	-8.14E+04	37864.6
PF5U	-25.22	4.40E+05	-19077.1
PF5L	-25.22	4.40E+05	19077.3
PF4L	4.39	-8.14E+04	-37864.8
PF3L	-6.13	6.07E+04	2480.0
PF2L	-0.16	1.37E+03	-608.8
PF1cL	10.39	-4.19E+04	23976.3
PF1bL	11.75	9.11E+04	38575.4
PF1aL	1.43	2.21E+04	-7979.4
OH	13.02	8.22E+06	0.4
Plasma	2000.00	3.86E+04	0.0

Table 2 Example of force calculation using influence matrices

WBS 1.5.2 Upgrade Moment Influence Coefficients
NSTXU-CALC-13-05-00 January 18 2011
Prepared By: Peter Titus,
Reviewed By: R. Woolley, Ron Hatcher, NSTX Cognizant Engineer

Executive Summary:

It is usual practice to utilize influence coefficient calculations to determine hoop and axial (vertical for tokamak's) loads from coil currents. However the centroid of the Lorentz loads may not be at the geometric center of the coils. Where there is significant offset between the Lorentz centroid and the geometric center, there will be a moment about the coil geometric center in addition to the net loads. This may be a significant contributor to the support reaction loads and to the stresses in the coils themselves. In design and analysis of coil systems, distributions of fields and forces are typically calculated for a useful structural/magnetic mesh which is typically fine enough to properly distribute the Lorentz forces and resolve any moments about the coil current centers. When influence coefficients are used in operating tokamaks to check coil stresses and support loading the effect of moments has been omitted. To the author's knowledge, this is true of Alcator C-Mod, TFTR and NSTX. Addition of the moment coefficients completes the three degrees of freedom available from the axisymmetric analysis of ring coils.
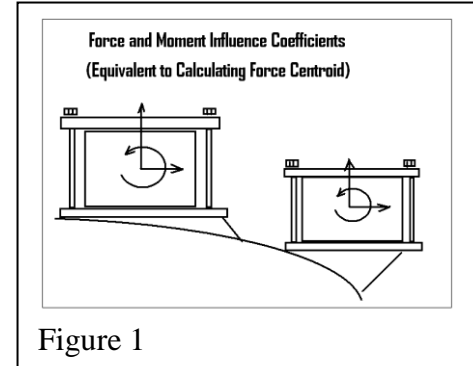

Force and Moment Influence Coefficients
(Equivalent to Calculating Force Centroid)

Figure 1

**Digital Coil Protection System (DCPS) Input**

The proposed DCPS is described in detail in a draft requirements document by Robert Woolley ref [7]. Force influence coefficients are already included in plans for the DCPS. Inclusion of these moment coefficients is proposed, depending on their usefulness in quantifying stresses for specific components. In the description of the DCPS, the "systems code" will actually be the analyses described in the filed structural calculations. There is a global model which is the closest thing we have to a single systems code, but this is augmented in many ways by separate calculations to address specific stress locations and components and support hardware. During the final design activity, each preparer of a calculation will be assigned the development of "mini algorithms" These may make use of moment influence coefficients. One example is:

PF 2,3 supports, welds bolts – At this stage, these are just calculated from influence coefficient matrix loads divided by weld or bolt area. Addition of moment influence coefficients adds overturning moments to the calculation of the bolt loads.

Addition of Moment Influence Coefficients to DCPS

Force Influence Coefficients
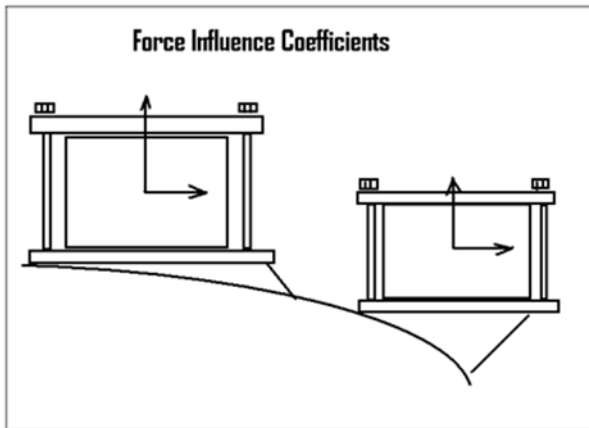
Bolt Loads are calculated only from the vertical force.

Force and Moment Influence Coefficients
(Equivalent to Calculating Force Centroid)
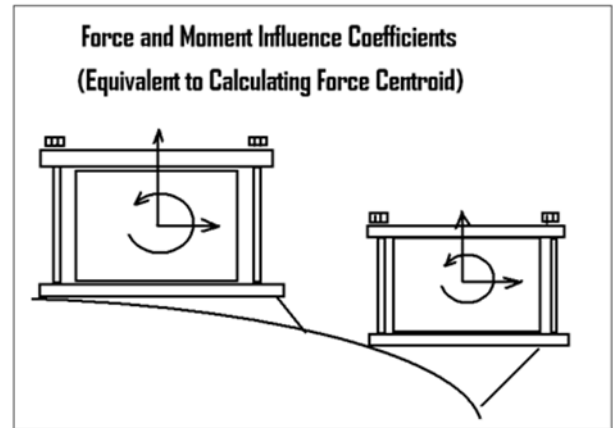
Bolt Loads are calculated from the vertical force and the moment divided by the width of the bolt pattern

WBS 1.5.5 Structural Analysis of PF1, TF & OH Bus Bars
NSTXU-CALC-55-01 Prepared By: Andrei Khodak
Reviewed by Peter Titus **Cognizant Engineer**: Mark Smith

NSTX upgrade scenarios call for increased loads for the coils. Thus bus bars will experience larger thermal and electromagnetic loads, so analysis of these effects is important for proper design. Three-dimensional numerical simulations were performed using ANSYS coupled solver for simultaneous structural, thermal and electromagnetic analysis. Thermal and electromagnetic simulations supported structural calculations providing necessary loads and strains. Model geometry was discretized into hexahedra elements using structured multi-block approach. Example of the mesh is presented on figure 1. Simulations were performed during design process to verify structural integrity.

The following parts of the coil assembly are included in the analysis:
- P1A,B,C upper and lower bus bars with flags supports and parts of coil assembly
- OH bus bar together with coaxial part
- TF bus bars with supports and parts of connecting structure

Remaining NSTX PF coils are modeled as current source elements, NSTX TF coils are modeled as current source elements within the center stack and as solid elements at the periphery. Constant elevated temperatures were imposed according to the analytical heat transfer calculations. Reference temperature of 20 ℃ was used for thermal strain calculation, as a temperature during assembly, of the device. Supporting brackets are fixed in places of attachment to other structures. Both ends of the TF and OH bus bars are fixed, as well as outer ends of the PF bus bars. Supporting faces of the PF coils are fixed to provide correct load structure on the flags. Positive vertical displacement of 1 cm is imposed on P1A, and PF1B upper coil boundaries to emulate thermal expansion of the center stack.

Results of the numerical simulations show, that bus bars experience very large values of local stresses due to magnetic forces and thermal expansion

Results for PF1 bus bars show that maximum values of stresses occur in flags where flags are connected to coil winding as shown on figure 2. With the current design of the flags and increased currents, coil connections experience excessive stresses at the narrowest cross-section. Coil cables have a cooling channel inside, which make them even weaker. Brackets connecting flags to coil insulation are proposed to improve strength of the connection. Introducing such brackets and/or extending insulation to the flags will eliminate narrow cross-section and improve stress situation. However even without flags stress levels in PF bus bars are significant. To reduce the level of stresses clamping of the in and out bus bar together will reduce the deformation and corresponding stress levels at the supports.

Maximum value of stress intensity in the TF bus bar occurs in flag attached to the outer leg. High value of the stress is caused by thermal expansion of the bus bar, fixed between the outer leg and the floor. Compensation measures for thermal expansion are recommended for this portion of the TF bus bar. Prolong unsupported sections of the TF bus bar experience strong deformation due to magnetic forces. Heat transfer analysis showed excessive temperature levels in the section of TF bus bars with a single conductor which is not cooled internally. Increase of the bus bar cross section is recommended in this area.

Maximum value of stress intensity in the OH bus bar occurs at the supporting bracket. Stronger bracket for OH bus bar is recommended
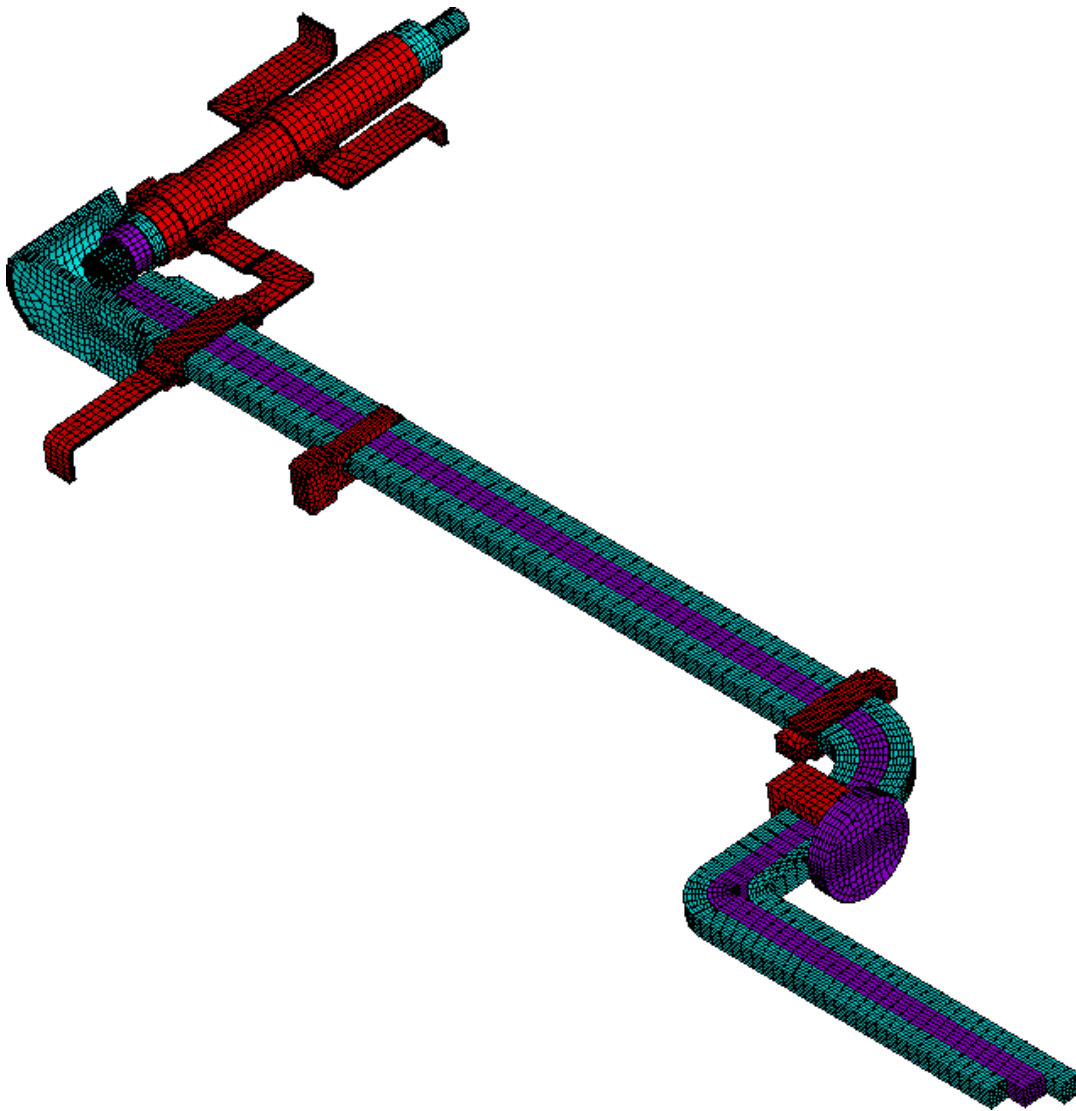
Figure 1 Mesh for OH bus bar
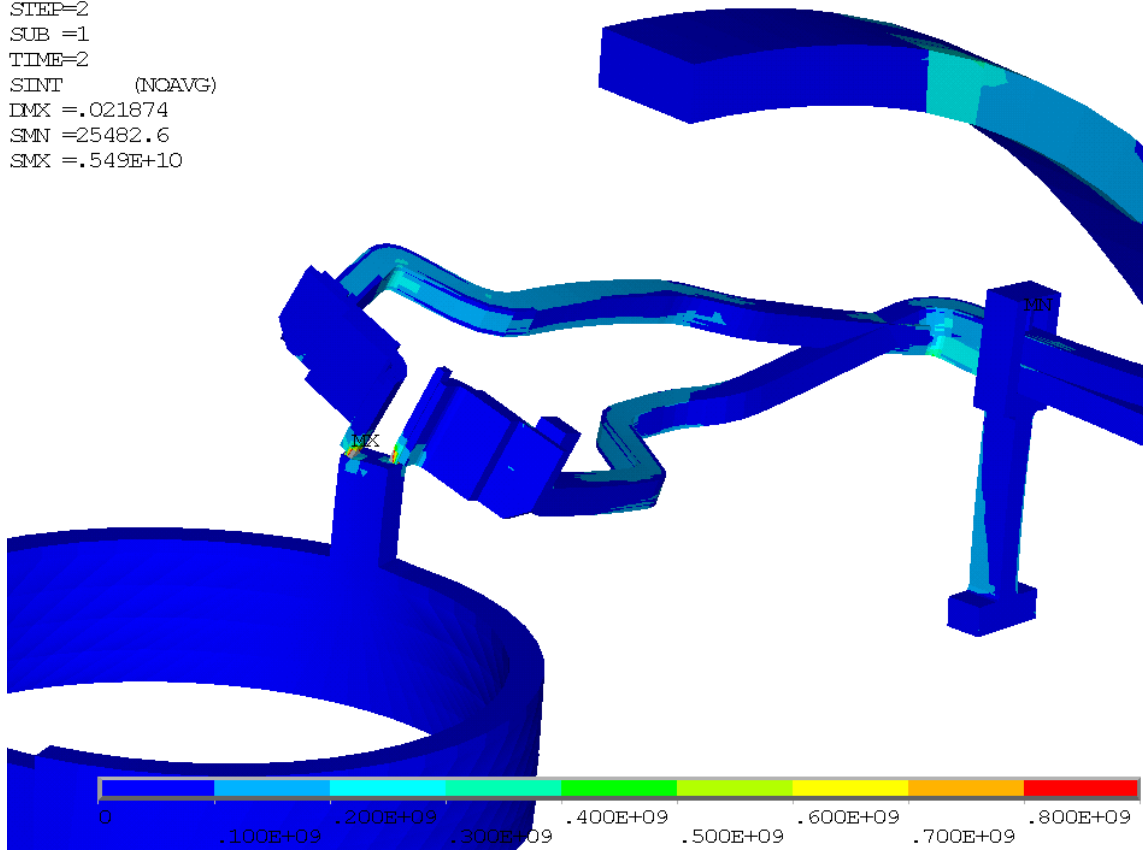
Figure 2 Stress intensity at PF1B upper bus bar coil connection